Scuola Normale Superiore di Pisa

Classe di Scienze

PhD Thesis

2011

Supersymmetry without a light Higgs boson

Roberto Franceschini

Advisor: Professor Riccardo Barbieri

Abstract

In this thesis I shall discuss a class of supersymmetric models characterized by a Higgs sector with a strongish self-coupling and a relatively heavy spectrum, with the mass of the lightest CP-even Higgs boson around 200-300 GeV. The effective field theory for these models is λSUSY [**1**] that is to say the Next-To-Minimal Supersymmetric Standard Model with large coupling $\lambda S H_1 H_2$ in the superpotential.

I shall discuss in detail a model with scale-invariant superpotential, with particular focus on the dynamical origin of the μ term and its relation with the mass of the Higgs boson.

I shall discuss the fine tuning of the model and various experimental constraints from LEP direct searches, precision data and direct DM searches. I shall argue that the model naturally accommodates the current limits and I shall discuss the main features of the signatures at the LHC.

The material of this thesis comes mostly from two papers [**2**, **3**]. Furthermore, during my PhD years in Pisa I have worked on other problems in collider phenomenology [**4**] and astro-particle physics [**5**]. As they do not have direct connection with supersymmetry and the Higgs boson they are not discussed in this thesis.

Ai miei genitori

"... i discorsi nostri hanno a essere sopra al mondo sensibile, e non sopra un mondo di carta."

Galileo Galilei - *Dialogo sopra i due massimi sistemi del mondo*, Firenze, 1632

Contents

CHAPTER 1

Introduction and plan of the work

What is known as the "standard model" of particle physics is a gauge theory with symmetry group

$$SU(3)_{\rm color} \times SU(2)_{\rm weak} \times U(1)_Y .$$

The dynamics of the gauge theory have been experimentally tested over a broad range of energies up to the high energies of LEP, about 200 GeV, TeVatron and recently the LHC that, as of the end of 2010, produced collisions up to more than 2 TeV of center of mass energy of the hard and central final state.

The $SU(3)_{\rm color}$ part of the Lagrangian is rather well established and QCD, the gauge theory of color, seems to be the correct theory of strong interactions, with quarks and gluons as fundamental degrees of freedom (DoF).

On the other hand the $SU(2)_{\rm weak} \times U(1)_Y$ part of the Lagrangian is still not completely established.

In fact the experiments at the LEP collider made precision tests of the interactions of quarks and leptons with the carriers of the $SU(2)_{\rm weak} \times U(1)_Y$ gauge forces, the gauge bosons $Z^0, W^{\pm}, \gamma$ [**6**]. LEP also tested the non-abelian interaction among the gauge bosons Z^0 and $W^{\pm}$ [**7**]. LEP produced more than 10^6 Z^0 bosons and the four experiments ALEPH, DELPHI, L3, OPAL studied their interactions with an accuracy of $\sim 10^{-3}$. The precision of these results required loop level calculations, that turned out to match very well with the precise data of LEP. As a matter of fact all the results of LEP point towards a $SU(2) \times U(1)$ gauge theory and the agreement with the theoretical calculations is impressive.

Despite the impressive agreement between LEP data and the predictions the $SU(2) \times U(1)$ gauge theory, we know that the gauge symmetry cannot be exact as the gauge bosons are observed to be massive. This requires that the gauge symmetry must be spontaneously broken, though we do not have yet observed what dynamics actually breaks the symmetry. The only ingredients that we are sure to be part of the sector that breaks the electroweak symmetry are the Goldstone bosons associated with the spontaneous breaking of the symmetry.

In Section 2.1 we shall use our knowledge of the interactions of Goldstone bosons to estimate the mass scale where we expect the EWSB sector to show up and reveal its dynamics. Here we can anticipate that the Goldstone bosons of the electroweak theory are in many respects similar to the pions of QCD, that are the Goldstone bosons of the chiral symmetry of the massless QCD Lagrangian. Their interaction is described by a non-linear sigma model, where the source of the breaking of the symmetry is left unspecified. The simplest, and probably most economic, way to introduce the breaking is to add to the model a scalar field, the Higgs boson, that has a VEV and triggers the breaking of the symmetry. One of the virtues of the addition of the Higgs field is that it

makes the model potentially valid up to arbitrary high energy[1], as the non-linear sigma model plus a Higgs boson with suitable couplings can be written as a renormalizable $\lambda\phi^4$ theory.

The existence of a fundamental scalar with VEV, however, poses some problem in a field theory at the quantum level. In Sections 2.2 and 2.3 we shall see that the potential of the scalar is very sensitive to the details of physics at energy scales much higher than the mass of the scalar. This comes from the fact that loop corrections to the potential tend to drive the mass of the Higgs boson toward the UV cut-off of the theory, rather than to correct the tree-level value by a small amount. The tendency of the Higgs mass, and its VEV, to become higher and higher as one pushes the validity of the theory to higher energies seems to clash with the fact that the non-linear sigma model plus the Higgs boson is potentially valid to arbitrarily high scales. Indeed we know that the VEV of the Higgs, measured to be around 246 GeV, sets the scale for the masses of the gauge bosons, and these are much smaller than any other scale expected to appear at higher energies, as for instance the scale of quantum gravity that is 17 orders of magnitude larger than m_W. In this sense the smallness of the masses of the gauge bosons seems a mere accident, or, better, calls for an explanation in terms of some dynamics that stabilizes the VEV of the Higgs. This puzzle goes under the name of "*hierarchy problem*" and motivated a great deal of theoretical work.

In Section 2.3 we shall see that one of the possible solutions to this problem is the introduction of a symmetry that stabilizes the VEV of the Higgs and that gets broken not far from the scale of the EWSB. Such symmetry is supersymmetry and, due to the fact that it must explain the size of the electroweak scale, we shall call it *electroweak scale supersymmetry*, or just SUSY.

The idea of SUSY as the symmetry that stabilizes the electroweak scale motivated the study of the supersymmetric extensions of the afore-mentioned "standard model", *i.e.* the “standard model” has been extended to become invariant under supersymmetry transformations, yielding the so-called Minimal Supersymmetric Standard Model (MSSM).

The MSSM predicts the existence of new particles at a mass scale close to the scale of the breaking of supersymmetry. These additional states happen to have the notable feature to modify the renormalization group flow of the gauge couplings of the SM such that in the MSSM the couplings nearly unify at an energy $M_{GUT} \sim 10^{16}$ GeV. Furthermore the model predicts that the Higgs boson at tree-level must be lighter than the Z^0 boson.

For what said, at the dawn of the LEP era hopes were on the discovery of SUSY, that provided a symmetry principle as solution of the hierarchy problem of the Standard Model and a serious chance for the Higgs boson to be light and thus to be in the reach of that machine. The measurements of the gauge couplings performed at LEP turned out to be in very good agreement with the idea of a unification at scales $M_{GUT} \sim 10^{16}$ GeV, as foreseen in the Minimal Supersymmetric Standard Model. Unfortunately, the striking picture emerging from the study of the gauge couplings did not find a counterpart in the observation of neither a light Higgs boson nor of any of the numerous superpartners.

The absence of evidence for supersymmetry at LEP might be taken as strongly disfavoring SUSY. However, one has to acknowledge that the expectation for SUSY, and in particular for a light Higgs boson, to be discovered at LEP was mostly based

[1] We put aside for a moment possible issues due to the occurrence of a Landau pole.

on strict requirements of minimality in model building. The MSSM has in fact a scalar potential whose quartic part is entirely fixed by the gauge symmetry and this yields the famous result that the lightest Higgs boson of the MSSM has to be light. As we shall discuss in more detail later, such lightness of the MSSM Higgs boson can be understood noting that at tree-level the lightest Higgs boson mass can be upper-bounded by

$$m_Z \cos 2\beta \,, \tag{1.0.1}$$

and therefore can even be vanishing if $\tan\beta = 1$.

In the MSSM further contributions to the lightest Higgs mass arise at the one loop level and can lift the Higgs mass above the experimental lower-bound [**8**]

$$m_{h_{\rm SM}} > 114 \text{ GeV} \,. \tag{1.0.2}$$

However such large radiative corrections require soft masses much larger than the ElectroWeak Symmetry Breaking scale, which loosens the Naturalness argument to motivate supersymmetry at the TeV scale.

The necessity of large soft masses in the MSSM motivates the study of supersymmetric models that extend the MSSM and that can possibly alleviate the tension with LEP direct searches. Indeed a study of extensions of the MSSM with effective operators [**9**] indicates that departing from the minimal model one can have substantial corrections to the bound on the lightest Higgs mass in eq.(1.0.1) [2].

The positive results of LEP about a possible unification of the gauge couplings at high energies and the theoretical preference for models where unification is reached in a perturbative regime posed further constraints of minimality in model building. However relaxing the requirement of strictly perturbative unification does not necessarily conflict with the idea of unification, that might be reached in a less minimal way, for instance having the gauge couplings that run to the unified value while the other couplings of the theory do not necessarily stay perturbative at all energies [3]. In general this leads to non-minimal models with significant changes for the phenomenology [**10**] that are worth to be studied. Indeed, an attempt along this line has been made in [**11**–**14**], where the self-coupling of the Higgs sector has a strong coupling phase at some intermediate scale between the EWSB and the GUT scale. Handling such a strong coupling phase for the Higgs sector puts one in position to substantially increase the mass of the Higgs at the tree-level. The concrete example in [**11**] shows that this can be done with no substantial changes in the cherished pattern of unification of the gauge couplings. The idea has been further elaborated in [**13**] where it has been discussed a unification-compatible UV completion for the so-called Next to Minimal Supersymmetric Standard Model (NMSSM), *i.e.* for a model described by a superpotential of the form

$$W = \lambda S H_1 \cdot H_2 + f(S) \,, \tag{1.0.3}$$

where the superfields H_1 and H_2 are Higgs doublets and S is a SM singlet.

---

[2] These studies, however, must be taken just as an indication of the room available in going beyond the MSSM. Indeed to have a significant effect the scale that suppresses the operators relevant for the mass of the Higgs needs to be not far from the TeV. This signals the need to go beyond the operator analysis and specify a theory valid well above the TeV, such that higher dimensional operators at the cut-off of the theory do not endanger the precision measurements of LEP.

[3] The absence of effects in the QED coupling across the strong coupling scale of QCD seems to give support to the idea that such pattern of evolution of couplings can be realized in Nature.

With respect to the commonly studied case with perturbative unification, the low energy NMSSM of [**11**–**14**] can have larger couplings that become non-perturbative much below the gauge coupling unification scale. The extended range of acceptable couplings allows the mass of the lightest Higgs boson to reach 200-300 GeV, which leads to dramatic differences in the phenomenology of the Higgs sector with respect to the MSSM.

Indeed, if one considers a model with a superpotential that includes the term $\lambda S H_1 \cdot H_2$, as in (1.0.3), the upper-bound on the lightest Higgs mass is given by

$$\sqrt{m_Z^2 \cos^2 2\beta + \lambda^2 v^2 \sin^2 2\beta}\,, \tag{1.0.4}$$

which does not vanish for any value of $\tan\beta$ and becomes larger as one takes larger values for λ.

However the maximal value of λ at the EW scale that does not lead to a Landau pole below the GUT scale is ~ 0.7 [**15**], which only modestly affects the upper-bound on the Higgs mass, if compared to the MSSM.

Motivated by the strong constraints that follow from perturbative unification one can try to see what happens dropping the requirement of a perturbative λ up to M_{GUT} and impose only that λ stay perturbative up to a cut-off scale $\Lambda \gtrsim 50$ TeV, such that the model still makes sense as a calculable low-energy effective theory, *i.e.* that any effect from physics at the cut-off affects negligibly currently available measurements at energies up to hundreds of GeV. This guise of the NMSSM with coupling $\lambda \simeq 1-2$ will have a Higgs boson significantly heavier than what attainable in the perturbative case and this leads to profound changes in the phenomenology, which makes the model worth a study. Furthermore, the large Higgs mass attainable for $\lambda \simeq 1-2$ automatically reduces the sensitivity of the mass of the Higgs to UV effects, and consequently the model turns out to be less fine tuned, which adds further motivation to pursue this regime.

Ref. [**1**] analyzed the case where $\lambda \sim 2$ and (1.0.3) is taken as a low energy effective superpotential below a scale of $\mathcal{O}(50\ \mathrm{TeV})$. Given the great importance covered by the coupling λ in this regime of the NMSSM they dubbed this scenario λSUSY. In Ref. [**1**] a very detailed analysis of the Electroweak Precision Tests (EWPT) has been performed with the result that λSUSY can be in agreement with LEP data. Ref. [**1**] also studied the issue of the Naturalness of the model, finding that this kind of models typically does not need to be tuned. The absence of tuning is somehow expected because the major source of fine-tuning in the MSSM is due to the need to generate large loop corrections to raise the Higgs mass above m_Z. Including the tree-level contribution coming from the large coupling λ, this need is no longer a concern and one is not forced to push the model to an unnatural region of its parameter space because of the LEP bound on the Higgs mass. In this sense λSUSY is a remarkable candidate for a natural supersymmetric theory of Electroweak Symmetry Breaking.

Furthermore it has been shown that in λSUSY a singlino-like lightest supersymmetric particle (LSP) can be a weakly interacting massive particle (WIMP) dark matter candidate with the correct thermal relic abundance. Additionally, λSUSY has a strikingly different Higgs sector with respect to the one of the MSSM and the one of the perturbative NMSSM, which leads to testable distinctive signals for the LHC [**3**].

An additional virtue of the NMSSM, if compared to the MSSM, is the possibility of generating the Higgsino mass term μ dynamically. Indeed if the singlet S takes a VEV, the interaction in eq. (1.0.3) generates an effective mass for the Higgsinos $\mu = \lambda\langle S\rangle$. In the NMSSM the VEV of the singlet depends on the same soft masses that trigger the VEV of the doublets. Therefore the μ term is generated by the same dynamics that breaks the EW symmetry, rendering evident why μ is of the same order of the EW scale instead of being zero or of the order of some other energy scale that characterizes the (unspecified) UV theory.

In this sense the solution of the μ problem in the NMSSM is very economical and constitutes a testable alternative to other mechanisms that generate the μ term through the same mechanism that generates the soft masses [**16**–**18**] [**19**] [4].

Previous works on λSUSY [**1**] did not try to study the dynamical generation of μ and simply put the μ term by hand in the superpotential. In this thesis we shall address the issue of the dynamical generation of the μ term in λSUSY [**2**], which constitutes an important piece of information to complete the current picture of supersymmetry without a light Higgs boson.

In this thesis we shall discuss analytically the relation between the mass term μ generated thanks to the interaction $\lambda S H_1 \cdot H_2$ and the other mass scales of the model. In particular we shall discuss to what extent the dynamical generation of the μ term through the VEV of the singlet scalar requires the doublets H_1 and H_2 to be mixed with the singlet. Because of the necessity of non-negligible mixing between the doublets and the singlet, we will generalize the analysis of [**1**] including the effects of the mixing where appropriate, as for instance in the EWPT analysis, in the consideration of limits from the direct searches of dark matter, and in the phenomenology at the LHC.

A recent study of the NMSSM in the large λ regime has been performed in Ref. [**21**], where the importance of a dynamical generation of a μ term is not highlighted and a numeric scan of the parameter space allowed by the many experimental constraints is performed. Contrary to Ref. [**21**], we will pursue an analytic approach as much as we can. Moreover the set of constraints that we shall consider will be slightly different with respect to [**21**]. Notably, we shall not require the NMSSM to provide an explanation for the current discrepancy between the experimental value and the SM prediction of the $g-2$ of the muon. Furthermore, we do not impose the thermal production of lightest neutralinos to account for the observed relic dark matter abundance, as we content ourselves to not over-close the Universe with the lightest supersymmetric particle. At variance with [**21**] we shall take into account limits coming from direct dark matter searches through the elastic scattering of a weakly-interacting massive particle on a nucleus.

The rest of this work is organized as follows. In Chapters 2 and 3 we discuss the motivation for electroweak scale supersymmetry and we briefly overview the Higgs sector of the MSSM. In Chapter 3 we also discuss the unification of gauge couplings in the MSSM. Later in Chapter 4 we present the fat Higgs scenario as an example of complete model where the Higgs sector has a strong self-coupling and the pattern of the unification of gauge couplings can resemble very closely that of the MSSM. In

[4] As a matter of fact explicit models of supersymmetry breaking generically have difficulties [**17**] to generate correctly the μ term and special solutions for the generation of μ are needed. In this sense the NMSSM appears more suitable for an economic dynamical generation of μ. Indeed it has already been considered the possibility to generate μ from an NMSSM superpotential with soft masses generated by gauge mediated supersymmetry braking [**20**].

Chapter 5 we resume the studies on λSUSY of Ref. [**1**]. This serves to fix our starting point, to show some of the characteristic features of λSUSY in the more familiar set-up of the two-Higgs-doublets-model and to introduce the notation.

Chapters 6, 7, and 8 are devoted to the exposition of the original work contained in this thesis [**2**, **3**]. In particular Chapter 6 describes how the NMSSM with large λ can dynamically generate the μ mass term for the Higgsinos through the VEV of the singlet S. In Section 6.4 we shall describe how the generation of the μ terms differs from the usual case of perturbative λ and we shall work out the relation between the generated μ and the other mass scales of the theory, in particular with the Higgs mass. Then in Section 6.5 we shall quantify the necessity of tuning the parameters of the model to get a viable phenomenology and we shall obtain limits from Naturalness on the spectrum of the theory. In Chapter 7 we discuss the experimental bounds that the theory has to satisfy. In particular, in Section 7.2 we discuss the limits from LEP direct searches. Then, in Section 7.3 we study the indirect constraints coming from Electroweak Precision Tests. In Sections 7.4 and 7.5 we discuss the relic abundance of the LSP of the model and its detection in current experiments. Finally in Chapter 8 we present our expectation for the phenomenology of λSUSY at the LHC. In Section 8.3 we shall discuss the generic features of the phenomenology of the regimes of λSUSY where the singlet is significantly mixed with the doublets, *i.e.* the regime suggested by the possibility of generating the μ term dynamically. In Section 8.5 we shall present a detailed study of the observability of the distinguishing signatures of λSUSY in the more elusive case of a singlet that does not mix with the doublets. Finally in Chapter 9 we give our conclusions.

CHAPTER 2

Motivation for supersymmetry

2.1. WW scattering and unitarity constraints on m_h

The Fermi theory is a four fermion contact interaction theory which successfully accounts for what in modern language we describe as low energy weak interactions. It is an effective field theory with interaction given by:

$$\mathcal{L}_{int} \sim G_F \bar{\psi}_\mu \psi_{\nu_\mu} \bar{\psi}_e \psi_{\nu_e},$$

and can be used to compute the muon lifetime with very good agreement with measurement. Although low energy physics is beautifully accounted for, the theory cannot be more than "effective". Indeed, the cross section of the two fermions to two fermions scattering processes increase with energy and exceeds unitarity bounds at energy scales around $G_F^{-1/2}$. In the past this has been considered as a signal for the need of a more fundamental description and led to the modern formulation of weak interactions. The W boson has been speculated to be the unitarizer of the four fermions scattering process and then it has been actually observed.

With almost the same script we can introduce the Higgs boson as the unitarizer of the standard model and find constraints on its mass.[1]

After spontaneous symmetry breaking (SSB) has occurred the standard model has massive weak gauge bosons with both transverse and longitudinal polarization. The longitudinal modes are the eaten Goldstone bosons and this make them special probes of the properties of the Higgs. Indeed, the amplitude of the $W_L W_L \to W_L W_L$ scattering is a powerful tool to understand how heavy the standard model Higgs can be [**22**]. To this aim, we focus on

$$\{W_L^+ W_L^-, Z_L^0 Z_L^0, hh\} \to \{W_L^+ W_L^-, Z_L^0 Z_L^0, hh\} \tag{2.1.1}$$

processes. These nine reactions constitute a coupled set of scattering processes among all the degrees of freedom of the Higgs sector[2]. To study unitarity of these processes we decompose each amplitude in partial waves according to $S = 1 + iT$ with

$$T(s,t) = 16\pi \sum_J (2J+1) a_J(s) P_J(\cos\theta) = \sum_J t_J$$

where s and t are the usual Mandelstam variables, J is the angular momentum eigenvalue, P_J are a set of angular momentum eigenfunctions that we use as a basis for the expansion and $a_J(s)$ the partial wave amplitudes. Given that the polarization vector of

[1] One does not need to say how fruitful and effective the introduction of the Higgs boson can be. Indeed it provides Fermi scale masses for the weak gauge boson while preserving massless photons, it breaks undesired global symmetries like the axial baryonic and leptonic number otherwise exact the SM, it provides a mechanism for mass generation of fundamental fermions.

[2] $HZ_L^0 \to HZ_L^0$ is the only missing possibility and, since it is decoupled from the three considered channels, is left out.

the longitudinal gauge bosons can be chosen $\epsilon_L^\mu(k) \sim (|k|, 0, 0, E)/m_{W,Z}$ and given the momentum dependence of the coupling between gauge bosons, one can show that for $k \gg m_W$

$$a_J = A\left(\frac{k}{m_W}\right)^4 + B\left(\frac{k}{m_W}\right)^2 + C\ .$$

The part A of the amplitude depends only on pure gauge diagrams, while B and C feel also the Higgs boson.

Due to the structure of the couplings among gauge bosons in a gauge theory A is vanishing. If the Higgs boson is an elementary scalar coupled as dictated by gauge invariance the amplitude B for the scattering of 4 on-shell gauge bosons vanishes as well. Thus the amplitude of a gauge theory with an elementary scalar does not grows with the energy. This means the theory can be extrapolated to very high energy and still make sense. However the C part of the amplitude, despite being constant w.r.t the energy of the process, is an increasing function of the Higgs mass. For instance

$$a_0\left(W_L^+W_L^- \to W_L^+W_L^-\right) \xrightarrow[s\gg m_h^2]{} -\frac{G_F m_h^2}{4\pi\sqrt{2}}$$

and imposing $\left|a_0\left(W_L^+W_L^- \to W_L^+W_L^-\right)\right| \leq 1$ one finds

$$m_h^2 \leq \frac{4\pi\sqrt{2}}{G_F}\ .$$

Computing the nine amplitudes of Eq. (2.1.1) and taking the $J = 0$ partial wave in the large s limit one finds

$$t_0 \xrightarrow[s\gg {m_h}^2]{} -\frac{G_F m_h^2}{4\pi\sqrt{2}} \begin{pmatrix} 1 & \frac{1}{\sqrt{8}} & \frac{1}{\sqrt{8}} \\ \frac{1}{\sqrt{8}} & \frac{3}{4} & \frac{1}{4} \\ \frac{1}{\sqrt{8}} & \frac{1}{4} & \frac{3}{4} \end{pmatrix}\ . \tag{2.1.2}$$

The tightest bound that one can place comes from the combination of channels $2W_L^-W_L^+ + Z_L^0Z_L^0 + hh$. This combination corresponds to the highest eigenvalue of Eq. (2.1.2), which is $3G_F m_h^2/8\pi\sqrt{2}$ and yields the bound:

$$m_h^2 \leq \frac{8\pi\sqrt{2}}{3G_F} \simeq (1\ \text{TeV})^2\ . \tag{2.1.3}$$

This bound implies that a standard model Higgs boson lighter that 1 TeV is compatible with a perturbation theory description of weak interactions, while a heavier Higgs would be the trace of a strong coupling in the Higgs sector[3].

Broadening the scope of the discussion, we can say that any physics beyond the standard model (BSM) needs a "unitarizer" of the longitudinal gauge bosons scattering and the calculation above suggests that this has to be lighter than about 1 TeV. Therefore, the LHC, colliding protons with 14 TeV center of mass energy, has the potential to asses the nature of the unitarization mechanism. In this respect it is interesting the fact that weak boson fusion (see Fig.2.1.1), which is mainly due to longitudinal bosons, is considered a discovery channel for a heavy enough Higgs boson.

It is worth to notice that other unitarization mechanisms can occur in BSM. These typically rely on new vectorial resonances either coming from an enlarged gauge group

[3]However there are strongly coupled theories where the Higgs is kept light with some mechanism [**23**–**25**].

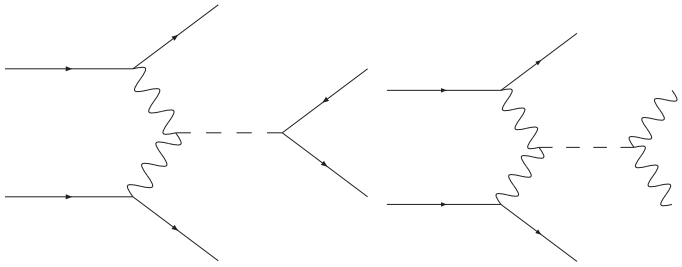

FIGURE 2.1.1. Weak boson fusion diagram for Higgs production and decay into fermions(left) and into vectors(right).

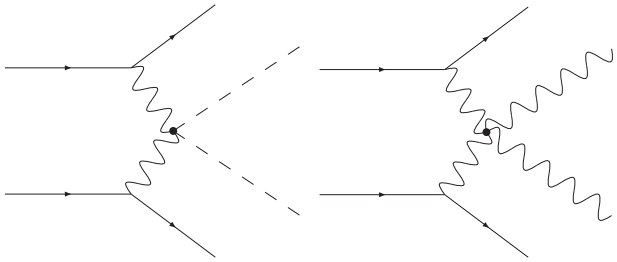

FIGURE 2.1.2. Double Higgs production through gauge boson scattering(left). Double gauge boson production through gauge boson scattering (right).

[**23**, **24**] or as mesons of a strong dynamic [**26**] or from compactification of extra-dimensions [**27**]. These states would be more likely discovered in the direct production followed by the observation of their decay products.

However, one can also find their traces in precise measurement of the Higgs width, couplings, production rate and branching fractions [**25**], that are of more direct relevance to assess the role of these states in the breaking of the electroweak symmetry. Indeed the most direct probe of the role of these states in the electroweak symmetry breaking is the study of the scattering of longitudinal vectors, *i.e.* the energy dependence of weak boson fusion production of $W_L^- W_L^+, Z_L Z_L, hh, f\bar{f}$ (see diagrams in Fig. (2.1.1) and in Fig.2.1.2). As such longitudinal gauge bosons are a key tool to understand the SSB of the gauge symmetry.

2.2. Stability of the running mass of a scalar

We have seen how important is the value of the mass of the Higgs in the standard model. Unfortunately, when one includes quantum corrections to the Higgs mass these bring in a quadratic sensitivity to the UV scale. Precisely this means that if one regularize the divergences with a physical cut-off, *i.e.* we assume that the SM is valid up to the scale Λ, where some new physics enters in the dynamics, then

$$\delta m_h^2 \sim -N_f \frac{y_f^2}{8\pi^2} \left[\Lambda^2 + \ldots\right] \tag{2.2.1}$$

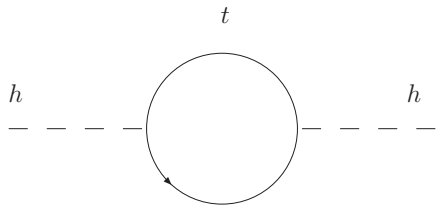

FIGURE 2.2.1. SM contribution to the one-loop Higgs mass.

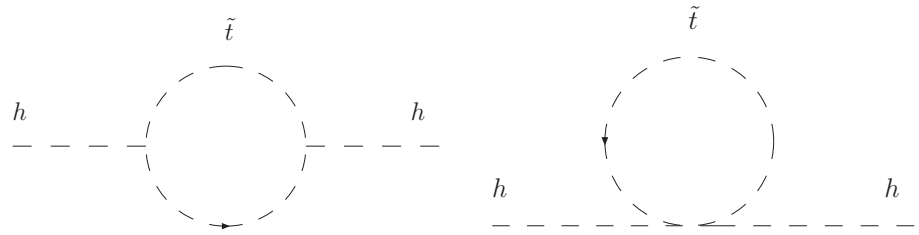

FIGURE 2.2.2. SUSY contribution to the one-loop Higgs mass.

where y_f is the Yukawa coupling of the Higgs with the fermion f, N_f is the number of helicity states of the fermion and the dots stand for less divergent and finite pieces [4]. Eq. (2.2.1) singles out the top loop (see Fig. 2.2.1) as the main contribution.

Taking $\Lambda \sim M_{pl}$ and $m_h^2 \sim (1 \text{ TeV})^2$ means that the "bare mass" and the one-loop contribution must cancel with an accuracy of 10^{-30}. Such need of fine tuning (FT) of the parameters of the theory is a highly unpleasant feature of the quantum corrections to the Higgs mass. On the other hand, when one compute loop corrections to the mass of a fermion one finds corrections of the form

$$\delta m_f \sim m_f^0 \left(1 + c \cdot \log \Lambda\right),$$

where c is a constant, meaning that the mass of the fermion is not sizably affected by physics at the physical cut-off Λ where some new physics starts to modify the SM.

The difference between this "multiplicative" correction to fermion mass and the "additive" correction to the scalar mass can be traced back to the chiral symmetry of the massless Dirac Lagrangian. The point is that the kinetic term $\bar{\psi}\partial_\mu\gamma^\mu\psi$ preserves chirality, while a mass term $\bar{\psi}m\psi$ mixes left and right-handed fermions. Therefore a massless fermion cannot acquire mass radiatively unless chirality is violated. The scalar has no symmetry to protect its mass, that is to say $m_h = 0$ does not enhance the symmetry of the Lagrangian [5]. This is the reason of its sensitivity to UV effects.

Adding N_S scalars $\tilde{t}_{i=1..N_S}$ with trilinear and quadrilinear coupling to the Higgs given by $v\lambda$ and λ, respectively, we have the two new diagrams of Fig. 2.2.2 in the one

[4] Here we concentrate on the loops with fermions of the SM, that are numerically more important than the contributions form the bosons of the SM.

[5] One might object that for $m_h = 0$ the Lagrangian becomes invariant under conformal transformations at the classical level. However the conformal symmetry is broken at the quantum level, therefore we do not consider it as a symmetry to protect the mass of the scalar.

loop mass shift. Precisely

$$\begin{aligned}\delta m_h^2 =& N_f \frac{y_f^2}{8\pi^2}\left[-\Lambda^2 + 6m_f^2 \log\left(\frac{\Lambda}{m_f}\right) - 2m_f^2\right] + \\ &+ \sum_i^{N_S} \frac{\lambda}{16\pi^2}\left[-\Lambda^2 + 2m_{\tilde{t}_i} \log\left(\frac{\Lambda}{m_{\tilde{t}_i}}\right)\right] + \\ &- \frac{\lambda^2 v^2}{16\pi^2}\left[-1 + 2\log\left(\frac{\Lambda}{m_{\tilde{t}_i}}\right)\right] ,\end{aligned} \tag{2.2.2}$$

where we denoted with m_f the mass of the fermion and with $m_{\tilde{f}}$ the mass of the N_S scalars that we introduced.

If we introduce as many scalars as the fermionic degrees of freedom, $N_S = 2N_f$, and set

$$\lambda = -y_f^2 \tag{2.2.3}$$

the Λ^2 term vanishes yielding

$$\delta m_h^2 = \sum_i^{N_F/2} \frac{y_f^2}{4\pi^2}\left[(m_f^2 - m_{\tilde{t}}^2)\log\left(\frac{\Lambda}{m_{\tilde{t}_i}}\right) + 3m_f^2 \log\left(\frac{m_{\tilde{t}_i}}{m_f}\right)\right] . \tag{2.2.4}$$

This can be seen as an accident in the coupling space or as the consequence of a symmetry: supersymmetry (SUSY).

We refer to [**28**, **29**] for an introduction to SUSY and details about the derivation of what follows. We content ourselves with quoting the interesting result that SUSY, being a symmetry between scalars and fermions, forces us to have the same number of fermionic and bosonic degrees of freedom with couplings that in our case must be related through Eq. (2.2.3). In case SUSY is exact one also has

$$m_t = m_{\tilde{t}} , \tag{2.2.5}$$

that puts to zero the one-loop correction to the Higgs mass. However, Eq. (2.2.5) is phenomenologically not acceptable because such scalar partner for every known fermion has not been observed. Thus one has to introduce a violation of the supersymmetric mass relation Eq. (2.2.5), which can potentially yield a large $\delta m_h^2 \sim m_f^2 - m_{\tilde{t}}^2$. If we want to exploit supersymmetry to explain the Fermi scale in a natural way, we are forced to assume $m_f^2 - m_{\tilde{t}}^2 \lesssim (1\text{ TeV})^2$ that is to say "TeV scale SUSY". In this way we can *motivate* SUSY through the requirement of a protection mechanism for the Higgs mass. This relation between the Higgs mass and the scale of supersymmetry puts the LHC in position to discover TeV-scale supersymmetry in the first months of operation at design energy and luminosity.

2.3. Naturalness and scalars

Other kinds of stabilization of the UV sensitivity of the Higgs mass are possible. Instead of reviewing the proposed mechanisms I would like to spend time to recast the problem of the UV sensitivity of the Higgs mass in another way, that allows to understand it more generally.

Indeed our problem with the Higgs boson is a generic problem of the braking of a symmetry with a fundamental scalar. To give masses to electroweak bosons we need this scalar to take vacuum expectation value of the order of the Fermi scale. This in turn

requires that the potential of the scalar has a quadratic negative term of size similar to the VEV. More precisely for a potential

$$V = -\mu^2 h^2 + \lambda h^4 \,,$$

the VEV is $v = \frac{\mu}{\sqrt{2\lambda}}$. Experiments tell that the VEV, and therefore the Fermi scale, is roughly 246 GeV.

The SM with a Higgs boson is a theory in principle valid up to arbitrary high energy. However to generate a VEV of the correct order of magnitude it is necessary to impose a size for the quadratic term of the potential that seems completely unnatural in a quantum field theory. Indeed our computation of Section 2.2 of the loop corrections to the quadratic parameter of the potential shows that it should be as large as the maximal scale up to which the theory is valid. Thus, if we pretend the SM to be valid up to the Planck scale, *i.e.* 10^{19} GeV, we expect a VEV of the same size. The quest for an explanation of the hierarchy between the maximal scale of the SM and the Fermi scale is what we call the hierarchy problem of the SM.

Indeed the hierarchy problem is related to a more general problem of field theories, the problem of the natural generation of mass scales. The general issue and the reasons why the SM with a Higgs boson is problematic can be visualized as follows [**30**].

Imagine to have a theory valid at a scale Λ_{UV}. The theory is defined at the scale Λ_{UV} by a set of parameters p_i. The parameters p_i can be taken to be the coefficients of the operators that appear in the Lagrangian. These coefficients have some value at the scale Λ_{UV} that we denote as $p_{i,UV} \equiv p_i(\Lambda_{UV})$.

We want to study how the theory looks like at a lower energy scale that we call Λ_{IR} . We assume that in a large range of energies $E \gg \Lambda_{IR}$ the theory is very close to be a conformally invariant theory.

Due to the renormalization flow [**31**], the parameters change value as one considers the Lagrangian at a different energy. In the limit of a conformal field theory (CFT) the scaling of the coefficients is given by

$$p_i(E) = p_i(\Lambda_{UV})(\frac{E}{\Lambda_{UV}})^{4-d_i} \,, \tag{2.3.1}$$

where by d_i we denote the dimension of the operator O_i whose coefficient in the Lagrangian is p_i.

The operators with $d_i = 4 - \epsilon \lesssim 4$ are the operators whose coefficients grows when one consider the Lagrangian at scales $E < \Lambda_{UV}$. Given the behavior of their coefficient they are called relevant operators. From eq. (2.3.1) we can derive the scale $\hat{\Lambda}_{IR}$ at which the running coefficient $p_i(E)$ of the relevant operators O_i becomes ~ 1,

$$\hat{\Lambda}_{IR} = p_{i,UV}^{1/\epsilon} \cdot \Lambda_{UV} \,.$$

This shows how the dimensional transmutation behind the renormalization flow of the Lagrangian can generate the scale $\hat{\Lambda}_{IR}$, that is the scale where the phenomena connected to the operator O_i become relevant. For sufficiently small ϵ one can generate a large separation between the scales Λ_{UV} and $\hat{\Lambda}_{IR}$.

In the cases where exist some operator O_k with $4 - d_k \gtrsim 1$ the scaling law eq. (2.3.1) is no longer accurate and one must consider the full renormalization group equations (RGE) of the coefficients p_k. The coefficients p_k of the relevant operators still tend to grow when one consider energies $E < \Lambda_{UV}$ but with a different behavior.

If one wants to generate a large separation between $\hat{\Lambda}_{IR}$ and Λ_{UV} it is necessary to take very small values of the $p_{i,UV}$.

However one can limit the size of the p_i imposing a symmetry on the system that enforces certain p_i to be zero. The size of the $p_i(E)$ will be in this case determined not by the scale Λ_{UV} but by the scale of the symmetry breaking, $\Lambda_{s.b.}$. This is for instance the case of the masses of the quarks that are protected by the chiral symmetry of the QCD Lagrangian.

The SM with the Higgs boson fails to respect the above assumptions as it has operators of dimension 2 in its Lagrangian and it does not encompass any symmetry to protect them. The fact that the SM do not fall in neither of the two categories outlined above renders unclear what is the mechanism that keeps the Fermi scale so small compared to the Planck scale.

This observation motivated extensions of the SM that incorporates some mechanism to generate the value of the Fermi scale.

One such attempt is the supersymmetric extension of the SM. In supersymmetry (SUSY) the coefficients of the operators involving the Higgs boson must be related to those involving fermions. The coefficients of the fermionic operators are in turn controlled by a chiral symmetry analogous to the symmetry that controls the masses of the quarks in QCD. Thus the Fermi scale is generated by the breaking of SUSY, i.e. the symmetry preventing the Higgs mass from becoming very large. This breaking must occur not far from the Fermi scale to not reintroduce an unnatural separation between the Fermi scale and the symmetry breaking scale.

Other solutions to the hierarchy problem exploit the dimensional transmutation mechanism explained above. The paradigm of this class of BSM theories is a model with a strong dynamics characterized by the scale f at which the strong dynamics produces a scalar composite with the quantum numbers of the Higgs boson. The scale f cannot be too large compared to the Fermi scale or a new unexplained hierarchy of scales would appear in the model. The scale f in turn naturally emerges as a consequence of the UV dynamics of the model as explained above in the language of CFT.

The presence of a dynamically generated scale not far from the Fermi scale or the existence of a new symmetry broken around the TeV are motivations to expect new physics in the reach of the LHC. This discovery potential for BSM physics is complementary to the discovery potential expected from the study of the high energy behavior of the scattering of longitudinal W bosons. This is why the LHC is expected to discover the missing pieces of the SM and the *necessary* beyond the standard model physics present at the TeV scale.

CHAPTER 3

Supersymmetric Higgs bosons: a brief overview

3.1. Electroweak precision tests and the prejudice of the light Higgs boson

As of 2010 the Higgs boson has not been observed and therefore all we said in the previous Sections is after all speculative, the Higgs boson could even not be there at all. However there have been attempts to find measurable effects of the Higgs boson in electroweak precision observables (EWPO). Obviously, these analysis should be taken as guide in the direct search for the Higgs more than an attempt to discover it. Figure 3.1.1 reports the EWPO measurements, while Figure 3.1.2 shows the m_h values suggested by a χ^2-fit of the EWPO. These analyses clearly point towards a light Higgs boson with a 2.5σ bound of 144 GeV. However, two comments are in order: this result is valid only in the pure SM (or in case the BSM does not affect these observables); the sensitivity to m_h is only logarithmic, thus small changes in the input parameters of the fit can change significantly the result.

This logarithmic sensitivity deserves a comment, indeed it arises from symmetry features of the SM. In fact, the standard model Higgs potential is symmetric under $SO(4)$ transformations among the the four real components ϕ_i of the complex Higgs doublet Φ. This is because the potential is a function of the invariant $\Phi\Phi^\dagger = \sum_i \phi_i^2$. This symmetry implies that, in absence of hypercharge interactions the gauge boson get all the same mass $m_{W_i}^2 = \frac{1}{2} g_2^2 v$. Taking into account hypercharge and the weak angle mixing necessary to conserve electric charge, one gets the tree level relation

$$\frac{m_W^2}{m_Z^2 \cos^2\theta_W} \equiv \rho = 1 \,, \tag{3.1.1}$$

which can be ascribed to the $SO\left(4\right)$ symmetry. At one-loop, the Yukawa interaction responsible for the top loop vacuum polarization breaks the $SO\left(4\right)$ down to the $SU(2)$ of the weak interactions yielding a correction $\delta\rho \sim m_t^2$ of order 10^{-2}. This sensitivity to m_t^2 allowed to make a rather precise prediction of the top mass. Unfortunately we have no such strong predictive power for m_h. Indeed the $SO(4)$ symmetry forbids any one loop correction to ρ proportional to the Higgs self-coupling $\lambda \sim m_h^2$ and we are left with a milder logarithmic sensitivity $\delta\rho \sim \log m_h$. Despite this mild sensitivity, the huge statistic achieved at LEP severely constrains the vacuum polarization amplitudes of gauge bosons. Thus it is worth to define some phenomenological quantities to parametrize the precision observables and then use them to constrain the Higgs both in SM and in BSM [**32**, **33**]. To this aim we introduce 4 one-loop vacuum polarization amplitudes $\Pi\left(q^2\right)$ through

$$\mathcal{L}_{pheno} = -\frac{1}{2} W_\mu^3 \Pi_{33}\left(q^2\right) W_\mu^3 \; -\frac{1}{2} W_\mu^+ \Pi_{+-}\left(q^2\right) W_\mu^- \; -\frac{1}{2} B_\mu \Pi_{00}\left(q\right)^2 B_\mu \; -\frac{1}{2} B_\mu \Pi_{03}\left(q^2\right) W_\mu^3 \,.$$

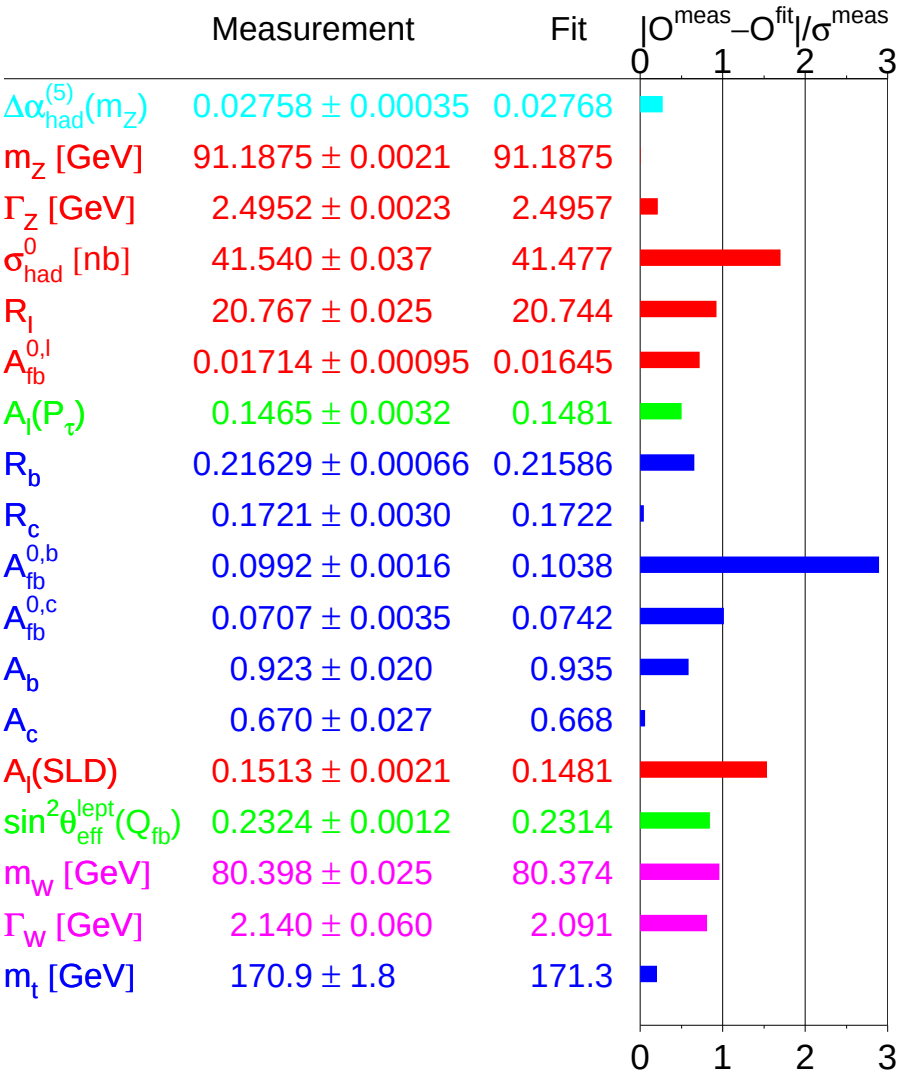

FIGURE 3.1.1. LEP electroweak working group (LEPEWWG) results for precision observables and corresponding χ^2-fit of m_h in the SM [**62**]. All data shown comes from LEP except for m_t from Tevatron, m_W and Γ_W which are a combination of LEP and Tevatron data, and the leptonic average polarization A_l from SLD. A^x_{fb} stands for forward-backward asymmetries in the spatial distribution of x, $A_l(P_\tau)$ is the average τ polarization. R_x is the fraction $\Gamma(Z \to xx)/\Gamma(Z \to$ hadrons), σ^0_{had} is the hadronic cross section at the Z pole, $\Delta\alpha_{had}$ is the shift in the fine-structure constant due to light quarks and photon as measured at the Z pole and $\sin^2\theta_{eff}$ is the weak mixing angle obtained combining several measure in a large range of energies (from atomic scale to Z-pole!).

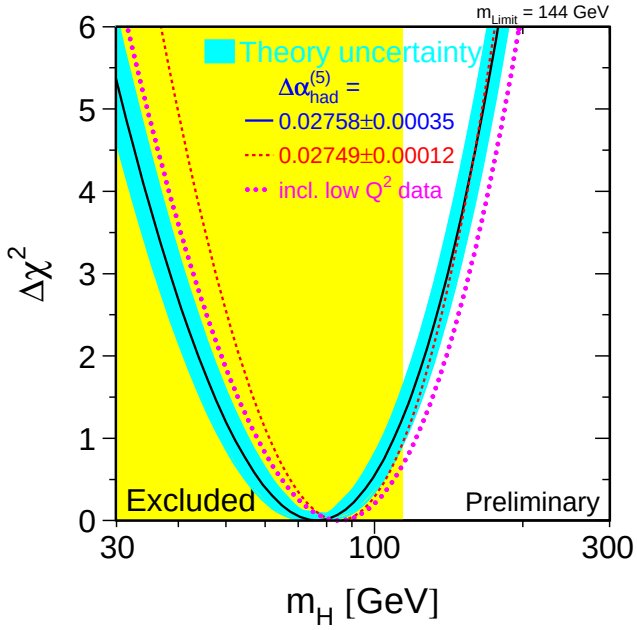

FIGURE 3.1.2. LEP electroweak working group (LEPEWWG) χ^2-fit of m_h in the SM [**62**].

Assuming that the scale at which SM is replaced by some other theory is far enough, we can expand each $\Pi_{xy}(q^2)$ in powers of q^2 around $q^2 = 0$. Dimensional analysis establishes that only $\Pi(0)$ and $\Pi'(0)$ can be sensitive to the growth of m_h. Therefore we have a set of 4 $\Pi(0)$ and 4 $\Pi'(0)$ which feel the value of m_h. Since the Lagrangian has input values g_2, g_1, v and the vanishing mass of the photon requires $\Pi_{\gamma\gamma}(0) = \Pi_{Z\gamma}(0) = 0$, we are left with only three independent quantities.

The three quantities can be chosen as:

$$\hat{S} = \frac{4 s_W c_W}{\alpha_{em}} \Pi'_{30}(0) \ ,$$
$$\hat{T} = \frac{\Pi_{33}(0) - \Pi_{+-}(0)}{m_W^2} \ ,$$
$$\hat{U} = \frac{\Pi'_{33}(0) - \Pi'_{+-}(0)}{m_W^2} \ .$$

The parameters $\hat{T}$ and $\hat{U}$ are responsible for the violation of Eq. (3.1.1). Involving higher derivatives, $\hat{U}$ is numerically smaller than $\hat{T}$ and in the following we shall set it to zero. These two parameters are associated to the breaking of a global $SO(4)$ symmetry, the so-called *custodial* symmetry of the Higgs potential, that implies eq. (3.1.1).

The breaking of the custodial symmetry can be understood in terms of higher-dimensional operators that we can add to the renormalizable interactions of the SM and change the accidental relation eq. (3.1.1). Among the gauge invariant operators

that involve only gauge bosons there is the operator

$$\frac{c_{HH}}{\Lambda^2}\left|H^\dagger D_\mu H\right|^2 ,$$

which after the EWSB generates a splitting between the mass of the W and the Z boson and is in one-to-one correspondence to $\hat{T}$. On the other hand, the parameter $\hat{S}$ is not related to the breaking of the custodial symmetry and is generated by the effective operator

$$\frac{c_{BW}}{\Lambda^2}H^\dagger\sigma^a H\, W^a_{\mu\nu}B_{\mu\nu} ,$$

that after the EWSB produces a kinetic mixing between the B and W_3.

In the SM one can compute $\hat{S}$ and $\hat{T}$ for variable Higgs mass. This can be done using

$$\begin{aligned}\Pi(0) =&\frac{1}{16\pi^2}\left[\frac{m_1^2+m_2^2}{2}-\frac{m_1^2m_2^2}{m_1^2-m_2^2}\ln\frac{m_1}{m_2}\right]\\ \Pi'(0) =&\frac{1}{96\pi^2}\left[-\ln\frac{\Lambda^4}{m_1^2m_2^2}+\frac{4m_1^2m_2^2}{(m_1^2-m_2^2)^2}+\right.\\ &\left.+\frac{m_1^6+m_2^6-3m_1^2m_2^2(m_1^2+m_2^2)}{(m_1^2-m_2^2)^3}\ln\frac{m_1^2}{m_2^2}\right]\end{aligned}$$

for a generic bosonic loop with internal masses m_1 and m_2 and coupling $\imath W_\mu\phi_1\overleftrightarrow{\partial}\phi_2$. In case that one of the particles in the loop is a scalar that takes a VEV, say the Higgs boson, the parameter $\hat{S}$ has an additional contribution stemming from the diagram with a W and a h in the loop:

$$\frac{m_W}{2\pi}\left[\frac{2m_h^2m_W^2}{(m_h^2-m_W^2)^2}\ln\frac{m_h}{m_W}-\frac{m_h^2+m_W^2}{(m_h^2-m_W^2)^2}\right].$$

For a fermionic loop with masses m_1 and m_2 and coupling $W_\mu\bar{\psi}_1\gamma^\mu\psi_2$ one has:

$$\begin{aligned}\Pi(0) =&\frac{1}{16\pi^2}\left[(m_1-m_2)^2\ln\frac{\Lambda^4}{m_1^2m_2^2}-2m_1m_2+\right.\\ &\left.+\frac{2m_1m_2(m_1^2+m_2^2)-m_1^4-m_2^4}{m_1^2-m_2^2}\ln\frac{m_1^2}{m_2^2}\right]\\ \Pi'(0) =&\frac{1}{24\pi^2}\left[-\ln\frac{\Lambda^4}{m_1^2m_2^2}-\frac{m_1m_2(3m_1^2-4m_1m_2+3m_2^2)}{(m_1^2-m_2^2)}+\right.\\ &\left.+\frac{m_1^6+m_2^6-3m_1^2m_2^2(m_1^2+m_2^2)+6m_1^3m_2^3}{(m_1^2-m_2^2)^3}\ln\frac{m_1^2}{m_2^2}\right]\end{aligned}$$

The result is shown in the yellow area of Figure 3.1.3 together with the 1σ ellipse coming from the experimental data. This plot obviously confirms the result of Figure 3.1.2 that the SM Higgs has to be light, but it can also be used in a more model independent way. Indeed, these phenomenological quantities can be computed in any model BSM and every model must be checked against these EWPT. This is of great importance, since until the LHC or the TeVatron will pose significant bounds on the Higgs, the EWPT and other constraints from flavor physics [**34**] are the only significant way to restrict the wide range of possibilities beyond the standard model. In this respect it is important to underline that there is no need to have a light Higgs in BSM. Indeed one can build models with new particles whose contributions to $\hat{S}$ and $\hat{T}$ (almost) balance with the contribution from the heavy Higgs [**35**]. This observation

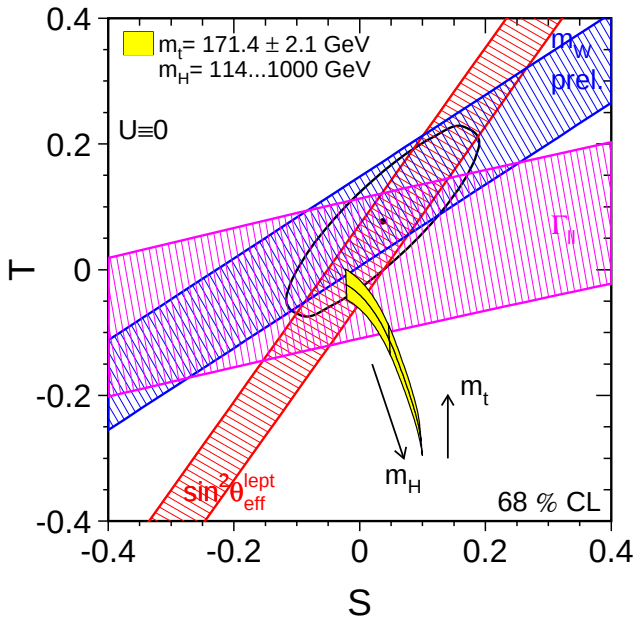

FIGURE 3.1.3. The ellipse shows the experimental determination of $S = 4\sin^2\theta_W/\alpha_{em}\hat{S}$ and $T = \hat{T}/\alpha_{em}$ from the LEPEWWG [**62**]. The yellow area is the SM prediction for variable m_h and m_t. The arrow points the direction in which the result shifts for increasing m_h or m_t.

opens a wide range of possibilities in model building. In particular one can imagine a phenomenology completely different from the SM or other standard scenarios of BSM like the Minimal Supersymmetric Standard Model (MSSM).

3.2. The MSSM

The structure of a supersymmetric theory beyond the gauge interactions can be specified through an analytic function of fields called *superpotential*, $W(\phi)$, and of a non analytic function $K(\phi, \phi^\dagger)$. For sake of brevity we shall not talk about superspace techniques and we shall deal with the these potentials as a tool to formulate a renormalizable Lagrangian theory invariant under SUSY transformations. We refer to [**28**,**36**] for a deeper and more detailed treatment, while here we shall just list some result in terms of component fields.

The superpotential is a function of "*super*-fields" that are multiplets containing the same number of bosonic and fermionic degrees of freedom (DoF). We shall need two kind of superfields: the chiral and the vector superfield. Chiral superfields are those containing a Weyl fermion and a complex scalar. They are the superfields that contains the chiral fermions of the SM and the Higgs boson(s) of the MSSM. Vectorial superfields are those containing massless gauge fields and Weyl fermions that transform in the adjoint of the gauge group. The vector superfields are needed to introduce gauge interactions in a manifestly supersymmetric way.

Given a superpotential $W(\varphi_i)$ function of the chiral superfields φ_i we obtain the resulting interaction Lagrangian terms through:

$$\mathcal{L}_{int}^{W} = |\frac{\delta W}{\delta \varphi_i}|^2 + \psi_j \frac{\delta W}{\delta \varphi_j \delta \varphi_i}\psi_i, \tag{3.2.1}$$

where δ means functional differentiation evaluated in terms of the *sfermion* ϕ, the scalar components of the chiral superfield, and ψ is the corresponding fermion. From Eq. (3.2.1) we conclude that, to get a power-counting renormalizable Lagrangian, the superpotential must have mass-dimension less or equal to 3.

Kinetic terms for the chiral fields can be introduced as well and by the proper "minimal coupling" procedure one can introduce gauge interaction such that eq. (3.2.1) is completed by the necessary gauge-covariant kinetic term for all the introduced fields. These yields the interactions:

$$\mathcal{L}_{int}^{G} = g\sqrt{2}\lambda^a \psi T^a \phi + g\sqrt{2}\lambda^a \psi T^a \phi + g^2(\phi^* T^a \phi)^2, \tag{3.2.2}$$

where λ^a is the gaugino, the fermionic partner belonging to the vector superfield, and the last term comes from the auxiliary fields needed to have a consistent SUSY- and gauge-invariant theory.

Gathering together eqs. (3.2.2) and (3.2.1), the resulting scalar potential is

$$V = \sum_i |\frac{\delta W}{\delta \varphi_i}|^2 + \sum_a g_a^2 (\phi^* T^a \phi)^2 \,, \tag{3.2.3}$$

where the first term comes from the superpotential and is know as F-term, while the second term comes from gauge interactions and is known as D-term.

All this shows that, once one specifies the gauge group and the representations of the fields, the only freedom in building a SUSY model lies in the choice of the superpotential. The Minimal Supersymmetric Standard Model is specified by:

$$W_{MSSM} = \hat{u}\mathbf{y}_u \hat{Q} \cdot \hat{H}_u + \hat{\bar{d}}\mathbf{y}_d \hat{Q} \cdot \hat{H}_d + \hat{e}\mathbf{y}_e \hat{L} \cdot \hat{H}_d + \mu \hat{H}_u \cdot \hat{H}_d,$$

where y are the dimension-less Yukawa couplings, μ is a parameter of the model with the dimensions of a mass and the hat on top of the fields denotes that they are superfields.

First of all we note that there are two Higgs doublets. The reason is twofold. First, we cannot use H_u^*, as happens in the SM, because W has to be analytic. Thus, if we want to have Yukawa interactions for down-type fermions, we need a H_d. Second, the introduction of one single Higgs superfield would add a fermion to matter content of the SM, spoiling anomaly cancellation. Therefore, one can introduce a second doublet with opposite hypercharge, such that the fermions in $\hat{H}_u$ and $\hat{H}_d$ form a vector-like representation of the gauge group that give a net zero contribution to the anomaly.

The final phenomenological Lagrangian of the MSSM must take into account the breaking of SUSY. This breaking is needed to explain why we did not observe scalar partners of the SM fermions. However, we do not want to spoil the reason for introducing SUSY, that is we do not want to reintroduce quadratic divergences in the mass of the Higgs eqs. ((2.2.1)) and (2.2.2)). This requires in particular that one does not alter the relation eq. (2.2.3) between Yukawa and scalar self-couplings. The two involved couplings are dimensionless parameters, as such their RGE is not changed by the introduction of relevant operators that break supersymmetry, *i.e.* a soft breaking of SUSY. The general form of such a breaking has been studied in Ref. [**37**] and for the MSSM the soft Lagrangian terms are:

$$\begin{aligned}\mathcal{L}_{soft} = &-\frac{1}{2}(M_3\tilde{g}\tilde{g} + M_2\tilde{W}\tilde{W} + M_1\tilde{B}\tilde{B} + h.c.)+ \\ &+ \tilde{Q}^\dagger m_{\tilde{Q}}^2\tilde{Q} + \tilde{L}^\dagger m_{\tilde{L}}^2\tilde{L} + \tilde{\bar{u}}^\dagger m_{\tilde{\bar{u}}}^2\tilde{\bar{u}} + \tilde{\bar{d}}^\dagger m_{\tilde{\bar{d}}}^2\tilde{\bar{d}} + \tilde{\bar{e}}^\dagger m_{\tilde{\bar{e}}}^2\tilde{\bar{e}} \\ &- (\tilde{\bar{u}}\mathbf{a}_u\tilde{Q}\cdot H_u - \tilde{\bar{d}}\mathbf{a}_d\tilde{Q}\cdot H_d - \tilde{\bar{e}}\mathbf{a}_e\tilde{L}\cdot H_d + h.c.)+ \\ &- m_u^2|H_u|^2 - m_d^2|H_d|^2 - B\mu(H_u\cdot H_d + h.c.),\end{aligned} \tag{3.2.4}$$

where tilde denotes partners of the SM particle.

3.3. Gauge coupling unification in the MSSM

The supersymmetric extension of the standard model to the MSSM brings new fields charged under the gauge group of the SM, thus affecting the value of the beta function of the gauge couplings. Indeed the evolution of the gauge couplings of the SM is determined at one loop level by the RGE equations

$$\frac{dg_i}{dt} = \frac{b_i}{16\pi^2}g_i^3\,, \tag{3.3.1}$$

where $t = \log\frac{Q}{Q_0}$ and the coefficients b_i depends on the content of fields charged under the gauge group.

A generic expression for the b_i of a supersymmetric model with arbitrary content of fermions F, scalars S, and gauge group G is:

$$b_i = -\left(\frac{11}{3}C_2(G) - \frac{4}{3}\kappa_F S_2(S) - \kappa_S\frac{1}{6}S_2(F)\right)\,,$$

where the $C_2(r)$ are the Casimir for the representation r, i.e. for the generators $t^{(r)}$

$$(t^{(r)}t^{(r)})_{ij} = C_2(r)\delta_{ij}\,,\quad S_2(r) = \frac{\dim(R)}{\dim(G)}C_2(r)\,,$$

$\kappa_F = \frac{1}{2}$ for a single Weyl fermion and $\kappa_S = 1$ for a real scalar or $\kappa_S = 2$ for a complex scalar, *i.e.* a complete chiral superfield corresponds to $\kappa_F = \frac{1}{2}$, $\kappa_S = 2$.

In the MSSM the coefficients b_i are $b_1 = 33/5$, $b_2 = 1$, $b_3 = 3$ where we have chosen a GUT normalization of the hypercharge $g_1 = \sqrt{5/3}\frac{e}{\cos\theta_W}$. The RGE can be recast in the form

$$\frac{d}{dt}\alpha_i^{-1} = -\frac{b_i}{2\pi}\,,$$

and inserting the coefficients b_i for the MSSM the resulting evolution of the gauge couplings at energies above the Fermi scale is shown in figure 3.3.1. The figure shows that the matter content of the MSSM is suitable to have unification of the gauge couplings within a significant accuracy. This accuracy can be quantified assuming that the gauge couplings unifies at the scale of grand unification and running the coupling α_3 to the scale of the mass of the Z boson, where it has been determined with a precision of about 6×10^{-3}. Depending on the details of the MSSM spectrum assumed, the measured value of $\alpha_3(m_Z) = 0.1184 \pm 0.0007$ [**38**] is compatible within roughly 1-σ with the one-loop prediction [1].

[1] A proper prediction of the low energy value of α_3 with uncertainties compatible with the experimental measure requires the integration of the RGE from the GUT scale to m_Z, including two-loops effects and a proper matching at the thresholds of the heavy particles of the theory [**39**]. For a thorough discussion of these effects we refer to Refs. [**40**].

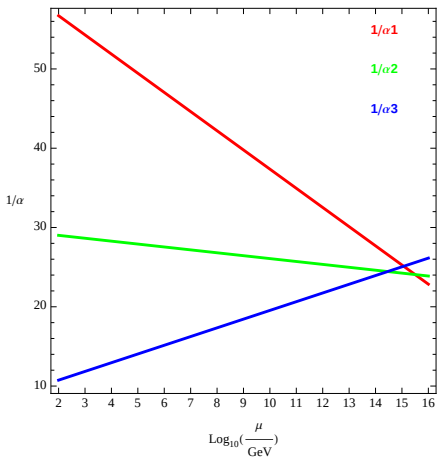

FIGURE 3.3.1. MSSM evolution of the gauge couplings at the scale μ from the experimental values at m_Z.

3.4. Tree-level Higgs mass of the MSSM

From eqs. (3.2.3) and (3.2.4) we can compute the scalar potential. We introduce the shorthand notation for the fundamental parameters $m^2_{1,2} = m^2_{u,d} + |\mu|^2$ and $m^2_3 = B\mu$ and decompose the Higgs doublets in weak-isospin components

$$H_u = \left(H_u^+, H_u^0\right)^t ,$$

and similarly for H_d. The potential reads:

$$V = m_1^2(|H_d^0|^2 + |H_d^-|^2) + m_2^2(|H_u^0|^2 + |H_u^+|^2) - m_3^2(H_u^+ H_d^- - H_2^0 H_1^0 + h.c.) + \\ + \frac{g_2^2 + g_1^2}{8}(|H_d^0|^2 + |H_d^-|^2 - |H_u^0|^2 + |H_u^+|^2)^2 + \frac{g_2^2}{2}|H_d^{-*} H_d^0 + H_u^{0*} H_u^+|^2 .$$

All the three m_i^2 can be taken real exploiting the re-phasing freedom on the fields. Furthermore one can see that the stable minima with broken $SU(2) \times U(1)$ automatically preserve the electric charge and CP [**41**].

Now we can exploit the gauge freedom and parametrize the fields around the ground state as

$$H_u = (H^+, v_u + \frac{h_u + \imath P_2}{\sqrt{2}}), \quad H_d = (v_d + \frac{h_d + \imath P_1}{\sqrt{2}}, 0) ,$$

and compute the Higgs sector spectrum. Since CP is conserved we can deal with the CP-odd and the CP-even states separately. This amount to compute the appropriate matrices of second derivatives evaluated at the ground state (GS):

$$M^\phi_{ij} = \frac{\partial V}{\partial\phi_j \partial\phi_i}, \qquad \phi = (P_1, P_2) \quad \text{or} \quad (h_u, h_d)$$

When $\phi = (P_1, P_2)$ we have a massless eigenstate that is one of the three Goldstone bosons we owe to gauge-invariance, and a massive pseudo-scalar, A, with mass

$$m_A^2 = -\frac{2m_3^2}{\sin 2\beta},$$

where we used the customary definition $\tan\beta = v_u/v_d$.

When $\phi = (h_u, h_d)$ the mass matrix in interaction basis is diagonalized by a rotation of angle α defined by

$$\tan\alpha = \frac{(m_A^2 - m_Z^2)\cos 2\beta + \sqrt{(m_A^2+m_Z^2)^2 - 4m_A^2 m_Z^2\cos^2 2\beta}}{(m_A^2+m_Z^2)\sin 2\beta}\,. \tag{3.4.1}$$

The resulting eigenstates are

$$h = -h_d^0\sin\alpha + h_u^0\cos\alpha, \quad H = h_u^0\sin\alpha + h_d^0\cos\alpha\,, \tag{3.4.2}$$

and the masses are

$$m_{h,H}^2 = \frac{1}{2}\left(m_A^2 + m_Z^2 \mp \sqrt{(m_A^2+m_Z^2)^2 - 4m_A^2 m_Z^2\cos^2 2\beta}\right), \tag{3.4.3}$$

where we have used $m_Z^2 = \frac{1}{2}(g_1^2+g_2^2)(v_u^2+v_d^2)$. From Eq. (3.4.3) one can find the *tree level* mass ordering

$$m_h < m_Z|\cos 2\beta| < m_Z < m_H. \tag{3.4.4}$$

3.5. Radiative corrections to m_h in the MSSM

Eq. (3.4.4) does not mean that the MSSM Higgs boson had to be observed at LEP, since the Higgs mass m_h get significantly corrected when one includes one-loop corrections. The reason is that the scalar potential at tree level does not contain all the terms allowed by gauge symmetry in the most general two Higgs doublets model (2HDM) potential. The supersymmetric structure results in the accidental vanishing of some terms that receive their leading contribution at one loop level. Such correction to the potential are controlled by the supersymmetry breaking parameters, *i.e.* the soft masses, and can be found from the zero of the inverse propagator computed from the one-loop effective action [**42**]. Precisely, the effective action Γ generates the n-point functions for one-particle-irreducible diagrams through n functional differentiations:

$$\frac{\delta\Gamma(\phi)}{\delta\phi^n}|_{\phi=0} = \Gamma^{(n)}.$$

As such, the Fourier transform of $\Gamma^{(2)}$, $\tilde{\Gamma}^{(2)}$, is the inverse propagator of the field. Thus one can define the mass of the particle as the p^2 value that satisfies

$$\tilde{\Gamma}^{(2)}(p) = p^2 - m^2 + \Sigma(p^2) = 0 \quad ,$$

where Σ denotes one-loop self-energy of the particle.

That is to say $m_{phys}^2 = m^2 - \Sigma(m_{phys}^2) = -\tilde{\Gamma}^{(2)}(0) - \Sigma(m_{phys}^2) + \Sigma(0)$. Expanding the effective action in powers on the derivative operator one sees that $\Gamma(\phi) = -V(\phi) + \mathrm{derivatives}$, which yields

$$m_{phys}^2 = \frac{\partial V}{\partial\phi\partial\phi} - \Sigma(m_{phys}^2) + \Sigma(0)$$

In the case of a light particle this formula gets simpler. In fact, denoting the mass of the particle in the loop as m_{loop} and taking $m_{phys}^2 \ll 4m_{loop}^2$, the self-energy amplitude $\Sigma(m_{phys}^2)$ is never resonant, thus one can assume $\Sigma(m_{phys}^2) \simeq \Sigma(0)$. This result allows us to compute the physical mass of the lightest Higgs boson just diagonalizing the proper second derivative matrix of a one-loop corrected potential. This is the effective potential of the Coleman-Weinberg formalism.

Softly broken supersymmetry does not have quadratic divergences, therefore the effective potential induces only a field-dependent logarithmic shift on the classical potential:

$$\frac{1}{64\pi^2}\mathrm{Str}\mathcal{M}^4(\log\frac{\mathcal{M}^2}{Q^2}-\frac{3}{2}) \tag{3.5.1}$$

where $\mathrm{Str}f(\mathcal{M}^2)=\sum_i(-1)^{2J_i}(2J_i+1)f(m_i^2)$, J_i is the spin of the i-th particle in the sum and m_i^2 is the i-th eigenvalue of the field-dependent mass matrix $\mathcal{M}^2$.

An interesting limiting case is suggested by current experimental data. We ignore stop mixing and taking $m_{\tilde{t}}\gg m_Z$ we compute the field dependent masses from the leading terms only:

$$\mathcal{L}\supset\bar{\psi}_t h_u\psi y_t+\frac{1}{2}y_t^2(h_u\tilde{t})^2+\frac{1}{2}\tilde{t}m_{\tilde{t}}^2\tilde{t}$$

We find $m_t^2(h_u)=y_t^2h_u^2$ and $m_{\tilde{t}}^2(h_u)=y_t^2h_u^2+m_{\tilde{t}}^2$. This in turn can be plugged in Eq. (3.5.1) yielding

$$\Delta V=\frac{1}{32\pi^2}[m_{\tilde{t}}^4(\log\frac{m_{\tilde{t}}^2}{Q^2}-\frac{3}{2})-m_t^4(\log\frac{m_t^2}{Q^2}-\frac{3}{2})]$$

Adding this shift to the classical potential we can look for the new minimum condition and compute the new value of the second derivative evaluated at this new minimum. This amounts to find the one-loop corrected physical mass of the Higgs. The minimization condition now reads:

$$\frac{\partial(V+\Delta V)}{\partial h_u}=\frac{\partial V}{\partial h_u}+\frac{1}{16\pi^2}\frac{\partial m_t^2(h_u)}{\partial h_u}[m_{\tilde{t}}^2(\log\frac{m_{\tilde{t}}^2}{Q^2}-1)-m_t^2(\log\frac{m_t^2}{Q^2}-1)]=0$$

where we exploited $\partial m_t^2(h_u)/\partial h_u=\partial m_{\tilde{t}}^2(h_u)/\partial h_u$ (again barring sub-leading D-term). Choosing the appropriate $Q=\hat{Q}$ one can set the square bracket to zero and keep the tree level minimum condition $\partial V/\partial h_u=0$. Once this scale choice is made also the second derivative is simpler, at the ground state it reads:

$$\begin{aligned}\frac{1}{2}\frac{\partial^2(V+\Delta V)}{\partial h_u^2}|_{h_u=v_u}&=\frac{1}{2}\frac{\partial^2 V}{\partial h_u^2}|_{\phi=v_u}+\frac{1}{32\pi^2}\left(\frac{\partial m_t^2(h_u)}{\partial h_u}\right)^2\log\left(\frac{m_{\tilde{t}}^2}{\hat{Q}^2}\right)\Bigg|_{\phi=v}\\&=\frac{1}{2}\frac{\partial^2 V}{\partial h_u^2}|_{h_u=v_u}+\frac{g_2^2}{32\pi^2}\frac{m_t^4}{m_W^2}\log\left(\frac{m_{\tilde{t}}^4}{m_t^4}\right)\end{aligned} \tag{3.5.2}$$

where $m_W^2=\frac{1}{2}g_2^2v^2$ has been used in the last line. We see from the last line that the physical Higgs boson mass has a potentially large contribution from the breaking of supersymmetry. Indeed this contribution is crucial to make the MSSM compatible with the null results of LEP Higgs boson searches.

However, the lift induced by the radiative corrections cannot be too large, because a large scale for the soft masses would reintroduce an unwanted and unexplained hierarchy in the model.

Limiting the stop mass to 2 TeV yields an upper bound $m_h\lesssim 140$ GeV for $m_t=175$ GeV. This means the Higgs boson of the MSSM is only slightly heavier than the Z_0, thus the lore of the *light* Higgs of the MSSM. The lightness of the Higgs boson is apparent from Figure 3.5.1, which shows the one-loop Higgs mass in the MSSM as function of $\tan\beta$ and the scale of the soft masses Δ_S, that for our purposes corresponds to the mass of the stop.

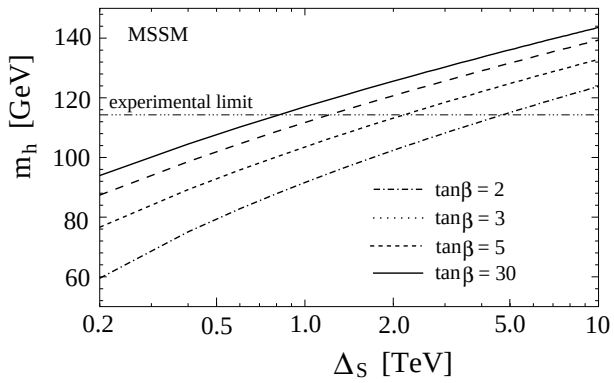

FIGURE 3.5.1. One-loop Higgs mass in the MSSM as function of $\tan\beta$ and the scale of the soft masses Δ_S.

3.5.1. An effective derivation of the loop corrected Higgs mass. The loop corrected Higgs boson mass eq.(3.5.2) can be computed alternatively in the language of effective field theory [**43**]. This derivation allows to quickly estimate the correction from the loops and gives some further insight on the origin of the shift in the Higgs mass.

One can imagine that the spectrum of supersymmetric particles is heavy with respect to m_Z and sufficiently compressed to consider the sparticles as degenerate. Denoting as m_{SUSY} the common mass of the sparticles one can describe physics above the mass scale m_{SUSY} as if supersymmetry were exact, while below m_{SUSY} we can assume that the correct effective field theory is just the SM.

With this set-up in mind we can approximate the mass eigenstates and the mixing angle α taking $m_A \gg m_Z$ in equation (3.4.2) and eq. (3.4.1), i.e.

$$h = \sin\beta\, h_u^0 + \cos\beta\, h_d^0\,.$$

The Higgs boson renormalization group improved effective potential is

$$V_h = -\frac{1}{2}\mu(t)^2 h^2 + \frac{\lambda(t)}{4}h^4,$$

where $t = \log(h/m_{SUSY})$. At the leading order the potential is minimized requiring that

$$\left.\frac{\partial V}{\partial h}\right|_{h=v} = 0$$

and the resulting Higgs mass is then

$$m_h = \left. v\lambda\right|_{h=v}\,.$$

The structure of the MSSM enforces a boundary condition for the quartic coupling

$$\lambda = \frac{1}{8}(g_2^2 + g_1^2)\cos^2 2\beta\,.$$

Starting from this boundary condition at the scale m_{SUSY} we can run the quartic coupling according to the RGE of the SM quartic

$$\frac{d\lambda}{dt} = \frac{1}{16\pi^2}\left(-6y_t^4 + 12\lambda y_t^2 + \frac{3}{8}\left(2g_2^4 + \left(g_1^2+g_2^2\right)^2\right) - 3\left(g_1^2+3g_2^2\right)\lambda + 24\lambda^4\right)\,,$$

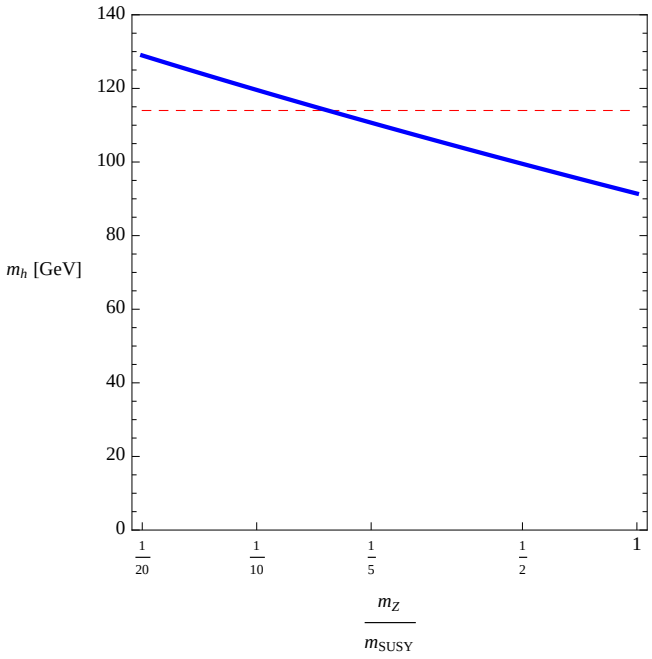

FIGURE 3.5.2. One-loop Higgs mass in the MSSM.

supplemented with the eq. (3.3.1) for the running gauge couplings and the RGE of top Yukawa coupling

$$\frac{dy_t}{dt} = \frac{1}{16\pi^2}\left(\frac{9}{2}y_t^2 - 8g_3^2 - \frac{17g_1^2}{12} - \frac{9g_2^2}{4}\right) .$$

The resulting mass of the Higgs is given in figure 3.5.2 as a function of the ratio m_Z/m_{SUSY}. From this result it is clear that a separation of at least a factor ~ 5 is necessary to increase the mass of the Higgs above the LEP bound.

3.6. How to raise the mass of the Higgs boson is supersymmetric theories

The strict tree-level bound of eq. (3.4.4) and the missed observation of a Higgs boson at LEP triggered several attempts to raise the mass of the Higgs boson. Besides the effect of loops from the MSSM matter sector that we already discussed in Section 3.5 several other mechanism have been proposed and this Section will be devoted to a brief review of these mechanisms.

The simplest possibility to raise the Higgs boson mass is to pursue the solution of loop corrections and try to augment the effect discussed in Section 3.5. The increase of the Higgs mass that can be obtained in this way is sensitive to the effective mass of the sector that is coupled to Higgs boson. Indeed in the case considered in Section 3.5 the most important effect arose from the stop squark and the size of the effect was controlled by $m_{\tilde{t}}$.

As such we can try to couple new matter to the Higgs boson and take this matter as heavy as possible to have a large effect on the mass of the Higgs. To not induce large effects on the EWPT this heavy matter is forced to be in a real representation of the SM gauge group. In this way they can have large gauge invariant mass terms that

only mildly affect the precision measurements. This solution however do not yield a large increase of the Higgs mass and therefore we prefer to not give any further detail on it. For a recent and extensive discussion on this possibility see Ref. [**44**].

In general the mass of the Higgs boson can be augmented adding new sources of quartic coupling in the potential. Due to the supersymmetric origin of the potential we shall differentiate two possible sources for the new quartic: the D-terms and the F-terms. The former are present in models with an extended gauge group with respect to the SM group and the latter are a consequence of the choice of the superpotential.

3.6.1. Tree-level mass induced by non-decoupling effects from abelian D-terms. In models with extended gauge symmetry it is possible to increase the mass of the Higgs boson through the new D-terms that must appear in the scalar potential due to the supersymmetric structure of the model. An extra $U(1)$ factor will suffice to explain the mechanism [**45**].

Let us consider a model with a new $U(1)_x$ gauge symmetry and a superpotential

$$W = \lambda N(\phi\phi^C - w^2)\,. \tag{3.6.1}$$

The charges of the MSSM matter under this new group are $Y + (B-L)/2$. The new matter fields N and ϕ, ϕ^C are SM singlets and under the new $U(1)$ they have charge 0 and $q, -q$ respectively. The soft Lagrangian for the scalar degrees of freedom is

$$\mathcal{L}_{soft} = -m_\phi^2\left(|\phi|^2 + \left|\phi^C\right|^2\right) - m_N^2 N^2 + (B_s\phi\phi^C + h.c.) \tag{3.6.2}$$

and the scalar potential has F-term contributions

$$V_F = \lambda^2\,|\phi|^2\left|\phi^C\right|^2 - \lambda w^2(\phi\phi^C + h.c.) + \lambda^2\left(|N\phi^C|^2 + |N\phi|^2\right)\,. \tag{3.6.3}$$

The D-term contributions from the new $U(1)$ factor is

$$V_{D_x} = \frac{1}{2}g_x^2\left(\frac{1}{2}\,|H_u|^2 - \frac{1}{2}\,|H_d|^2 + q\,|\phi|^2 - q\left|\phi^C\right|^2\right)^2\,. \tag{3.6.4}$$

Assuming that N is not taking a VEV the quadratic part of the potential for ϕ and ϕ^C is

$$V_2 = m_\phi^2\left(|\phi|^2 + \left|\phi^C\right|^2\right) - (B_s + \lambda w^2)(\phi\phi^C + h.c.). \tag{3.6.5}$$

When the following condition holds

$$m^2 < B_s + \lambda w^2\,, \tag{3.6.6}$$

the origin of the ϕ, ϕ^C field space is not stable and the fields ϕ and ϕ^C develop a VEV

$$\langle\phi\rangle^2 = \left\langle\phi^C\right\rangle^2 = \frac{B_s + \lambda w^2 - m_\phi^2}{\lambda^2}\,. \tag{3.6.7}$$

After this spontaneous breaking of the new $U(1)$, its vector boson will acquire a mass $m_{Z'} = g_x\,\langle\phi\rangle$. Also the scalars ϕ and ϕ^C get a mass from the breaking of the symmetry and for $B \gg v$ they become heavy degrees of freedom with respect to the SM states. This fact allow us to make an effective field theory where the states ϕ and ϕ^C do not propagate and can be integrated out. This results in a shift in the quartic of the light states H_u and H_d from the new $U(1)$ interaction

$$\frac{g_x^2}{2}\left(\frac{1}{2}\,|H_u|^2 - \frac{1}{2}\,|H_d|^2\right)^2 \times \left(\frac{2m_\phi^2}{2m_\phi^2 + m_{Z'}^2}\right)\,. \tag{3.6.8}$$

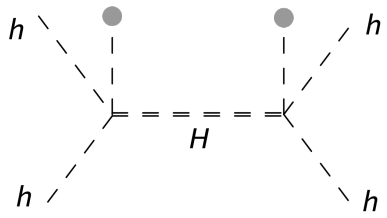

FIGURE 3.6.1. Diagrams originating from the interactions contained in the new D-terms, which contribute to the quartic of the light Higgs boson h after that the heavy state H has been integrated out.

This new quartic can be used to raise the mass of the Higgs boson, however there are several limitations on the size of this new contribution. The maximal shift of the quartic corresponds to $m_{Z'}/m_\phi \to 0$. This situation cannot be realized taking a vanishing $m_{Z'}$ because this is strongly constrained by direct and indirect limits on new vector bosons. Thus we must take $m_{Z'}$ at least a few TeV and a soft mass m_ϕ large compared to $m_{Z'}$, say tens of TeV. This solution would be phenomenologically viable but not very satisfactory. Indeed this large soft mass of the order of tens of TeV would induce a tuning. This tuning can be quantified by mean of

$$\Delta \equiv \left| \frac{\partial \log m_{Z'}^2}{\partial \log m_\phi^2} \right| = \frac{m_\phi^2}{B_s + \lambda w^2 - m_\phi^2} \,. \tag{3.6.9}$$

The relation between this tuning and the achievable Higgs boson mass is made apparent observing that

$$\frac{m_{Z'}^2}{2m_\phi^2} = g_x^2 \frac{B_s + \lambda w^2 - m_\phi^2}{2\lambda^2 m_\phi^2} = \frac{g_x^2}{2\lambda\Delta}. \tag{3.6.10}$$

This in turn allows to express the new upper bound on the mass of the Higgs in terms of the tuning

$$m_h \leq m_Z^2 + \frac{g_x^2 v^2}{2} \frac{1}{1 + \frac{g_x^2}{2\lambda^2\Delta}} \,, \tag{3.6.11}$$

which shows that the model need to be tuned to have a shift of the mass of the Higgs. This relation between the Higgs boson mass and the tuning of the model is rather generic of models which exploit the non-decoupling of D-terms from an extended gauge sector. Indeed in this kind of models there are are two clashing requirements, the decoupling of the effects of the broken gauge dynamics and the effect of the same dynamics on the quartic. In the following section we give an example of non-abelian extension to make the point more general.

3.6.2. Tree-level mass induced by non-decoupling effects from non-abelian D-terms. We take a model with two $SU(2)$ gauge groups $SU(2)_A$ and $SU(2)_B$ which are broken to the diagonal subgroup $SU(2)_{A+B}$ by the VEV of a bi-doublet field $\Sigma \sim (2_A, 2_B)$. The unbroken combination of these two $SU(2)$ factors is identified with the gauge group of the SM, which at this stage has massless vector bosons W_i. The orthogonal combination is the broken $SU(2)$ associated to a heavy triplet of vectors

X_i. The expression of the SM gauge coupling g_2 in terms of the coupling g_A and g_B is

$$\frac{1}{g_2^2} = \frac{1}{g_A^2} + \frac{1}{g_B^2}\,, \tag{3.6.12}$$

as it can be found by writing explicitly the covariant derivatives and then going in the mass basis. In the same way one can see that the heavy mass eigenstates are present in the interaction eigenstates in a fraction controlled by g_A/g_B. For later convenience we define the angle ϕ such that

$$\cos\phi = g_2/g_B\,, \quad \sin\phi = g_2/g_A. \tag{3.6.13}$$

In a fashion similar to the $U(1)$ example we take the superpotential

$$W = \frac{1}{2}\lambda N(\Sigma\cdot\Sigma - w^2) \tag{3.6.14}$$

where N is a singlet of $SU(2)_A \times SU(2)_B$ and $\Sigma\cdot\Sigma = Tr(\Sigma\epsilon\Sigma^t\epsilon)$. This yields the F-terms contribution to the superpotential

$$V_F = \frac{1}{4}\lambda|\Sigma\cdot\Sigma|^2 + \lambda w^2(\Sigma\cdot\Sigma + h.c.) \tag{3.6.15}$$

plus terms containing the singlet. From the gauge structure we have the D-terms contribution to the potential

$$V_D = \frac{g_A^2}{8}\left(Tr\left(\Sigma^\dagger\sigma^a\Sigma\right) + H_u^\dagger\sigma_a H_u - H_d^\dagger\sigma_a H_d\right)^2 + \frac{g_B^2}{8}\left(Tr\left(\Sigma^\dagger\sigma^a\Sigma\right)\right)^2\,. \tag{3.6.16}$$

The relevant soft terms for the fields that we added with respect to the MSSM are

$$\mathcal{L}_{soft} = -m_\Sigma^2|\Sigma|^2 + B_s(\Sigma\cdot\Sigma + h.c.)\,. \tag{3.6.17}$$

The origin of the field space $\Sigma = 0$ is not stable when holds the condition

$$B_s + \lambda w^2 > m_\Sigma\,. \tag{3.6.18}$$

In this case the field Σ develops a VEV

$$\langle\Sigma\rangle = u\mathbf{1} \tag{3.6.19}$$

where

$$u^2 = (B_s + \lambda w^2 - m_\Sigma^2)/\lambda^2\,. \tag{3.6.20}$$

This VEV leaves unbroken the diagonal combination of $SU(2)_A$ and $SU(2)_B$. Furthermore, when $u^2 \simeq \frac{\omega^2}{\lambda}$ the potential at the VEV is vanishing, that is to say supersymmetry is restored when $m_\Sigma, B_s \ll \lambda\omega^2$.

As seen in the case of the $U(1)$ extension the VEV of Σ gives mass to some component of Σ itself and we can make an effective field theory below the mass of these states. The quartic coupling of the Higgs boson in this effective theory is lifted by the effect of the analogous of the diagrams of figure 3.6.1 . The resulting upper bound for the mass of the Higgs is

$$m_h^2 < \frac{v^2}{2}(g_1^2 + \eta g_2^2)\,, \tag{3.6.21}$$

where

$$\eta = \frac{1 + \frac{\delta}{g_2^2}\cos^2\phi}{1 + \frac{\delta}{g_2^2}\sin^2\phi\cos^2\phi} \tag{3.6.22}$$

with $\delta = 2m_\Sigma^2/u^2$. From these expressions is clear that $\eta = 1$ corresponds to the usual MSSM case and that to increase the mass of the Higgs we have to take η as large as possible. To achieve this goal we need some degree of tuning. Indeed we can quantify the tuning of the VEV u with respected to m_Σ and find

$$\Delta \equiv \left| \frac{\partial \log u^2}{\partial \log m_\Sigma^2} \right| = \frac{m_\Sigma^2}{\lambda^2 u^2} = \frac{\delta}{2\lambda^2} \,. \tag{3.6.23}$$

This allows us to express η, and thus the limit on the mass of the Higgs, in terms of the tuning

$$\eta = \frac{1 + \frac{2\lambda^2\Delta}{g_2^2} \cos^2\phi}{1 + \frac{2\lambda^2\Delta}{g_2^2} \sin^2\phi \cos^2\phi} \tag{3.6.24}$$

When $\lambda^2\Delta$ is small compared to g_2^2 the factor η grows linearly with Δ and for infinite tuning it reaches the value $1/\sin^2\phi$. Thus we see that, as in the abelian case, to increase the mass of the Higgs boson we have to accept some tuning. However for $\Delta \sim 10/\lambda^2$ we can obtain significant shift such that $m_h \simeq \text{few } m_Z$. The precise value of the mass of the Higgs boson that can be reached depends on the parameter ϕ which is in turns subject to several limitations.

Firstly the parameter ϕ cannot be 0 nor $\frac{\pi}{2}$ because this corresponds to take infinite gauge gauge couplings in the new gauge groups. For a given value of ϕ one can study the RGE of g_A, g_B and λ and find up to which scale the couplings are perturbative. Thus the range for ϕ depends on the limitations that one wants to impose on the perturbativity of the couplings. we shall comment later on this point.

The parameter ϕ also control the coupling of the heavy vectors X_i to the SM matter and thus has to respect some limitation. The tightest bounds arise from the measurements of four fermions contact interactions and oblique corrections to the gauge bosons propagators. These limits can be encoded in the parameters X, Y and S, T of Ref. [**33**]. An analysis for the case considered in this example has been performed in Ref. [**33**, **46**] and gives

$$u > \max(6.5\cos^2\phi, 3.7\cos^2\phi) \text{ TeV} \,. \tag{3.6.25}$$

This lower bound on u implies an $m_\Sigma^2 = \lambda^2 u^2 \Delta$ very large compared to the electroweak scale. Thus one can expect large loop level contributions to the soft masses of the MSSM Higgs bosons.

A detailed study of the effect the large m_Σ^2 has been performed in [**10**]. The analysis of [**10**] also addresses the issue of the maximal scale of perturbativity of the model once the shift on the mass of the Higgs boson is connected to the running of λ, g_A and g_B. The result is that for $m_h = 2m_Z$ and $\Delta < 10$ the theory needs a mechanism for the generation of the soft terms that operates not much above few hundreds of TeV and that some coupling goes non-perturbative at scales below M_{GUT}.

From this brief analysis and the more general results of [**10**] we can conclude that D-term are a viable possibility to lift the mass of the Higgs boson. They are particularly suitable to get the modest increase needed to have a tree-level mass compatible with LEP. However to get a large correction to the MSSM tree-level prediction is rather generic to have a significant tuning and some coupling that goes non-perturbative at scales below M_{GUT}.

3.6.3. Tree-level mass from F-terms. The source of the new quartic coupling responsible for lifting the Higgs mass can be obtained changing the superpotential of the MSSM. This solution to the tension between the LEP result and the prediction of the MSSM relies on new Yukawa couplings and in principle does not require any extension of the SM gauge group.

To get a new F-term contribution the Higgs quartic we need to introduce a chiral superfield X linearly coupled to a Higgs bilinear

$$W = y_X X H_u H_d \,. \tag{3.6.26}$$

The field X must be either a SM gauge singlet, that we denote by S, or a SU(2) triplet, that we denote by T. The resulting extension of the MSSM has the most general superpotential

$$W = \lambda H_u \cdot H_d S + \lambda_2 H_u \cdot T_0 H_d + \chi_1 H_u \cdot T_+ H_d + \chi_2 H_d \cdot T_- H_u, \tag{3.6.27}$$

which yields the tree level bound for the mass of the Higgs boson:

$$\frac{m_h^2}{v^2} \leq \frac{1}{2}(g_1^2+g_2^2)\cos^2 2\beta + \left(\lambda^2 + \frac{1}{2}\lambda_2^2\right)\sin^2 2\beta + 4\chi_1^2\cos^4\beta + 4\chi_2^2\cos^4\beta \,. \tag{3.6.28}$$

The $SU(2)$ triplet affects the running of the gauge couplings and alters the prediction of the unification. Furthermore the presence of a triplet with a VEV is rather constrained by the EWPT. For these reasons we consider the case with just the singlet S and from now on we shall set the couplings $\chi_{1,2}$ and λ_2 to zero. Going to this limit the model that we want to study is an incarnation of the so-called NMSSM.

How large can be the bound eq. (3.6.28) depends only on how large we allow the coupling λ to be at the weak scale. This is a Yukawa couplings and because of to the structure of supersymmetric theories it runs according to an RGE that has the form

$$\frac{d\lambda}{dt} \sim \frac{\lambda}{16\pi^2}(\lambda^2 - g^2)\,, \tag{3.6.29}$$

where g is some combination of the gauge couplings experienced by the fields involved in the interaction mediated by λ.

When $\lambda < g$ the evolution of the Yukawa is driven by the gauge dynamics. The Yukawa will run to zero in the UV when g is UV-free or will grow in the UV following the growth of g.

When $\lambda > g$ the Yukawa grows in the UV and eventually hits a Landau pole. The choice of the lowest scale at which we tolerate a Landau pole reflects how fundamental we want our model to be. If the Landau pole is above the scale of the unification of gauge couplings our model has the right to be considered fundamental up to the scale where a theory of Grand Unification should onset. A model with a Landau pole at lower energies is just as meaningful as the model valid up to the GUT scale, but it has a limited range of energies at which it makes sense perturbatively.

Traditionally models where the Yukawa couplings hits a Landau pole before the GUT scale have been considered less appealing and great effort have been done to compute the maximal value of λ that still allow for *manifest*[2] unification. Adding suitable matter in complete representations of $SU(5)$ one can reach $\lambda = 0.7$ [**47**]. Hence, insisting on manifest unification yields an upper bound on the mass of the Higgs of about 150 GeV.

[2] read "à la MSSM"

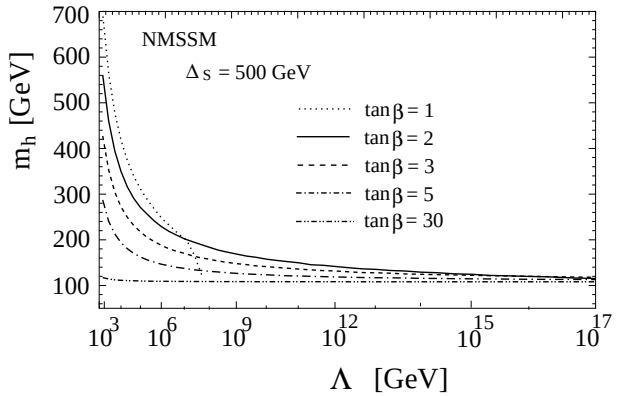

FIGURE 3.6.2. One-loop Higgs mass in the NMSSM computed for the maximal λ that stay perturbative up to Λ.

The increase of the Higgs mass that can be obtained in this way is already sufficient to go above the LEP limit, however the maximal value of the mass of the Higgs boson is strongly limited by the requirement of perturbative unitarity. Therefore it is worth considering how large the Higgs mass can be if one allows non-perturbative couplings at some scale Λ. Once the value of λ at the weak scale is fixed we can integrate the RGE of λ

$$\frac{d\lambda}{dt} = \frac{\lambda}{16\pi^2}\left(4\lambda^2 + 3y_t^2 - 3g_2^2 - g_1^2\right) , \tag{3.6.30}$$

and find the scale Λ where the coupling is equal to 4π. Figure 3.6.2 shows the corresponding maximal m_h in the NMSSM with couplings perturbative up to Λ. We can see that for $\Lambda \simeq 50$ TeV one can have a Higgs of few hundreds GeV mass that corresponds to $\lambda = 2$ at the weak scale.

This strongish coupling at low energy is surely affecting the phenomenology of the model. The most striking difference with respect to the MSSM is certainly the large mass of the Higgs boson, which implies a rather different decay pattern of the states in the Higgs sector. Other peculiar features of this class of models are expected to originate from this large couplings. Indeed we shall see in the rest of this work that many parts of the supersymmetric paradigm of the MSSM should be reconsidered and changed when we study a model with a strongish self-interacting Higgs sector.

CHAPTER 4

Gauge couplings unification and the UV completion of a Higgs sector with a strongish self-coupling

4.1. The fat Higgs scenario

We have already discussed in Section 3.6 how the addition of new quartic couplings through F-terms can raise significantly the mass of the Higgs boson. The price to pay to raise this mass is the low energy at which the Higgs self-coupling blows up hitting a Landau pole. This has not to be regarded as a fault of the theory. Rather it may reflect the fact that the description given in terms of a Higgs boson is not fundamental in the sense that the Higgs is not a degree of freedom of the theory that holds at higher energy.

A very fitting example of such phenomenon is provided in Nature and is the one of the interaction of pions at low energy. As a matter of fact at energies well below the GeV the pions interact a with coupling that shows an energy dependence characteristic of the interaction of non fundamentals objects. Indeed their interactions are mediated by effective operators of dimension greater than 4 and the strength of their coupling grows with the energy until a scale where it is necessary to change the degrees of freedom used to describe the interactions. This change in favor of quarks and QCD represent a familiar case of UV completion that one does when the energy of the processes with pions crosses the dynamical scale of QCD, Λ_{QCD}.

In a similar fashion we can imagine that the Higgs sector consists of composite objects that play the role of the pions and experience a coupling that stay perturbative up to energies comparable with the dynamical scale of the analogous of QCD and at larger energies hits a Landau pole. As in the previous case we can make sense of this phenomenon providing a UV completion whose onset lies at energies well below the Landau pole of the sector of composites.

This idea is the basic of the so-called "fat Higgs" scenario, that solves the problem of lifting the tree-level mass of the Higgs boson taking an NMSSM set-up where the three Higgs states H_u,H_d,S are composites formed at some scale $\Lambda \gg m_W$ and giving them a large self-coupling at the Fermi scale, such that the increase in the Higgs mass can be substantial. The RGE of the self coupling sets the order of magnitude for the scale of the onset of the UV completion that can be estimated running the self-coupling and finding the scale where it reaches 4π.

Concrete examples of fat Higgs models have a confining gauge theory in the UV with matter degrees of freedom which form condensates with the quantum numbers of the Higgs states of the NMSSM. The UV theory is defined choosing an appropriate number of flavors, to be UV free and to have a IR conformal phase. In this way the scale of compositeness is generated by the evolution of the UV gauge coupling and the value of the couplings at this scale have only little sensitivity to the choice of the UV boundary conditions.

It is important to stress that these are just the details of this particular realization of the idea and nothing prevents the UV completion to be something completely different still sharing the same IR properties of the models studied in the literature. In this respect the effective low energy approach of λSUSY proves particularly useful as it encompasses all the testable features of this class of models and disregards the details of the UV theory.

However we believe that the issue of the gauge coupling unification, although not *directly* testable at low energy, deserves some discussion as it is a conceptually important feature of the UV completion. Furthermore the measures of the gauge couplings performed at LEP provide a strong hint for this unification to happen. This fact is very evocative of the features of the UV theory and we believe that is not very plausible that the results of LEP are fooling us.

In the original formulation of the fat Higgs [**12**] and in some of its variants [**14**] the unification of gauge couplings can be achieved but only with addition of rather ad-hoc matter that compensate for the fact that some state charged under the standard model gauge group, such as the three Higgs states of the NMSSM or the third generation quarks, is not elementary. The existence of these models proves that unification is not in contradiction with the idea of the fat Higgs. However we consider very important that one can formulate models where the unification is reached in a way very close to what happens in the MSSM [**11**] and in the following we shall give more details on the so-called "new fat Higgs".

Another major difficulty with the original fat Higgs scenario that motivates in going beyond it is the generation of large Yukawa couplings. As a matter of facts the large top mass can hardly fit in the original scenario because the top quark is an elementary fermion while the MSSM Higgs boson H_u is a composite that is formed at the dynamical scale of the model Λ_{FH} where the fundamental constituents go to strong coupling. As such the interaction of the composite Higgs and the top quark is actually an interaction with the constituents of the Higgs and can be estimated as

$$y_{top} \simeq \frac{y_{tm} \cdot y_{hm}}{M} \frac{\Lambda_{FH}}{4\pi} \tag{4.1.1}$$

where M is the mass of the mediator state that interact directly with both the constituents of the Higgs and with the top and y_{tm} and y_{hm} are the coupling of the mediator with the top and the components of the Higgs. Generically on can expect to have the mass of the mediator to be above, and not necessarily close to, the dynamical scale of the Fat Higgs model implying a certain difficulty to get a large effective Yukawa for the top quark. Furthermore the direct couplings of the messenger need to be large in order to achieve a sizeable effective Yukawa coupling and this is not generic as well.

The simple solution pursued in the “new fat Higgs model” is to arrange for the MSSM Higgs boson to be elementary in such a way that the standard Yukawa interaction can be written in the Lagrangian in the usual way. Pursuing this solution the only composite state of the model is the SM singlet, who has no effect in the RGE. Thus the running of the gauge coupling follows the same pattern of the MSSM, in other words making the MSSM Higgs bosons elementary one gets back for free the standard pattern of gauge coupling unification [1].

[1] Subtleties connected with the presence of a strong coupling phase in the rest of the Higgs sector can be raised, however they are at the same level of uncertainty of the anyway unknown threshold corrections due to the unknown matter content present in the energy range from the weak scale to the scale of unification.

Alternatively one can solve the issue of the mass of the top quark giving some degree of compositeness to the third family of quarks or to part of it [**14**]. In this way a large top mass can be understood in terms of large couplings in a composite sector. However to reach the unification the model needs some ad-hoc adjustment. Therefore this latter possibility will not be discussed here and we shall concentrate on the "new fat Higgs" model.

4.2. A specific fat Higgs model

The new fat Higgs model consists in taking SM $SU(2)$ doublets X, X^c and singlets ϕ, ϕ^c with the superpotential

$$W = \lambda_1 \phi H_u X + \lambda_2 \phi H_d X^c + M_X X X^c + ... \tag{4.2.1}$$

For the sake of gauge coupling unification *à la* MSSM one can add $\tilde{X}, \tilde{X}^c$ to complete a fundamental of $SU(5)$ with the X and X^c, though this is not necessary for the argument about the generation of large Yukawa couplings. Altogether we have

$$\phi \sim (\underline{1}, \underline{1}, 0)\,, \quad X \sim (\underline{1}, \underline{2}, -\frac{1}{2})\,, \quad \tilde{X} \sim (\underline{3}, \underline{1}, \frac{1}{3}) \tag{4.2.2}$$

under $SU(3) \times SU(2) \times U(1)$. All the fields $X, \tilde{X}, \phi$ transforming as fundamentals under a new strong gauge group $SU(4)$ under which the field content of the MSSM is completely singlet.

Below the scale M_X the heavy X, X^c fields can be integrated out generating the effective superpotential term

$$W_{eff} = \frac{\lambda_1 \lambda_2}{M_X} H_u H_d \phi \phi^c\,. \tag{4.2.3}$$

The bilinear $\phi\phi^c$ has the quantum numbers of the SM singlet of the NMSSM and if one can arrange the strong $SU(4)$ dynamics to make it form a composite the effective Yukawa coupling generated is

$$\lambda_{eff} = \frac{\lambda_1 \lambda_2}{M_X} \frac{\Lambda_{FH}}{4\pi}\,. \tag{4.2.4}$$

The size of the effective Yukawa coupling is controlled by the size of the Yukawa couplings in the fundamental theory and is remarkable that the strong dynamics of $SU(4)$ can be used at the same time to have large couplings $\lambda_{1,2}$. Indeed $\lambda_{1,2}$ can be taken as UV-free Yukawa couplings that run to a quasi-fixed point in the IR pretty much in the same way the top Yukawa coupling could be generated in the SM [**48**]. Indeed in the context of supersymmetric strongly coupled gauge theories this kind of argument is put on firmer ground compared to the SM case by the existence of methods to account for the non-perturbative effects in the RGE. The RGE of $\lambda_{1,2}$ is

$$\frac{d\lambda_{1,2}}{dt} = \lambda_{1,2} \left(\frac{7}{16\pi^2} \lambda_{1,2}^2 + \gamma_* \right) \tag{4.2.5}$$

where γ_* is the contribution to the anomalous dimension from non perturbative dynamics. The RGE has an IR fixed point for

$$\lambda_{1,2}^2 = -\frac{16\pi^2}{7} \gamma_* \tag{4.2.6}$$

whose value can be computed using the results of [**49**]. The anomalous dimension of a gauge invariant operator made of chiral superfield in a strongly coupled supersymmetric $SU(N_c)$ gauge theory with N_f active flavors is given by $\gamma_* = 1 - 3N_c/N_f$. In

a $SU(4)$ gauge theory with just the fields $\phi, X, \tilde{X}$ that transform in the fundamental of $SU(4)$ and as in eq.(4.2.2) under the SM gauge group we would have $N_f = 6$ above M_X and $N_f = 1$ below M_X, where the $\underline{5}$-plet $X \oplus \tilde{X}$ is decoupled. In this case the theory below M_X would not have $N_f > N_c$ that is a necessary condition to have a s-confining supersymmetric gauge theory. In order to achieve the s-confining phase is necessary to add 4 additional flavors active below M_X such that the theory goes to a s-confining phase in the IR and gives negative values of γ_* that drive the Yukawa couplings to be UV-free and to have the desired IR fixed point.

The presence of additional flavors lead to a larger sets of gauge invariant operators made of chiral superfields and thus to a larger set of composites than just the needed singlet of the NMSSM. We shall not comment further on their presence assuming that they are made heavy enough to not be of relevance for the phenomenology.

Using the IR fixed point of the fundamental Yukawa couplings one can see that the maximal effective coupling in the NMSSM at the scale Λ_{FH} is

$$\lambda_{max} \simeq \frac{4\pi}{7}\gamma_* < \max(\lambda_1, \lambda_2)\,. \tag{4.2.7}$$

Running this coupling down to the electroweak scale can give sizeable couplings $\lambda \sim 2$ that are of phenomenological interest as they lead to a very non standard supersymmetric Higgs sector.

CHAPTER 5

The effective low-energy approach of λSUSY

5.1. The NMSSM

A recent review on the NMSSM can be found in [**50**], but for sake of completeness and to fix our notation, we give here some details on the model.

We take $SU(3)_C \times SU(2)_L \times U(1)_Y$ as gauge group. We consider the same matter sector of the MSSM and a Higgs sector made of the Higgs fields of the MSSM plus a singlet chiral field denoted by S. The most general superpotential that we can assign to the theory is

$$W_{gen}(\Phi_i) = \mu H_1 \cdot H_2 + \frac{M}{2} S^2 + \lambda S H_1 \cdot H_2 + \frac{k}{3} S^3 \,, \tag{5.1.1}$$

where H_1 and H_2 are the Higgs superfields with $-1/2$ and $1/2$ hypercharge respectively.

This superpotential generalizes the superpotential of the MSSM and still contains dimensionful parameters such as μ and M. These parameters appear in the superpotential and therefore they are not subject to large effect from renormalization. However their size is crucial to have an acceptable phenomenology. For instance studying the minimization of the potential of the MSSM one can see that μ needs to be close to the electroweak scale and such a coincidence of scales calls for an explanation. One of the topics of the rest of our work will be study of a dynamical mechanism to generate these terms.

The D-terms of the model are exactly the same of the MSSM:

$$V_Y = \frac{1}{8} g_1^2 (|H_2|^2 - |H_1|^2)^2 \,, \tag{5.1.2}$$

$$V_2 = \frac{1}{8} g_2^2 \left(H_1^\dagger T^i H_1 + H_2^\dagger T^i H_2 \right)^2 \,, \tag{5.1.3}$$

where $T^i = \frac{\sigma^i}{2}$. Using the identity for canonical generators of $SU(2)$ $\sum_i T^i_{ab} T^i_{cd} = 2\delta_{ad}\delta_{bc} - \delta_{ab}\delta_{cd}$, we can write the total gauge potential as

$$V_D \equiv V_Y + V_2 = \frac{1}{8} \left(g_2^2 + g_1^2 \right) (|H_2|^2 - |H_1|^2)^2 + \frac{1}{2} g_2^2 |H_1^\dagger H_2|^2 \,. \tag{5.1.4}$$

5.2. λSUSY

As explained in the Introduction and Section 3.6.3, there is a class of extensions of the MSSM that contains large extra contributions to the quartic part of the Higgs potential. These models are not fundamental models in the sense that they reach a strong-coupling regime well below the scale of the unification of the gauge couplings. All of them have a different dynamic in the UV but they all

share the fundamental feature of having a sector with a Higgs sector with a strongish self-interaction at the Fermi scale. The UV dynamics sets-in at some scale Λ and below this scale we can make use of an effective theory where the heavy degrees of freedom of the UV have been integrated out.

In the effective theory the details of the UV-completion are lost and the theory contains just the superpotential term $\lambda S H_1 \cdot H_2$, where the fields S, H_1 and H_2 are suitable combinations of the fundamental degrees of freedom. Ref. [**1**] studied the class of effective theories characterized by the superpotential:

$$W = \mu(S) H_1 H_2 + f(S)\,, \tag{5.2.1}$$

where f is a generic function of the field S. For later convenience we define $\lambda = d\mu/dS$.

5.3. Spectrum of the scalar sector

From the superpotential 5.2.1 we can compute the F-terms contribution to the potential

$$V_F = \mu_1^2(S)|H_1|^2 + \mu_2^2(S)|H_2|^2 - (\mu_3^2(S) H_1 H_2 + \text{h.c.}) + \lambda^2 |H_1 H_2|^2 + V(S). \tag{5.3.1}$$

For our purpose we shall neglect the D-term contributions to the quartic term of eq. (5.1.4), which are small compared to the superpotential contribution for the largish values of $\lambda \sim 2$ that we shall consider in our analysis [1]. The mass parameters of the potential also include contributions from the soft SUSY-breaking Lagrangian. For simplicity, we assume CP invariance of V and W.

Many of the phenomenologically relevant properties of λSUSY can be characterized by the functions $\mu_i^2(S)$, $\mu(S)$, and $M(S) = f''(S)$ evaluated at the Vacuum Expectation Value (VEV) s of the field S. These background values will be denoted below as μ_i^2, μ and M leaving their argument s understood. For example, the electroweak symmetry breaking (EWSB) is described by the equations

$$\tan\beta \equiv \frac{v_2}{v_1} = \frac{\mu_1}{\mu_2}, \tag{5.3.2}$$

$$\lambda^2 v^2 = \frac{2\mu_3^2}{\sin 2\beta} - \mu_1^2 - \mu_2^2\,, \tag{5.3.3}$$

where $v_{1,2}$ are the VEVs of the Higgs fields ($v \equiv (v_1^2 + v_2^2)^{1/2} = 175$ GeV).

The mass of the charged Higgs bosons $H^\pm$ is

$$m_{H^\pm}^2 = \mu_1^2 + \mu_2^2.$$

In this Chapter we shall simplify the analysis of the the general superpotential 5.2.1 making the approximation of negligible mixing of the singlet with the doublet scalars. This decoupling can be realized in explicit model where the superpotential mass of the singlet M is large. As a matter of fact this mass can be few TeV without reintroducing any fine-tuning [**1**]. For such large masses

[1] The D-terms increase the mass of the lightest Higgs boson of the model by $5 - 10$ GeV compared to the expressions given below.

we can legitimately neglect the mixing between the neutral components of the Higgs doublets and the real and imaginary components of S. Indeed a numerical analysis shows that the decrease in the masses of h, H, A due to this mixing does not typically exceed $5 - 10$ % and that the singlet admixture in h, H, A stays below $0.2 - 0.3$.

Neglecting the singlet-doublet mixing the masses of the light neutral scalars can be expressed via μ_i^2. In particular the mass of the pseudo-scalar A is then given by

$$m_A^2 = \frac{2\mu_3^2}{\sin 2\beta} = m_{H^\pm}^2 + \lambda^2 v^2.$$

The CP-even states h_i have mass matrix

$$\begin{pmatrix} m_A^2 \sin^2\beta & (\lambda^2 v^2 - \frac{1}{2} m_A^2) \sin 2\beta \\ (\lambda^2 v^2 - \frac{1}{2} m_A^2) \sin 2\beta & m_A^2 \cos^2\beta \end{pmatrix}.$$

The masses and compositions of the mass eigenstates h, H are

$$\begin{aligned} m_{H,h}^2 &= \frac{1}{2}(m_A^2 \pm X), \quad X^2 = m_A^4 - 4\lambda^2 v^2 m_{H^\pm}^2 \sin^2 2\beta\,, \\ H &= \cos\alpha\, h_1 + \sin\alpha\, h_2, \quad h = -\sin\alpha\, h_1 + \cos\alpha\, h_2\,, \\ \tan\alpha &= \frac{m_A^2 \cos 2\beta + X}{(\lambda^2 v^2 - m_{H^\pm}^2)\sin 2\beta}\,. \end{aligned} \tag{5.3.4}$$

It is convenient to parametrize the scalar sector of the model in terms of the parameters $\tan\beta$ and m_{H^+}.

Anticipating the result of the EWPT analysis, we observe from Figure 5.6.1 that large values of $\tan\beta$ tends to give too large values to T and are disfavored. The analysis of the supersymmetric contributions to the $b \to s\gamma$ transition, and in particular that of the charged Higgs boson, suggests a conservative bound on the mass of the charged Higgs boson [**51**]

$$m_{H^+} \gtrsim 350\ \mathrm{GeV}\,. \tag{5.3.5}$$

Taking these phenomenological indications together with Naturalness considerations the preferred parameter space is given by:

$$\begin{aligned} 1.5 \lesssim \tan\beta \lesssim 3\,, \\ 350\ \text{GeV} \lesssim m_{H^\pm} \lesssim 700\ \text{GeV}. \end{aligned} \tag{5.3.6}$$

The masses of neutral scalars in this range of parameters are given in Figure 5.3.1 and Figure 5.3.2. The key feature of the spectrum is that the lightest Higgs boson h is in the $200 - 300$GeV range, hence much heavier than in MSSM or the perturbative NMSSM. Another notable feature of the spectrum which is shown in Fig. 5.3.2 is the fixed ordering of the spectrum:

$$m_h < m_{H^+} < m_H < m_A\,.$$

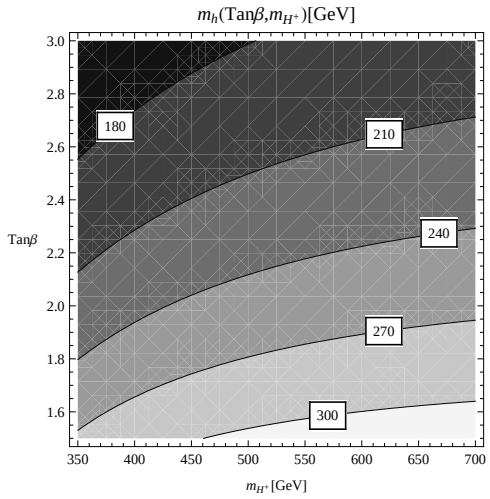

FIGURE 5.3.1. The mass of the lightest CP-even scalar h in the preferred region (5.3.6) of the parameter space. The coupling λ is fixed at $\lambda = 2$.

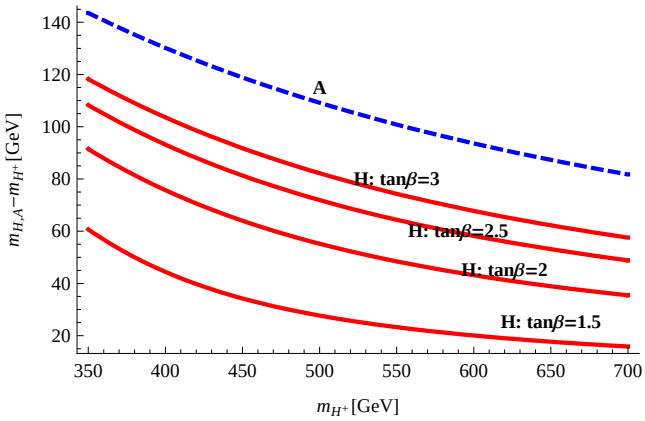

FIGURE 5.3.2. The second CP-even scalar H and the CP-odd scalar A are always heavier than the charged scalars $H^{\pm}$. This plot shows mass differences $m_H - m_{H^{\pm}}$ (solid red lines, $\tan\beta = 1.5, 2, 2.5, 3$ from below up) and $m_A - m_{H^{\pm}}$ (dashed blue line) as a function of $m_{H^{\pm}}$ in the preferred region (5.3.6) of the parameter space. The coupling λ is fixed at $\lambda = 2$.

5.4. Spectrum of the Higgsino/Singlino sector

In the fermion sector of λSUSY, we shall assume for simplicity that the electroweak gauginos are heavy and we shall neglect their mixing with the Higgsinos. This is justifiable since the Higgsinos are mixed with the Singlino $\tilde{S}$ by terms proportional to λv, while mixing with the gauginos are controlled by the relatively small terms of order gv.

In this approximation the lightest chargino is just a pure charged Higgsino and has mass μ. We shall denote it as χ^+.

We define the states

$$N_1 = \frac{1}{\sqrt{2}}\left(\tilde{H}_1 - \tilde{H}_2\right), \quad N_2 = \frac{1}{\sqrt{2}}\left(\tilde{H}_1 + \tilde{H}_2\right), \quad N_3 = \tilde{S}\,. \tag{5.4.1}$$

In the basis (N_1, N_2, N_3) the neutral Higgsino mass matrix is

$$M_N = \begin{pmatrix} \mu & 0 & \frac{v}{\sqrt{2}}\lambda(c_\beta - s_\beta) \\ 0 & -\mu & -\frac{v}{\sqrt{2}}\lambda(c_\beta + s_\beta) \\ \frac{v}{\sqrt{2}}\lambda(c_\beta - s_\beta) & -\frac{v}{\sqrt{2}}\lambda(c_\beta + s_\beta) & M \end{pmatrix}. \tag{5.4.2}$$

From this mass matrix one can see that there is a massless Higgsino state if holds the condition

$$\mu = -\frac{v^2\lambda^2 \sin 2\beta}{M}\,. \tag{5.4.3}$$

Furthermore the lightest neutralino is always lighter than the chargino

$$m_{\chi_1^0} \leq m_{\chi^\pm}\,. \tag{5.4.4}$$

Studying the stability of the potential one can see that exists an upper bound for the chargino mass

$$m_{\chi^\pm} \leq \cos\beta\, m_{H^\pm}\,, \tag{5.4.5}$$

which together with eq. (5.4.4) implies that the lightest neutralino typically has a mass in $100 - 200$ GeV range.

5.5. Other SUSY particles

The masses of the top squarks and of the gluino masses affects the running of μ_2^2 at the one- and two-loop level, respectively, and can thus be bounded from Naturalness considerations. For 20% fine tuning ($\Delta = 5$) and $\tan\beta$ as in (5.3.6) these masses have to satisfy [**1**]

$$\begin{aligned} m_{\tilde{t}} &\lesssim 600 - 800 \text{ GeV}\,, \\ m_{\tilde{g}} &\lesssim 1.2 - 1.6 \text{ TeV} \end{aligned} \tag{5.5.1}$$

(looser bounds corresponding to smaller $\tan\beta$). For larger fine tuning Δ these bounds increase by a factor $\sqrt{\Delta/5}$.

The masses of the electroweak gauginos, sleptons and all the other squarks except for the stops are taken to be several TeV. This is very similar to the approach of the "effective" supersymmetry [**52**] originally proposed to address the SUSY flavour problem. The analysis of [**53**] assesses that this separation of the spectrum can be done without introducing significant tuning.

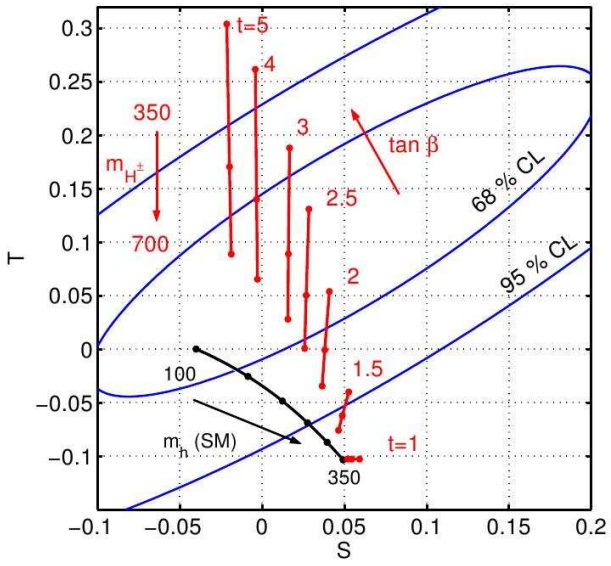

FIGURE 5.6.1. Result of the EWPT analysis of λSUSY. Red curves are the prediction of λSUSY for $\tan\beta$ as in the label and variable m_{H^+}. The red points corresponds to $m_{H^+} = 350, 500, 700$ GeV. For comparison, in black, is shown the SM with m_h from 100 GeV to 350 GeV with a stepping of 50 GeV.

5.6. EWPT

We have seen in the previous sections that λSUSY can have a Higgs boson as heavy as 300 GeV. In the pure SM such a mass of the Higgs boson would be hardly compatible with the EWPT because of a too large value of the parameter S. However this is not the case in λSUSY or in any other model that generate a significant contribution to T together with the contribution to S from the heavy Higgs.

In this respect λSUSY is very naturally in agreement with LEP precision data thanks to the combined effect of the Higgs/Higgsino sector on both the parameter T and the parameter S. As a matter of fact the potentially dangerous contribution to S coming from the heavy Higgs boson is controlled by the coupling λ, that is the same parameter controlling the mass splittings between the states of the Higgs sector and between the states in the Higgsino sector. As such the Higgs sector and the Higgsino sector will give contributions to T that bring the model back inside the ellipses of the $S - T$ plane.

This effect does not rely on any tuning because both the positive shift to T and the positive shift to S are controlled by λ. The systematic entanglement of the two contributions is apparent in Figure 5.6.1 where we report the result of [**1**] for the total contribution to the EWPT arising from the scalar sector.

CHAPTER 6

λSUSY with a scale-invariant superpotential

In this chapter we study the possibility to dynamically generate the μ term in λSUSY. As starting point we specialize the superpotential of λSUSY to a superpotential without dimensionful parameters. To forbid all the superpotential terms with a dimensionful constant we impose a continuous R-symmetry. Consequently our superpotential is

$$W_{\rm NMSSM}(\Phi_i) = \lambda S H_1 \cdot H_2 + \frac{k}{3} S^3 \,. \tag{6.0.1}$$

The corresponding soft supersymmetry breaking potential is [1]

$$V_{\text{soft}} = m_1^2 |H_1|^2 + m_2^2 |H_2|^2 + \mu_S^2 |S|^2 - (A\lambda S H_1 H_2 + G\frac{k}{3} S^3 + h.c.) \,. \tag{6.0.2}$$

The D-terms of our model are exactly the same of the MSSM and have already been given in eq. (5.1.4).

The total scalar potential of the theory will also include several terms involving the squark and slepton fields, but for our purposes it will not be necessary to deal with them. In the following we shall assume for simplicity that all the parameters of the Higgs-Higgsino potential are real. In addition, we conventionally choose the coupling λ to be positive and in all our examples we shall take positive k. A complementary study that deals with the case of negative k can be found in Ref. [**55**], that finds conclusions similar to ours.

6.1. Stability of the scalar potential

The first requirement we have to impose to the scalar potential is that it is bounded from below. At large values of the fields the quartic part of the potential dominates and, since its coupling is not negative, the only way to destabilize the potential is to make the quartic part vanishing along some direction. However, the quartic potential of the NMSSM is the sum of D-terms and F-terms which are each positive definite and, as we shall recall in the following, they cannot vanish at the same time, if not for the trivial field configuration. As such, the global stability of the potential is guaranteed by the supersymmetric structure of the theory and no constraint for the soft terms emerges.

[1] Note that this definition of the NMSSM superpotential and soft masses is not the same of the Les Houches Accord [**54**]. The parameters must be mapped according to: $k \to k$, $\lambda \to -\lambda, A \to -A_\lambda, G \to -A_k$ and consistently $\mu \to -\mu$.

The global stability of the potential can be explicitly shown as follows. The quartic part of the potential is given by $V^{(4)} = V_F + V_D$ where we denote the contributions from the F-terms and D-terms as V_F and V_D respectively. Since $V_F = \sum_i \left|\frac{\partial W}{\partial \Phi_i}\right|^2 \equiv \sum_i |F_i|^2$, the F-term part of the potential vanishes only if all the F_i vanish. This condition is satisfied, in general, along the direction

$$S = 0\,, \quad H_1 \cdot H_2 = 0\,, \tag{6.1.1}$$

and for $k = 0$ also along the direction of generic S and

$$H_1 = 0\,, \quad H_2 = 0\,. \tag{6.1.2}$$

The D-term part of the potential in eq. (5.1.4) is a sum of positive terms as well. Requiring each term to vanish, one finds that V_D vanishes only along the non-trivial direction

$$\begin{aligned} H_1^\dagger H_2 &= 0\,, \\ |H_1| - |H_2| &= 0. \end{aligned} \tag{6.1.3}$$

Consequently, for $k \neq 0$ the function $V^{(4)}$ vanishes only if both the conditions (6.1.1) and (6.1.3) hold, and this is only possible for the trivial configuration

$$H_1 = 0\,, \quad H_2 = 0\,, \quad S = 0\,. \tag{6.1.4}$$

Namely, in the $k \neq 0$ case there is no non-trivial direction in field space along which the whole quartic potential vanishes. Consequently the potential is always positive at large values of the fields, and there are no constraints on the parameter space resulting from the condition of stability of the potential.

In the $k = 0$ case, instead, there is the additional F-flat direction of (6.1.2). Along this direction the condition for vanishing V_D (eq. (6.1.3)) is always valid and therefore the whole quartic potential vanishes. As such, the large field behavior of the potential along this direction is dictated by the soft terms. Requiring the potential to be positive for large field values yields the condition $\mu_S^2 > 0$.

6.2. The minimum of the potential

The minimum of the potential has to be a stationary point, therefore the extremal point conditions with respect to $H_i = (H_1^0, H_2^0, S)$ must hold in a non-trivial point (v_1, v_2, s)

$$\frac{\partial}{\partial H_i}\, V|_{H_1^0 = v_1,\, H_2^0 = v_2,\, S = s} = 0\,, \tag{6.2.1}$$

which are equivalent to

$$\sin 2\beta = \frac{2s\lambda(A - ks)}{m_1^2 + m_2^2 + 2s^2\lambda^2 + v^2\lambda^2}\,, \tag{6.2.2}$$

$$\lambda^2 v^2 = \frac{2s\lambda(A - ks)}{\sin 2\beta} + \frac{m_1^2 - m_2^2}{\cos 2\beta} + m_Z^2\,, \tag{6.2.3}$$

and

$$4k^2s^3 - 2Gks^2 + 2s\left(v^2\lambda(k\sin 2\beta + \lambda) + \mu_S^2\right) - Av^2\lambda\sin 2\beta = 0\,. \tag{6.2.4}$$

The three conditions (6.2.2)-(6.2.4) will be used as relations to trade v, $\tan\beta$ and s for the soft parameters m_1, m_2 and μ_S.

For $k = 0$ we can write explicitly the solution of the last equation for the VEV s

$$s = \frac{A\lambda v^2\sin 2\beta}{2\left(\mu_S^2 + v^2\lambda^2\right)}\,. \tag{6.2.5}$$

Instead in the general case of $k \neq 0$ there are three different solutions of (6.2.4). As in the following we shall impose the CP invariance of the vacuum, we shall take the only real solution for s. This, however, will not be reported in the text, because of its quite complicated and not transparent expression.

This stationary point has to be a minimum and therefore we shall require the Hessian to be positive definite. In addition we want it to be a global minimum, hence we require it to be deeper than the origin

$$V(v_1, v_2, s) < V(0, 0, 0) = 0\,. \tag{6.2.6}$$

This latter condition reads

$$\mu_S^2 s^2 + k^2 s^4 - 2G\frac{k}{3}s^3 - \frac{\lambda^2}{4}v^4\sin^2 2\beta - \frac{m_Z^2 v^2}{4}\cos^2 2\beta < 0\,, \tag{6.2.7}$$

while the condition on the Hessian happens to have a rather complicated expression when $k \neq 0$ and therefore we do not give it explicitly here.

Additionally we have to require that no other stationary point of the potential is a minimum deeper than the electroweak symmetry breaking minimum. In particular we shall to require that

$$V(0, 0, s) > V(v_1, v_2, s) \tag{6.2.8}$$

for all solutions s of eq.(6.2.4).

For the potential to break the electroweak symmetry we have to ensure that the neutral Higgs boson potential has a global minimum in a point with non vanishing VEVs v_1 and v_2. Due to the structure of the potential the stability condition on the $SU(2)$ breaking point implies that CP is not broken at this point [**41**]. The conservation of CP allow us to treat the real and imaginary part of the scalar fields as non-mixing fields such that their mass matrices will be respectively a 3-by-3 and a 2-by-2 matrices, as opposed to the general case where a 5-by-5 mass matrix is needed.

In what follows we shall use the fact that CP conservation is a necessary condition for the stability of the minimum to derive constraints on the soft masses. This requirement amounts to impose that the VEVs of the scalar fields at the minimum of the potential have zero imaginary parts. The set of constraints from CP conservation are necessary conditions for the stability of the minimum and can result in analytically simpler expressions than those coming

from the constraint of the stability of the minimum, thus allowing a simpler discussion of some feature of the allowed region of the parameter space, see for instance the discussion around eq. (6.3.2).

The requirement of real VEVs v_1 and v_2 is given by

$$\lambda s(A-ks) > \sqrt{\lambda s\frac{A-ks}{\tan\beta}-\lambda^2 v^2\cos^2\beta+\frac{m_Z^2}{2}\cos 2\beta}\times \times\sqrt{(A-ks)\lambda s\tan\beta-\lambda^2 v^2\sin^2\beta-\frac{m_Z^2}{2}\cos 2\beta}\,, \tag{6.2.9}$$

where s is expressed by the real solution of (6.2.4).

To discuss the conservation of the $U(1)_{em}$ symmetry we go to the basis where only one Higgs doublet gets a VEV, v. In addition we exploit gauge invariance to set to zero the charged component of this same Higgs doublet such that we are left with a single charged scalar field that we call $\phi^{\pm}$. The absence of a VEV for $\phi^{\pm}$ is then expressed by the condition

$$\left.\frac{\partial^2 V}{\partial\phi^{\pm}\partial\phi^{\pm\dagger}}\right|_{\phi^{\pm}=0}>0\,, \tag{6.2.10}$$

which yields the condition on the soft breaking parameters

$$A>\frac{\lambda v^2}{2s}\sin 2\beta+ks-\frac{m_W^2}{2\lambda s}\sin 2\beta\,. \tag{6.2.11}$$

For the discussion of spontaneous CP breaking we set all the parameter of the Higgs potential to be real, we assume the condition (6.2.11) for the conservation of the electromagnetism to hold, so that we can write the potential at the minimum as

$$\begin{aligned} V_{\text{neutral}} &= \lambda^2|S|^2(|H_1^0|^2+|H_2^0|^2)+\lambda^2|H_1^0H_2^0|^2+ \\ &+ m_1^2|H_1^0|^2+m_2^2|H_2^0|^2+\mu_S^2|S|^2+k^2|S|^4+ \\ &- (A\lambda SH_1^0H_2^0+G\frac{k}{3}S^3-\lambda kS^2H_1^{0\dagger}H_2^{0\dagger}+h.c.)+ \\ &+ \frac{g_1^2+g_2^2}{8}(|H_1^0|^2-|H_2^0|^2)^2\,. \end{aligned} \tag{6.2.12}$$

With a suitable $U(1)$ rotation of the scalar fields we can cancel the imaginary part of H_1^0, so that we can write the three Higgs fields at the minimum as

$$\begin{aligned} H_1&=(v_1,0)\,,\\ H_2&=(0,v_2e^{\imath\phi})\,,\\ S&=se^{\imath\theta}\,, \end{aligned} \tag{6.2.13}$$

where v_1, v_2 and s are taken real and positive.

Replacing these fields in the scalar potential (6.2.12), and requiring a minimum in correspondence of the point $\phi = \theta = 0$, we find that for $k \neq 0$ the conditions

$$3Gks^2 - 5k\lambda v_1 v_2 s + 2A\lambda v_1 v_2 > 0\,, \tag{6.2.14}$$

$$\lambda k\,(Gs(A - ks) - 3A\lambda v_1 v_2) > 0 \tag{6.2.15}$$

that ensures that CP is not broken at the minimum and are necessary conditions for the stability of the extremal point. In the particular case of $k = 0$, these conditions get simplified to just the requirement that $A > 0$.

6.3. Parameter space

In this section we give explicit bounds on the parameter space arising from the various constraints discussed in Section 6.2. Each point of the parameter space is fixed by coordinates $\lambda, k, \tan\beta, s, A$ and G that are in principle unconstrained, however we shall focus on particular regions described and motivated in the following.

We are particularly interested in the large λ regime that helps in pushing the Higgs sector beyond LEP direct searches. Ref. [**1**] shows that this can be done for $\lambda > 1$ and a small $\tan\beta$. Remarkably this is precisely the regime where contributions to the precision observables from the Higgs sector are better fitting LEP data. In the same work, all the contributions to the T parameter were worked out in a particular model coming from a superpotential with the Peccei-Quinn (PQ) symmetry broken by the term MS^2. In that case the PQ-symmetric limit $M \to 0$ resulted in too large contributions to the EW oblique parameter T from the Higgsino sector. In close analogy, we shall explore the breaking of the PQ symmetry through the coupling k, with particular attention to the case of large k, where the symmetry is dramatically broken. A representative point of the interesting region of the parameter space is

$$\lambda = 2,\ \ \tan\beta = 1.5,\ \ \ k = 1.2\,, \tag{6.3.1}$$

which is singled out by the request of a moderate $\tan\beta$ and the maximal values of k and λ, such that the theory will stay perturbative at least up to $O(10\ \text{TeV})$ [2]. Having fixed a region of the parameters space in the surroundings of the point (6.3.1), the remaining parameter space is spanned by the VEV s and the soft breaking parameters A and G. Since the soft breaking terms are naturally expected to be of the same order of magnitude, we decide to make the simplifying assumption

$$G = A\,. \tag{6.3.2}$$

In fact, a large hierarchy between A and G is not possible since the requirement of absolute minimum given in (6.2.7) does not allow $G \gg A$ and the constraint

[2] Precisely we require that starting the supersymmetric one-loop RGE with boundary condition eq.(6.3.1) at 500 GeV the couplings are less than 4π at 10 TeV.

from CP invariance of (6.2.15) does not allow $G \ll A$. Variations on the assumption (6.3.2) are conceivable but we checked that they do not lead to any important change in our analysis.

Finally we decide to parametrize the two dimensional parameter space s, A in terms of the parameters μ and m_{H^+} that are parameters with direct relevance for the spectrum of the model and defined by

$$\mu = \lambda s\,, \quad m^2_{H^+} = m^2_W - \lambda^2 v^2 + \frac{2\mu(A - \frac{k}{\lambda}\mu)}{\sin 2\beta}\,. \tag{6.3.3}$$

For later convenience we also introduce the combination of parameters

$$\tilde{m}^2_A = m^2_{H^+} - m^2_W + \lambda^2 v^2\,. \tag{6.3.4}$$

The green shaded region in figure 6.3.1 shows the physical parameter space for the particular choice of parameters in (6.3.1) and (6.3.2). The lower-bound on m_{H^+} is given by the condition of absence of spontaneous CP violation given in (6.2.15), that in the new variables, after imposing the condition $G = A$, reads simply

$$m^2_{H^+} > 2\lambda^2 v^2 + m^2_W\,. \tag{6.3.5}$$

The other bound mainly shaping the allowed parameters space is given by the two conditions of absolute minimum of eq. (6.2.7) and eq. (6.2.8). The former in the new variables has the simple approximate form

$$m^2_{H^+} < m^2_W + 4\frac{\mu^2}{\sin^2 2\beta} + \frac{m^2_Z}{\tan^2 2\beta} + O\left(\frac{1}{\lambda}\right) \tag{6.3.6}$$

and cuts values of m_{H^+} in the upper part of the plane in Figure 6.3.1. The condition eq. (6.2.8) to not have further minima of the potential that are more shallow than the electroweak breaking minimum cuts the strip of parameter space that divides the two disconnected allowed regions.

The union of the requirements (6.3.5) and (6.3.6) gives a minimal allowed value for μ on which we further comment in Section 6.4.

6.4. Generation of the μ term

One of the original motivations of the NMSSM is the possibility to dynamically generate an effective μ term in the Lagrangian at the Fermi scale. This possibility is very interesting because in the MSSM such a term has to be fixed by hand to a value close to m_Z or the model would be badly unrealistic. Indeed such a term gives mass to the chargino and is crucial to have a correct EWSB. On the other hand in the NMSSM an effective μ-term is dynamically generated by EWSB through the VEV of the Higgs singlet resulting in

$$\mu = \lambda s\,. \tag{6.4.1}$$

This dynamical generation of μ in connection to EWSB is particularly welcome also in view of fine-tuning problems. In facts the minimization equation (6.2.2)

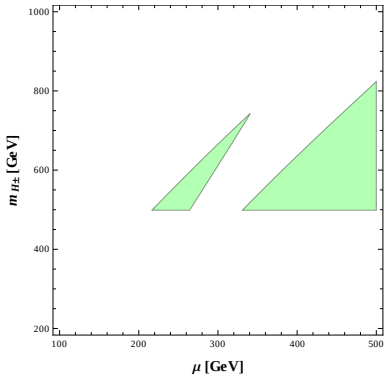

FIGURE 6.3.1. Region of the μ, m_{H^+} parameter space allowed by the conditions on the vacuum discussed in Section 6.2 for parameters fixed according to eqs. (6.3.1) and (6.3.2).

can be rewritten as

$$\mu^2 + \frac{1}{2}m_Z^2 - \frac{m_1^2 - m_2^2 \tan^2\beta}{\tan^2\beta - 1} = 0\,, \tag{6.4.2}$$

which shows that in a natural theory $\mu \sim m_Z$. Generating the μ term via EWSB relates the size of μ to that of the soft terms and therefore solves at the same time the issue of the presence of the term and the issue of its size.

In the traditional approach to the μ-problem within the NMSSM one requires that the coupling λ has to stay perturbative up the GUT scale, which means $\lambda \lesssim 0.7$ at the EW scale [**15**]. As such, to obtain a value of μ compatible with current searches and with the requirement of EWSB, one has to go in the regime $s \gtrsim v$. In particular, to have $\lambda s \sim m_Z$ when $\lambda \to 0$ one expects $s \gg v$, so that the minimization equation (6.2.4) has an approximate stable solution [**56**]

$$s \simeq \frac{1}{4k}(G + \sqrt{G^2 - 8\mu_S^2})\,. \tag{6.4.3}$$

This approximate solution generates larger values of μ as one takes larger λ and therefore seems to signal that the theory will be fine-tuned when a too large λ is considered. However this is not worrisome because the approximate solution (6.4.3) cannot be valid for any large value of λ as the approximation $s \gg v$ breaks down.

Indeed one can consider the minimization equation (6.2.4) in the large λ regime for generic s and find an approximate solution

$$s \simeq \frac{1}{2}\frac{A \sin 2\beta}{k \sin 2\beta + \lambda}\,, \tag{6.4.4}$$

that in the limit $\lambda \to \infty$ gives

$$\mu_\infty \equiv \lambda \lim_{\lambda\to\infty} s = \frac{1}{2} A \sin 2\beta\,.$$

The existence of such finite limit is not surprising as we have already noticed in Section 6.3 that μ cannot be taken arbitrarily large because of the incompatibility of the requirement of absolute minimum (6.2.6) and the requirement of positives masses squared of the CP-even scalars. Indeed one can be more quantitative and show that the presence of such maximal value of μ is a generic feature of the model due to the largeness of λ and that the value of the maximal μ is linked to the maximal mass of lightest Higgs boson.

The actual maximal allowed value of μ can be estimated observing that in the region close to the boundary defined by the condition of absolute minimum given in (6.2.7) and for $k < \lambda$ the condition $m_{s_1}^2 > 0$ can be approximated by

$$\sqrt{m_{H^+}^2 - m_W^2 + \lambda^2 v^2} > \mu \frac{3 - k/\lambda}{\sin 2\beta} + \frac{3}{2} v\lambda(k/\lambda - 1)\,. \tag{6.4.5}$$

This is a lower-bound on m_{H^+} that, for values of μ large enough, gets incompatible with the condition (6.2.7) for the minimum of the potential. The value of μ where the two conditions get incompatible can be estimated taking (6.2.7) in the approximate form given by the upper-bound on m_{H^+} of (6.3.6), yielding a relatively simple condition in terms of $\rho \equiv k/\lambda$

$$\mu < \frac{v\lambda \sin 2\beta}{2} \frac{3(\rho-4)\rho + \sqrt{8(\rho-1)(5\rho-7)} + 9}{(\rho-5)(\rho-1)} \simeq \frac{3}{2} v\lambda \sin 2\beta + O\left(\frac{k}{\lambda}\right)\,, \tag{6.4.6}$$

from which we observe that for generic $\tan\beta$ and generic $k < \lambda$ the model has a maximal allowed value of μ of the order of λv.

Furthermore, from the requirements of absolute minimum and of the absence of spontaneous CP breaking given in (6.2.7) and (6.2.15), we can see that there is a minimum allowed value for μ that can be estimated taking the approximate condition in (6.3.6) in place of (6.2.7) giving

$$\mu^2 > \frac{\lambda^2 v^2}{2} \sin^2 2\beta - \frac{m_Z^2}{4} \cos^2 2\beta\,. \tag{6.4.7}$$

Taking together this result and the condition (6.4.6) for the absolute minimum, we find that the model is consistent only for values of μ within an interval that, neglecting the term $m_Z \cos 2\beta/2$, reads

$$\frac{\lambda v}{\sqrt{2}} \sin 2\beta \lesssim \mu \lesssim \frac{3\lambda v}{2} \sin 2\beta\,. \tag{6.4.8}$$

In the large λ regime this relation automatically ensures that the chargino with mass μ is above the LEP bound (see later eq. (7.2.2)) and, at the same time, gives an upper-bound for μ linked to the mass of the lightest Higgs boson. In this sense eq. (6.4.8) shows that, specializing the generic λSUSY superpotential in (5.1.1) to a superpotential without dimensionful parameter gives a model where the μ term is phenomenologically acceptable and is necessarily close to m_Z, thus solving the so-called "μ-problem". It is important to stress

that eq. (6.4.8) holds only for $k < \lambda$ and that this is generically the case in the large λ regime of λSUSY.

Furthermore, we can use (6.4.8) to establish a relation between the mass of the chargino and the mass of the lightest Higgs

$$m_{\chi^+} \sim m_{s_1} \,, \tag{6.4.9}$$

which is of phenomenological interest for collider searches.

6.5. Naturalness

In this Section we want to quantify the degree of tuning of the fundamental parameters needed to get a realistic model. In particular we want to quantify how much tuning is needed to enforce the VEV of our fields to be of the order of the electroweak scale. The VEVs encode the dynamics of the breaking of the electroweak symmetry and therefore are the quantities where the tuning is expected to show up.

From the minimization equations (6.2.2), (6.2.4), and (6.2.3) we see that when the coupling λ is large the value of the VEVs can be understood by the approximate relations

$$v \simeq \frac{m_{soft}}{\lambda} \,, \quad s \simeq \frac{m_{soft}}{\lambda} \,, \tag{6.5.1}$$

where by m_{soft} we denote some suitable combination of the soft masses.

The non observation of superpartners neither at LEP nor at TeVatron generically requires a separation between the scale of the soft masses and the Fermi scale. From eq. (6.5.1) it is apparent that the choice of large λ naturally yields a moderate separation between the scale of the soft terms and the scale of the VEV. Thus in the large λ regime the needed separation of scales can be achieved with a low degree of tuning. The relation eq. (6.5.1) also shows that in the limit of large λ is generic to have the VEV s and the VEV v of the same order, as required by eq. (6.4.8) to solve the μ problem.

To quantify the tuning we want to study the sensitivity of the value of the VEV to the change of the fundamental parameters of the soft potential of the model. In particular we adopt the approach of [**57**] and for a fixed maximum amount of fine tuning $\frac{1}{\Delta}$ we impose

$$\Delta_{a_j} \equiv \left| \frac{a_j^2}{v^2} \frac{d\, v^2(a_i)}{d\, a_j^2} \right| < \Delta \,. \tag{6.5.2}$$

We shall consider the sensitivity to the parameters $a_j = (\mu_S, m_1, m_2, G, A)$. To compute the several logarithmic derivatives in (6.5.2), we have to consider the conditions of minimization of the potential (6.2.2) and (6.2.4).

To remove the implicit dependence on the soft parameters that feeds in the expression for the VEV v through the angle β we first combine eq. (6.2.2) and

eq. (6.2.3) in the new relation

$$\cos^2\beta = \frac{m_2^2 + m_Z^2/2 + \lambda^2 s^2}{m_1^2 + m_2^2 + m_Z^2 + 2\lambda^2 s^2}\,. \tag{6.5.3}$$

This relation is used to remove the dependence on β contained in the eqs. (6.2.3) and (6.2.4). Then we use eq. (6.2.3) to eliminate the dependence on the VEV v in the relation for the VEV s given by equation (6.2.4). After this treatment we can directly compute the several derivatives of s with respect to the dimensional parameters of the Lagrangian $\partial s/\partial a_j^2$ and express the level of fine tuning Δ_{a_j} as

$$\Delta_{a_j} = \left|\frac{a_j^2}{v^2}\frac{dv^2(a_i,s)}{da_j^2}\right| = \left|\frac{a_j^2}{v^2}\left(\frac{\partial v^2(a_i,s)}{\partial a_j^2} + \frac{\partial v^2(a_i,s)}{\partial s}\frac{\partial s}{\partial a_j^2}\right)\right|\,. \tag{6.5.4}$$

From our analysis it turns out that considering just the dimensional parameters m_1, m_2, G and μ_S the level of fine tuning required is in general very small in all the parameter space allowed by the conditions on the scalar potential analyzed in Section 6.2 and by the LEP bound on the mass of the lightest Higgs given in (1.0.2). The parameter that needs the largest degree of tuning is the soft trilinear coupling A. However the fine tuning required on this parameter is always relatively small. For example, for the reference point in (6.3.1) it is always smaller than ~ 25 when the mass of the lightest Higgs is in agreement with the LEP bound. Our result for the fine tuning on A is shown in Figure 6.5.1, as a function of the mass of the lightest Higgs, for the representative point of the parameter space presented in (6.3.1) for a representative choice of the mass the chargino $\mu = 230$ GeV (on the left panel) and $\mu = 400$ GeV (on the right panel). The result for fixed values of μ is rather representative of the general case. Indeed we checked explicitly that in the region allowed by LEP the fine tuning depends only mildly on the value of μ.

As expected from the considerations following eq. 6.5.1 the fine-tuning is a decreasing function of the mass of the Higgs. With this result in mind we can conclude that the non-observation of the the Higgs boson at LEP is pretty Natural in this model. Indeed we shall see in the following Section 7.1 that imposing the LEP bound on the Higgs mass will rule out only a tiny strip of the parameter space.

6.5.1. Naturalness bounds on sparticles masses. Using Naturalness arguments, we want to set upper bounds for the masses of sparticles. These bounds are particularly relevant to understand the expected size of the contributions of the sparticles to low-energy processes like the well studied flavour transitions and LEP precision data. Moreover with these bounds at hand one can estimate the timescale for the observation of such states at the LHC.

For the case of the stops-sbottoms, neglecting the mixing term proportional to the A-term, the physical masses of the stop and the sbottom squark are

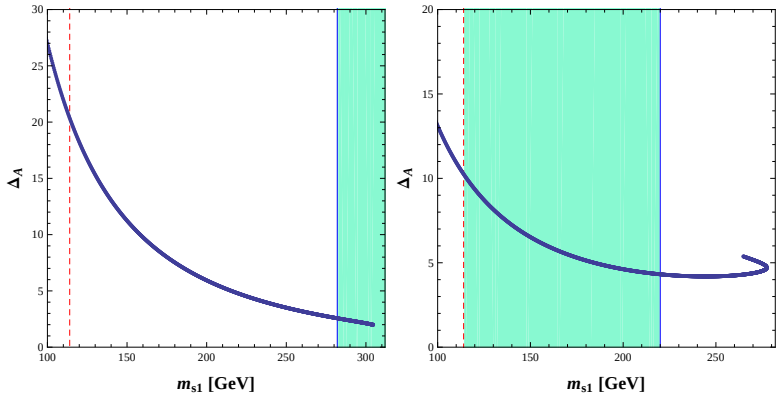

FIGURE 6.5.1. Logarithmic derivative of the VEV of the Higgs with respect to the dimensional parameter A as a function of the lightest Higgs boson mass m_{s_1}. The parameters are fixed as in the representative point eq. (6.3.1) and the chargino mass μ is fixed to 230 GeV (on the left), and 400 GeV (on the right). The blue shaded area denotes the range of Higgs masses allowed by the constraints on the scalar potential discussed in Section 6.2 for the parameters choice of eq. (6.3.1) and the two choices of μ. The vertical dashed line is the LEP limit of 114 GeV.

$$m_{\tilde{t}_L} = \sqrt{m_{\tilde{Q}}^2 + m_t^2 + m_Z^2 \cos 2\beta \left(\frac{1}{2} - \frac{2}{3}\sin^2\theta_W\right)}, \tag{6.5.5}$$

$$m_{\tilde{b}_L} = \sqrt{m_{\tilde{Q}}^2 + m_b^2 + m_Z^2 \cos 2\beta \left(-\frac{1}{2} + \frac{1}{3}\sin^2\theta_W\right)}, \tag{6.5.6}$$

We can put bounds on these masses observing that the soft mass $m_{\tilde{Q}}$ affects the soft Higgs mass m_2 through the one loop renormalization group equation (RGE) [**58**]

$$\frac{dm_2^2}{dt} = \frac{3}{8\pi^2}\lambda_t^2(m_{\tilde{Q}}^2 + m_{\tilde{t}_R}^2) + \cdots, \tag{6.5.7}$$

where the ellipsis stands for terms not dependent, in first approximation, on the soft squark masses. One can integrate these equations up to the messenger scale $\Lambda_{\rm mess}$, obtaining, at the leading log,

$$\delta m_2^2 \simeq -\frac{3}{8\pi^2}\lambda_t^2(m_{\tilde{Q}}^2 + m_{\tilde{t}_R}^2)\ln\frac{\Lambda_{\rm mess}}{1\ \text{TeV}}. \tag{6.5.8}$$

To give an estimate of the bound on the masses of stops and sbottoms, one can simply make the identification $m_{\tilde{Q}} = m_{\tilde{t}_R}$

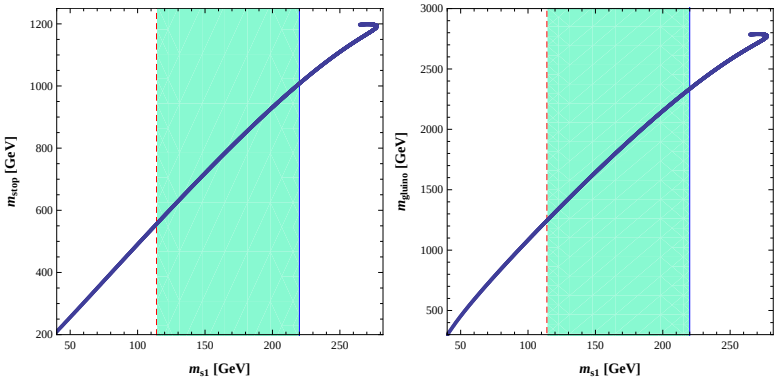

FIGURE 6.5.2. Upper bound on the mass of the stop (left panel) and of the gluino (right panel) for $\Lambda_{mess} \sim 100$ TeV an allowed fine tuning of 10%, computed for the representative point in (6.3.1) and for the chargino mass μ equal to 400 GeV. The blue shaded area denotes the range of Higgs masses allowed by the constraints on the scalar potential discussed in Section 6.2 for the parameters choice of eq. (6.3.1) and the two choices of μ. The vertical dashed line is the LEP limit of 114 GeV.

Imposing the Naturalness condition (6.5.2) with respect to the parameter $m_{\tilde{Q}}$ and using the approximate expression

$$\left| \frac{m_{\tilde{Q}}^2}{v^2} \frac{d\, v^2}{d\, m_{\tilde{Q}}^2} \right| \sim \left| \frac{m_{\tilde{Q}}^2}{v^2} \frac{d\, v^2}{d\, m_2^2} \frac{d\, m_2^2}{d\, m_{\tilde{Q}}^2} \right| , \tag{6.5.9}$$

one can find analytically the bound

$$m_{\tilde{Q}} \leq v \sqrt{\frac{4\pi^2}{3}} \sin\beta \frac{\sqrt{\Delta}}{\sqrt{\frac{dv^2}{dm_2^2}} \ln \frac{\Lambda_{\rm mess}}{1 \text{ TeV}}} . \tag{6.5.10}$$

The result for the bound on the mass of the stop for a messenger scale of 100 TeV and an allowed fine tuning of 10% is shown in the left panel of Figure 6.5.2 for the point of the parameter space presented in (6.3.1) and $\mu = 400\,$GeV [3]. From the figure it is evident that the upper bound on the stop mass $m_{\tilde{t}_L}$ increases when one increases the value of the mass of the lightest Higgs, and, for a Higgs mass satisfying the LEP bound, the stop mass bound is $m_{\tilde{t}} \lesssim 550$ GeV $-$ 1000 GeV for an allowed fine tuning of 10% depending on the lightest Higgs boson mass.

It is clear from eq. (6.5.8) that in the case of the sleptons and the first and second generation of squarks we would have a bound that is too loose to be useful because of the smaller Yukawa couplings. However, extending eq.

[3] There are no relevant changes in the curve for the bound on the stop mass, for μ fixed to be equal to the second reference value $(230\,\mathrm{GeV})$ discussed in the previous subsection.

(6.5.8) to include two-loops gauge effects the recent analysis of [**53**] shows that in our model Naturalness bounds on the sfermion masses are around $10\ \mathrm{TeV}$. We remark that squarks close to saturate these bounds are of no practical impact for our analysis of EWPT and for LHC phenomenology, but are still of potential relevance for flavor physics, which requires us to assume some structure in the sector of the first and second generation squarks to evade current bounds.

The mass of the gluino $m_{\tilde{g}}$ can be bounded as well as it contributes to m_2 via a two-loop effect enhanced by the large QCD coupling constant. At two loops, the main dependence of m_2 on the gluino mass is given by [**58**]

(6.5.11)
$$\frac{dm_2^2}{dt} \sim \frac{3}{8\pi^2}\left(\lambda_t^2(m_{\tilde{Q}}^2 + m_{\tilde{t}_R}^2) + h_t^2\right) + \frac{1}{8\pi^4} g_s^2 m_{\tilde{g}} \left(2\lambda_t^2 m_{\tilde{g}} - \lambda_t^\dagger h_t - \lambda_t h_t^\dagger\right) .$$

The second term is a purely two loop contribution directly dependent on the gluino mass, instead, in the first (one loop) term, we have dependence on the squark masses of third generation and on the third generation trilinear term h_t. At one loop, they are related to the mass of the gluino through the equations

$$\frac{dm_{\tilde{Q}}^2}{dt} \sim \frac{dm_{\tilde{t}_R}^2}{dt} \sim -\frac{2}{3\pi^2}\, g_s^2\, m_{\tilde{g}}^2 \,, \tag{6.5.12}$$

$$\frac{dh_t}{dt} \sim \frac{2}{3\pi^2}\, g_s^2\, \lambda_t\, m_{\tilde{g}} \,, \tag{6.5.13}$$

that can be solved, using the leading log approximation. Assuming that at the high scale h_t is small, if compared to its running, then it is easy to prove that numerically the most relevant contributions in (6.5.11) are those not involving the trilinear term h_t.

Plugging this finding in the RGE for m_2 where the squark masses are taken to be the solution of the differential equation (6.5.12) one finally obtains

$$\delta m_2^2 \approx \frac{g_s^2}{4\pi^2} \lambda_t^2\, m_{\tilde{g}}^2 \ln^2 \frac{\Lambda_{\mathrm{mess}}}{1\ \mathrm{TeV}} \,. \tag{6.5.14}$$

Imposing the Naturalness condition (6.5.2), with respect to the parameter $m_{\tilde{g}}$, and using the approximate expression

$$\left|\frac{m_{\tilde{g}}^2}{v^2}\frac{d\,v^2}{d\,m_{\tilde{g}}^2}\right| \sim \left|\frac{m_{\tilde{g}}^2}{v^2}\,\frac{d\,v^2}{d\,m_2^2}\,\frac{d\,m_2^2}{d\,m_{\tilde{g}}^2}\right| \,, \tag{6.5.15}$$

one can find analytically the bound

$$m_{\tilde{g}} \leq 2\pi^2 v \sin\beta\, \frac{\sqrt{\Delta}}{g_s \sqrt{\frac{dv^2}{dm_2^2}}\, \ln^2 \frac{\Lambda_{\mathrm{mess}}}{1\ \mathrm{TeV}}} \,. \tag{6.5.16}$$

The result for the bound on the mass of the gluino for a messenger scale of 100 TeV and an allowed fine tuning of 10% is shown in the right panel of Figure 6.5.2 for the parameter point presented in (6.3.1) and for $\mu = 400$ GeV. From the figure it is evident that the upper bound on the gluino mass $m_{\tilde{g}}$ increases when one considers increasing values of the mass of the lightest Higgs, and, for a Higgs mass satisfying the LEP bound, the mass of the gluino can be ~ 1.3 TeV for an allowed fine tuning of 10%.

The general conclusion of our study of Naturalness is that the model is less tuned when the lightest Higgs boson is heavier. This is somehow expected because the sensitivity to large corrections to the Higgs boson mass is necessarily smaller as the mass itself gets larger, for instance taking the usual measure of fine-tuning with respect to the mass of the stop

$$\frac{m_{\tilde{t}}^2}{m_h^2}\frac{\partial m_h^2}{\partial m_{\tilde{t}}^2} < \Delta$$

it is clear that the sensitivity is quadratically reduced as one takes larger m_h.

From this simple consideration it follows that the bounds on the third generation squarks and gluinos are rather loose when compared to the bounds in a light Higgs boson scenario. This means that these colored states of SUSY might not have any observable signature at the early LHC. As we shall see in Section 7.3 also LEP phenomenology is rather unaffected by the presence of this heavy superpartners of top and bottom.

Pretty much as for the stop and sbottom, one can find bounds on the masses of first and second generation squarks by requiring

$$\frac{m_{\tilde{q}}^2}{m_h^2}\frac{\partial m_h^2}{\partial m_{\tilde{q}}^2} < \Delta\,.$$

The limits originate dominantly from two-loops diagrams with squark and gauge bosons loops and turn out to be of the order of 10-20 TeV [**53**], that is a factor 3-4 larger than what obtained in the MSSM. The possibility of taking larger masses for the first and second generation of squarks of course helps to solve the flavor problem of SUSY by advocating a hierarchical spectrum.

It must be stressed that this improvement of the SUSY flavor problem is a peculiar feature of λSUSY and not of the other mechanisms to increase the Higgs boson mass reviewed in Section 3.6. Indeed the alternatives to λSUSY all introduce new gauge interactions that are needed to have new D-term contributions to the Higgs quartic. These new gauge interactions also bring new two-loops contributions to the Higgs soft masses from squark loops, thus reducing the possibility to take hierarchical squark masses [**53**] in the alternatives to λSUSY.

CHAPTER 7

Experimental constraints on scale-invariant λSUSY

7.1. The spectrum

The Higgs sector of the theory contains seven bosonic degrees of freedom. In particular, in the mass eigenstates basis we expect one charged Higgs, three neutral scalar fields and two neutral pseudo scalars, that do not mix with the scalars, since we imposed CP invariance. In order to investigate the spectrum of these six particles, it is convenient to express the scalar potential with the Higgs fields expressed by

(7.1.1)
$$S = s + \frac{S_1 + iS_2}{\sqrt{2}}\,, \quad H_1 = e^{-i\frac{\bar{\sigma}\bar{\pi}_1}{v_1}} \begin{pmatrix} v_1 + \frac{h_1}{\sqrt{2}} \\ 0 \end{pmatrix}, \quad H_2 = e^{-i\frac{\bar{\sigma}\bar{\pi}_2}{v_2}} \begin{pmatrix} 0 \\ v_2 + \frac{h_2}{\sqrt{2}} \end{pmatrix}.$$

After some algebra, we obtain the mass matrices given in the following, where we have used $s_\beta \equiv \sin\beta$, $c_\beta \equiv \cos\beta$, $t_\beta \equiv \tan\beta$, $s_{2\beta} \equiv \sin 2\beta$ and μ and $\tilde{m}_A$ as defined in (6.3.3) and (6.3.4) respectively. For the scalar Higgs bosons, in the basis (h_1, h_2, S_1) we get

(7.1.2)
$$M_S^2 = \begin{pmatrix} c_\beta^2 m_Z^2 + s_\beta^2 \tilde{m}_A^2 & c_\beta s_\beta \left(2v^2\lambda^2 - m_Z^2 - \tilde{m}_A^2\right) & \mu v(2\lambda c_\beta + s_\beta k) - s_\beta^2 c_\beta v\lambda \frac{\tilde{m}_A^2}{\mu} \\ . & m_Z^2 s_\beta^2 + c_\beta^2 \tilde{m}_A^2 & -\frac{v\lambda c_\beta^2 s_\beta \tilde{m}_A^2}{\mu} + v\mu(2\lambda s_\beta + k c_\beta) \\ . & . & 4\frac{k^2}{\lambda^2}\mu^2 - G\frac{k}{\lambda}\mu + \lambda^2 v^2 s_{2\beta}^2 \frac{\tilde{m}_A^2}{4\mu^2} + \frac{\lambda k}{2} v^2 s_{2\beta} \end{pmatrix}.$$

For the pseudoscalar we use the basis $(\pi^{(3)}, S_2)$, where $\pi^{(3)}$ is defined by $\pi^{(3)} = \sin\beta\pi_1^{(3)} - \cos\beta\pi_2^{(3)}$ and we get

(7.1.3)
$$M_{PS}^2 = \begin{pmatrix} \tilde{m}_A^2 & -\frac{v\lambda c_\beta s_\beta \tilde{m}_A^2}{\mu} - 3kv\mu \\ . & \lambda^2 v^2 c_\beta^2 s_\beta^2 \frac{\tilde{m}_A^2}{\mu^2} - 3k\lambda c_\beta s_\beta v^2 + 3G\mu\frac{k}{\lambda} \end{pmatrix}.$$

The charged Higgs boson mass is just equal to the parameter m_{H^+}

(7.1.4)
$$m_{H^\pm} = m_{H^+} = m_W^2 - \lambda^2 v^2 + \frac{2\mu(A - \frac{k}{\lambda}\mu)}{\sin 2\beta}\,.$$

For the neutralino and chargino sector we assume that the gaugino mass parameters M_1, M_2 are large. In this case the only light chargino is a pure

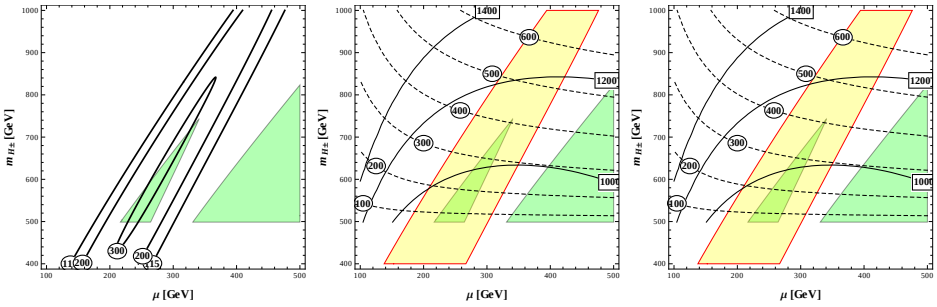

FIGURE 7.1.1. Masses (in GeV) of the neutral scalars in the plane μ, m_{H^+} for parameters fixed as in (6.3.1): (from the left to the right) the mass of the lightest CP-even (m_{s_1}), the masses of the two heavy CP-even ($m_{s_{2,3}}$), and the masses of the two CP-odd scalars ($m_{a_{1,2}}$). In all the panels the overlaid yellow area corresponds to $m_{s_1} > 114$ GeV and the overlaid green area corresponds to the parameter space where the $SU(2)$ breaking vacuum is the absolute minimum and CP is conserved.

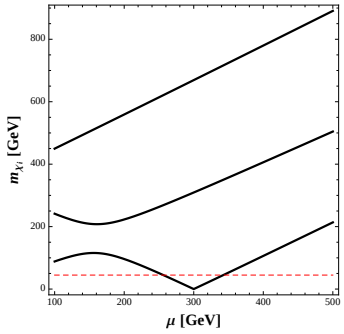

FIGURE 7.1.2. Higgsino masses (in GeV) as function of the chargino mass μ for fixed parameters as in (6.3.1). The dashed line corresponds to $m_Z/2$ which is taken as limit from LEP (eq. (7.2.4)).

Higgsino and has exactly the mass

$$m_{\chi^+} = \mu\,. \tag{7.1.5}$$

For the neutralinos we choose the basis defined by

$$N_1 = \frac{1}{\sqrt{2}}\left(\tilde{H}_1 - \tilde{H}_2\right)\,, \quad N_2 = \frac{1}{\sqrt{2}}\left(\tilde{H}_1 + \tilde{H}_2\right)\,, \quad N_3 = \tilde{S}\,, \tag{7.1.6}$$

and the mass matrix reads

$$M_N = \begin{pmatrix} \mu & 0 & \frac{v}{\sqrt{2}}\lambda(c_\beta - s_\beta) \\ 0 & -\mu & -\frac{v}{\sqrt{2}}\lambda(c_\beta + s_\beta) \\ \frac{v}{\sqrt{2}}\lambda(c_\beta - s_\beta) & -\frac{v}{\sqrt{2}}\lambda(c_\beta + s_\beta) & -2\frac{k}{\lambda}\mu \end{pmatrix}\,. \tag{7.1.7}$$

From this mass matrix one can see that there is a massless Higgsino state if

$$\mu^2 = \frac{\lambda}{k}\frac{v^2\lambda^2 \sin 2\beta}{2}\,, \tag{7.1.8}$$

and that

$$\sum_{i=1,2,3} m^2_{\chi_i} = 2\left[\mu^2\left(\frac{2k^2}{\lambda^2}+1\right)+v^2\lambda^2\right]\,. \tag{7.1.9}$$

All the masses given in this section are plotted in Figures 7.1.1 and 7.1.2 in the plane μ, m_{H^+} for the choice of parameters in (6.3.1). Few comments are in order. Firstly, we note that, due to the large value of λ, the spectrum consists of relatively heavy Higgs bosons with a lightest CP-even mass of roughly (200-300) GeV and, due to the large value of k, there is no light state in the CP-odd sector, in fact the lightest CP-odd has mass of few hundreds GeV. This shows how this realization of the NMSSM is rather at odds with the widely studied case of small λ.

Another interesting point is the fact that the requirement of a mass for the lightest Higgs in accordance with the LEP bound tends to clash with the requirement of absolute minimum of (6.2.7). This implies that the model cannot have an arbitrarily large value of μ because this would yield a negative mass squared for the lightest Higgs boson. The existence of a maximal allowed μ can be understood taking the the CP-even mass matrix (7.1.2) in the large μ and large λ limit and observing that all the diagonal sub-matrices have negative eigenvalues independently of the other parameters. This fact is very welcome in view of the need to generate a μ term of the order of m_Z and we shall study the consequences of this fact in Section 6.4.

For later convenience, we conclude this section fixing some notation. We call the scalar and pseudoscalar mass eigenstates (from the lightest to the heaviest) s_1, s_2, s_3 and a_1, a_2 respectively and we shall denote the Higgsino mass eigenstates as χ_1, χ_2, χ_3 (still from the lightest to the heaviest).

We introduce the combination of doublet fields that take VEV, $h = h_1\cos\beta + h_2\sin\beta$, and its orthogonal one $H = h_1\sin\beta - h_2\cos\beta$. The rotation U from the mass basis to the basis (H, h, S_1) is defined by

$$\begin{pmatrix} s_1 \\ s_2 \\ s_3 \end{pmatrix} = U \begin{pmatrix} H \\ h \\ S_1 \end{pmatrix}\,. \tag{7.1.10}$$

Analogously for the pseudoscalars the rotation matrix P is defined such that

$$\begin{pmatrix} a_1 \\ a_2 \end{pmatrix} = P \begin{pmatrix} \pi^{(3)} \\ S_2 \end{pmatrix}\,. \tag{7.1.11}$$

For the Higgsinos we call V the rotation matrix from the basis (N_1, N_2, N_3) to the mass eigenstates χ_m such that

$$\chi_m = V_{im} N_i \,. \tag{7.1.12}$$

Finally, we introduce the rotation matrix $R^{(x)}$ for a generic angle x

$$R^{(x)} = \begin{pmatrix} \cos x & -\sin x \\ \sin x & \cos x \end{pmatrix} , \tag{7.1.13}$$

such that the states N_n can be written as

$$N_n = \delta_{n3}\tilde{S} + (1-\delta_{n3}) \sum_{i=1,2} R^{(\pi/4)}_{ni} \tilde{H}_i \,. \tag{7.1.14}$$

7.2. LEP direct searches

Using the formulas for the masses of the Higgs bosons and Higgsinos given in Section 7.1, we can impose the bounds from LEP direct searches [**59**], [**60**], [**8**], [**61**]

$$m_h > 114\,\text{GeV}, \tag{7.2.1}$$
$$m_{\chi^+} > 103\,\text{GeV}, \tag{7.2.2}$$
$$m_{H^\pm} > 79\,\text{GeV}, \tag{7.2.3}$$
$$m_{\chi_1} > m_Z/2\,, \tag{7.2.4}$$

and exclude regions of the parameter space accordingly[1].

The union of the constraints from vacuum stability found in Section 6.2 and the constraints from LEP is shown in Figure 7.2.1 for the choice of parameters in (6.3.1) and two variations of λ and $\tan\beta$. The strongest constraint on the parameter space comes from the bound on the neutralino mass given in (7.2.4), which cuts a region in μ around the value given in (7.1.8) where the lightest neutralino is massless. On the other hand, we see that chargino, charged and neutral Higgs boson searches have basically no impact on the physical parameter space, once that the constraints on the scalar potential of Sections 6.2 and 7.1 are imposed. Indeed the maximal chargino mass that could be probed at LEP is less than the minimum allowed μ given in (6.4.7). Analogously, for the neutral and the charged Higgs bosons the typical mass in our model is significantly larger than the bounds and therefore only little restrictions arise from (7.2.1) and (7.2.3).

[1] We are aware of the fact that a χ_1 with mass $m_{\chi_1} < m_Z/2$ might be sufficiently decoupled to not be observable at the Z pole and thus allowed by LEP. For sake of simplicity we shall not impose the exact limits on the cross-section for neutralino production and on the invisible width of the Z boson. For our purpose of showing that a phenomenologically allowed parameter space exists one can impose the simpler condition eq. (7.2.4) .

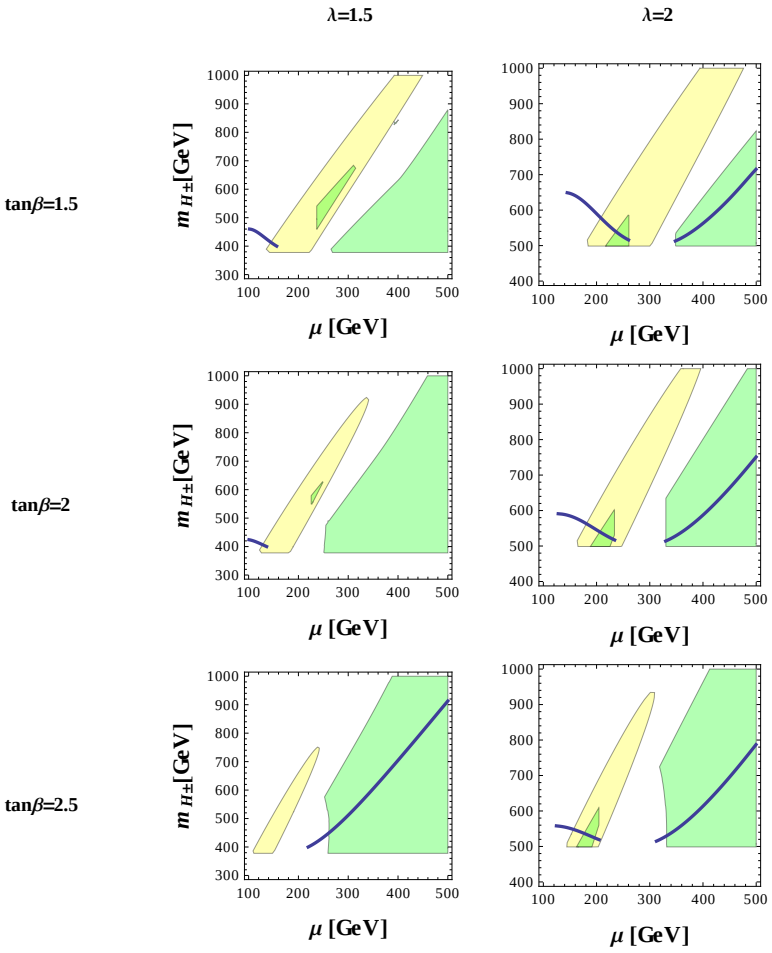

FIGURE 7.2.1. Six panels showing the area of the plane μ, m_{H^+} allowed by the constraints on the minimum discusses in Section 6.2 and LEP direct searches. The left column is for $\lambda = 1.5$ and the right column is for $\lambda = 2$. In each column is shown, from the top to the bottom, the result for $\tan\beta$ equal to 1.5, 2 and 2.5. In all the cases $k = 1.2$, that is representative of the all the cases with $k \sim 1$. The green (dark) region corresponds to the requirements on the minimum of Section 6.2. The yellow (lighter) area corresponds to allowed region by $m_h > 114$ GeV. The phenomenologically viable region is the overlap of the yellow and green regions. A solid blue line indicates the points where $2m_{\chi_1} = m_{a_1}$ and $m_\chi > 45$ GeV.

7.3. Indirect constraints from EWPT

The NMSSM in the large λ regime can have significant impact on the EWPT. Indeed a large λ increases the mass of the Higgs boson, which can have an impact on the EWPT. Furthermore there are other contributions to the

EWPT from the Higgs and Higgsino sector proportional to λ [**1**]. As such, we compute the new physics contributions to the oblique parameters T and S, coming from the new scalars and the new fermions of the model.

Scalar contributions arise from the enlarged Higgs sector and from the sfermions. All the sleptons, the first and second generation of squarks are not restricted to be particularly light by Naturalness arguments (see Section 6.5) and therefore their contribution can be neglected, assuming they are heavy. Third generation squarks are somehow special, indeed we have seen explicitly in Section 6.5 using Naturalness arguments, that they cannot be taken too heavy. Therefore the stop-sbottom system can potentially give a sizeable contribution to the electroweak precision observables T and S which we compute in Section 7.3.2. The contribution arising from the enlarged Higgs sector with a heavy spectrum will be discussed in Section 7.3.3. In the following section, instead, we discuss the contribution from the fermions that, in the limit of heavy gauginos, reduces just to the contribution of the Higgsinos.

7.3.1. Higgsinos. In the basis $N_{1,2,3}$ the interaction Lagrangian of the Higgsinos reads

$$\begin{aligned}(7.3.1)\qquad \mathcal{L} &= -\frac{g_2}{2}W_\mu^+\bar{\chi}^-\left(\gamma^\mu N_1-\gamma^\mu\gamma^5 N_2\right)+h.c.\\ &+ \frac{g_2}{2}W_\mu^3\left(\bar{\chi}^-\gamma^\mu\chi^- + N_1\gamma^\mu\gamma^5 N_2\right)\\ &+ \frac{g_1}{2}B_\mu\left(\bar{\chi}^-\gamma^\mu\chi^- - N_1\gamma^\mu\gamma^5 N_2\right)\,.\end{aligned}$$

Therefore the contributions to T and S can be given using the loop functions $\tilde{F}$ and $\tilde{A}$ given in Appendix A by the expressions

$$\begin{aligned}(7.3.2)\qquad T &= \sum_{i=1,2}\sum_{m=1,2,3}V_{mi}^2\tilde{A}(\mu,m_{\chi_m})+\\ &- \sum_{m=1,2,3}\sum_{n>m}(V_{1m}V_{2n}+V_{1n}V_{2m})^2\tilde{A}(m_{\chi_m},-m_{\chi_n})+\\ &- \frac{1}{2}\sum_{m=1,2,3}(V_{1m}V_{2m}+V_{2m}V_{1m})^2\tilde{A}(m_{\chi_m},-m_{\chi_m})\,,\\ (7.3.3)\qquad S &= \sum_{m=1,2,3}\sum_{n>m}(V_{1m}V_{2n}+V_{1n}V_{2m})^2\tilde{F}(m_{\chi_m},-m_{\chi_n})+\\ &+ \frac{1}{2}\sum_{m=1,2,3}(V_{1m}V_{2m}+V_{1m}V_{2m})^2\tilde{F}(m_{\chi_m},-m_{\chi_m})+\\ &- \tilde{F}(\mu,\mu)\,,\end{aligned}$$

where V is the rotation matrix for the Higgsinos defined in (7.1.12).

In Figure 7.3.1 we present the result as functions of μ and the coupling k for several representative values of $\tan\beta$ and λ. The figure shows that the generic value of the contribution to S is sizable but of the same order of the

experimental uncertainty; on the other hand the value of T is more problematic and deserves some more discussion.

The result of Figure 7.3.1 shows that T prefers small values of both λ and $\tan\beta$, as expected from the dependence of the mass splittings of the Higgsinos on these two parameters. Moreover it shows that values of k close to zero or close the perturbative bound of ~ 1.2 give the best results, with the latter generically giving a better result than the former. This can be understood noting from (7.1.9) that the mass scale of the Higgsinos for fixed λ goes like the product $k\mu$, thus, in general, larger values of k and μ tend to give a smaller contribution to T. However, for any finite value of μ, there is a non-vanishing value of k given by (7.1.8) that renders massless the lightest neutralino. In the regions of the μ, k plane where (7.1.8) is satisfied, and of course in the vicinity of them, the contribution to T is enhanced by the presence of the light state. From this discussion it is clear that for k large enough the critical value of μ is pushed to be smaller than the minimal phenomenologically interesting $\mu \simeq 100$ GeV and that, away from the line where (7.1.8) is satisfied, a larger k gives a smaller contribution to T.

This preference of the EWPT for large values of k gives further motivation to consider the regime of the NMSSM with large coupling k (see eq. (6.3.1)), namely the regime where the PQ symmetry is broken by a large coupling and hence all the states in the CP-odd sector are heavy.

7.3.2. Stop and sbottom squarks. We compute the contribution to S and T in the limit of diagonal squark mass matrices so that the interaction eigenstates for squarks coincide with mass eigenstates and the contribution to S and T are just

$$T = 6A(m_{\tilde{t}_L}, m_{\tilde{b}_L}), \tag{7.3.4}$$

$$S = F(m_{\tilde{b}_L}, m_{\tilde{b}_L}) - F(m_{\tilde{t}_L}, m_{\tilde{t}_L}), \tag{7.3.5}$$

where the loop functions A and F are reported in the Appendix A and the masses of the third generation squarks are given by (6.5.5) and (6.5.6) respectively. In order to estimate the minimal effect of the stop-sbottom, we assume that the soft mass $m_{\tilde{Q}}$ saturates the upper bound due to fine tuning constraints given in (6.5.10).

Both the contributions to T and S are rather small compared to the experimental uncertainties. In Figure 7.3.2 we show the value of T in the plane μ, m_{H^+}, for an allowed fine tuning of 10% and the point of parameter space presented in (6.3.1). We find that, for a 10% fine tuning and for a lightest Higgs boson in accordance with the LEP bound (yellow region in the Figure 7.3.2), the contribution to T is always smaller than ~ 0.04, which is small compared to the contribution coming from Higgsinos. This feature is due to the relatively heavy stops and sbottoms, allowed by Naturalness constraints, and does not change significantly for larger values of $\tan\beta$.

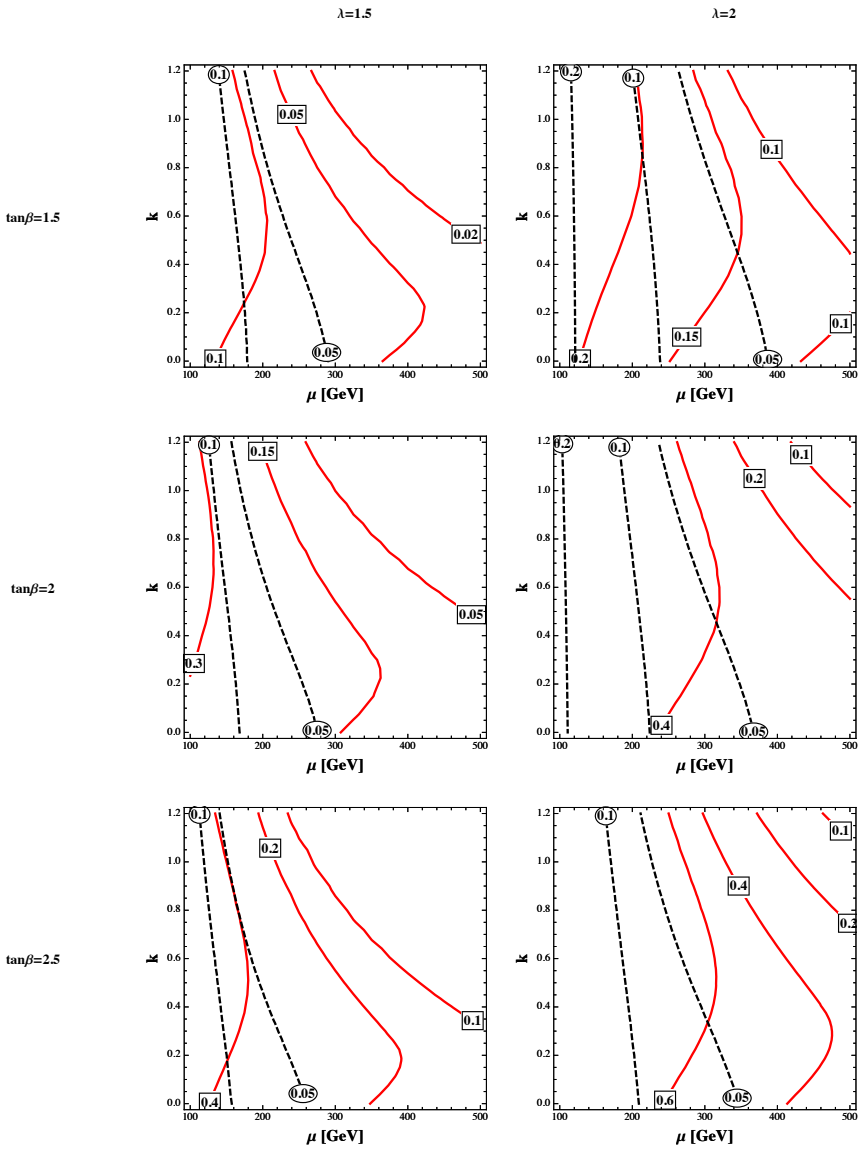

FIGURE 7.3.1. Contribution of the Higgsinos to T and S in the parameter space μ, k for different values of $\tan\beta$ and λ. The left column is for $\lambda = 1.5$, the right column is for $\lambda = 2$. From the top to the bottom of each column are shown the results for $\tan\beta$ equal to 1.5, 2 and 2.5. Solid red lines with squared labels are the contributions to T, dashed black lines with round labels are the contributions to S.

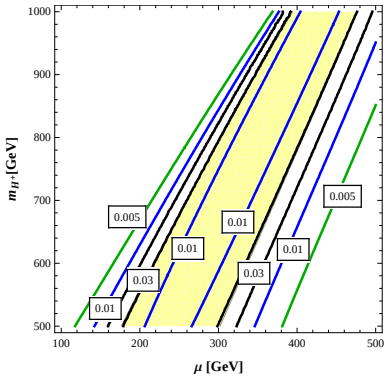

FIGURE 7.3.2. Minimal contribution to T coming from the stop-sbottom sector in the plane μ, m_{H^+} for the reference point of parameter space presented in (6.3.1), in the approximation of no mixing between $\tilde{t}_L$ and $\tilde{t}_R$, and with the stop mass saturating the upper-bound (6.5.10). The overlaid yellow area corresponds to $m_{s_1} > 114$ GeV.

7.3.3. CP-odd and CP-even Higgs bosons . For the Higgs sector we compute the contribution to T and S coming from the three CP-even states and the two CP-odd states. We compute the total value of S and T, taking as zero the value of the LEP Electroweak Working Group [**62**] minus the contribution that arises in the SM from a Higgs boson with a reference mass just above the LEP bound $m_{h_{\rm SM}} = 115\ \ {\rm GeV}$. This latter contribution is given by

$$T(m_{h_{\rm SM}}) = 3\left(A(m_{h_{\rm SM}}, m_Z) - A(m_{h_{\rm SM}}, m_W)\right)\,, \tag{7.3.6}$$

$$S(m_{h_{\rm SM}}) = F(m_{h_{\rm SM}}, m_Z) + m_Z^2 G(m_{h_{\rm SM}}, m_Z)\,, \tag{7.3.7}$$

with the loop functions A, F and G given in the Appendix A.

Subsequently, we add the contributions coming from the enlarged Higgs sector of the theory

$$\begin{aligned} T &= \sum_{i=1}^{3} U_{i2}^2\, T(m_{s_i}) + \sum_{i=1}^{3} U_{i1}^2 A(m_{H^+}, m_{s_i}) + \\ &+ \sum_{j=1}^{2} P_{j1}^2 A(m_{H^+}, m_{a_i}) - \sum_{i=1}^{3}\sum_{j=1}^{2} U_{i1}^2 P_{j1}^2 A(m_{s_i}, m_{a_j})\,, \end{aligned} \tag{7.3.8}$$

$$\begin{aligned} S &= \sum_{i=1}^{3} U_{i2}^2 S(m_{s_i}) + \sum_{i=1}^{3}\sum_{j=1}^{2} U_{i1}^2 P_{j1}^2 F(m_{a_j}, m_{s_i}) + \\ &- F(m_{H^+}, m_{H^+})\,, \end{aligned} \tag{7.3.9}$$

where m_{s_i} and m_{a_i} are the masses of the scalar and pseudoscalar Higgs respectively, the rotation matrices U and P are defined in (7.1.10) and (7.1.11) respectively, and the loop functions F, T, S and A are given in the Appendix A.

Once $\tan\beta$, λ and k are fixed, the mass spectrum and the mixing matrices still depend on the parameters μ, m_{H^+}. Therefore, in place of the customary plot of the position of the model in the S-T plane, we show in Figure 7.3.3 the contribution to T and S in the μ, m_{H^+} plane for representative values of $\tan\beta$ and λ. The contributions are generically well within the experimental uncertainty and sub-dominant with respect to the contributions from the Higgsinos sector computed before.

7.4. Relic abundance of neutralinos

The relic abundance of a heavy particle that decouples as a non-relativistic species can be computed solving its Boltzmann equation [**63**]. The resulting relic abundance is given by the approximate formula

$$\Omega h^2 \simeq \frac{1.07\times 10^9\ \mathrm{GeV}^{-1}}{\sqrt{g_*}M_P(a x_{f.o.}+b x_{f.o.}^2/2)}\,, \tag{7.4.1}$$

where a and b are constants related to the annihilation cross-section of the LSP, $g_*=86.25$ for $m_b \ll T_{f.o.} \lesssim m_W$ is the number of SM degrees of freedom at the time of freeze out, M_P the Planck mass and $x_{f.o.}$ the normalized freeze-out point temperature $x_{f.o.}=T_{f.o.}/m_{LSP}$, with m_{LSP} the mass of the LSP, that in our model is supposed to be the lightest Higgsino χ_1. The freeze-out point can be found solving numerically the equation

$$\frac{1}{x_{f.o.}} \simeq \log\frac{0.037 g_\chi M_P\, m_{LSP}\,\langle\sigma v\rangle\,\sqrt{x_{f.o.}}}{\sqrt{g_*}}, \tag{7.4.2}$$

with $g_\chi=2$.

The only relevant quantity from particle physics is the thermally averaged annihilation cross-section σv of the LSP which can be expanded around its non-relativistic limit as

$$\langle\sigma v\rangle = a + bx\,. \tag{7.4.3}$$

As far as $m_{LSP}<m_W$, the only available contributions to (7.4.3) are those coming from the annihilation $\chi\chi\to f\bar f$. In general this process can be mediated by a s-channel exchange of a Higgs boson or a Z boson, and by the t-channel exchange of a sfermion. Since in this paper we are interested in the case of heavy sfermions (see Section 6.5.1), we shall only investigate the s-channel contributions. The most important contributions to the s-channel can be understood in terms of symmetry arguments. Indeed the annihilation cross-section, as expanded in (7.4.3), corresponds to a partial wave expansion of the annihilation process. Using CP properties of the mediators and the chirality

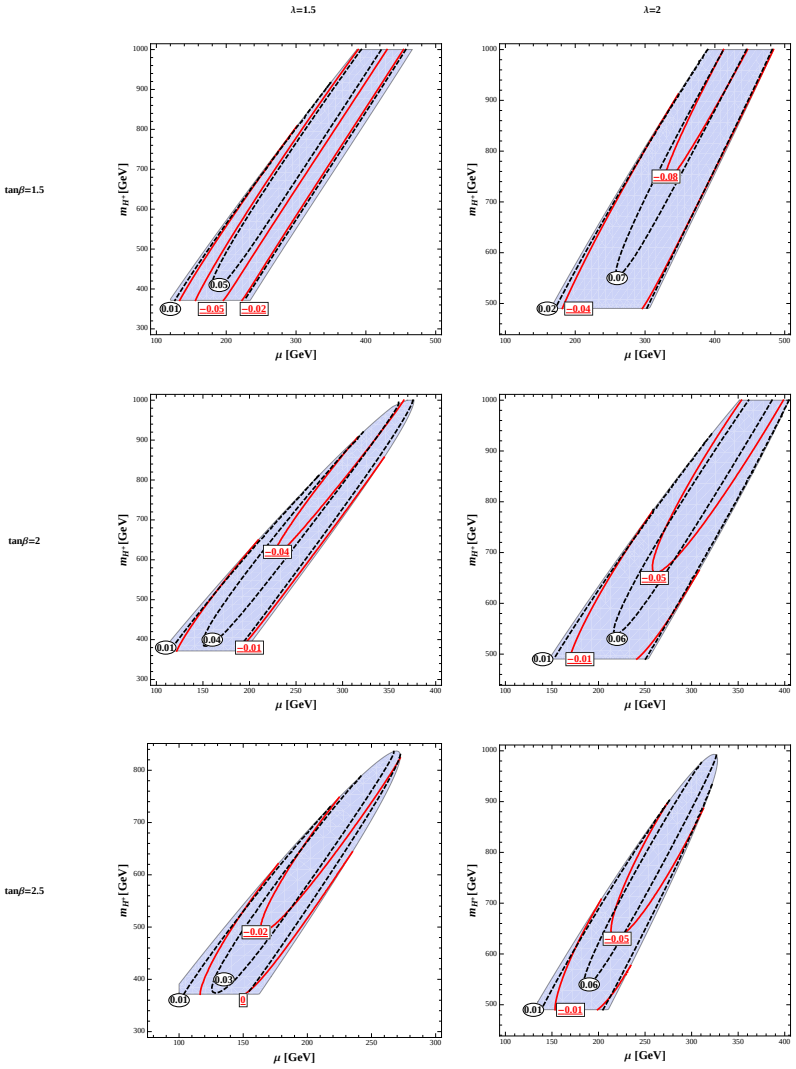

FIGURE 7.3.3. Contribution of the scalar sector to S and T in the plane μ, m_{H^+} for different values of $\tan\beta$ and λ. The left column is for $\lambda = 1.5$, the right column is for $\lambda = 2$. From the top to the bottom of each column are shown the results for $\tan\beta$ equal to 1.5, 2, 2.5. In all the cases $k = 1.2$ and for $k \sim 1$ the results are qualitatively unchanged. Solid red lines with squared labels are the contributions to T, dashed black lines with round labels are the contributions to S. The blue area denotes the region of the plane where all scalars have positive mass squared.

structure of the intervening interactions, one can find that the s-wave annihilation can be mediated only by CP-odd scalars, while the p-wave receives contributions from both a CP-even scalar and the Z boson [**64**]. The s-wave part of the cross-section is typically suppressed by the smallness of the Yukawa couplings involved, with the only exception of the on-shell production of the CP-odd scalar. The line in the parameter space where this condition is fulfilled is shown in Figure 7.2.1 as a solid line. Away from this line we can just repeat the analysis of the previous investigations of Higgsino DM in the large λ regime [**1**]. In fact, making the identification $M \to -2k\mu/\lambda$, the Higgsino sector of our model is equivalent to the one studied in [**1**] and therefore the resulting relic abundance is the same in the two cases.

Above the WW and ZZ threshold new channels open and the LSP can now annihilate via a s-channel exchange of a Z boson or a CP-even Higgs boson, and a t-channel exchange of a chargino. Once again by symmetry arguments the s-channels contribute only to the p-wave, while the t-channel contributes to the s-wave and the p-wave. Also in this case the resulting relic abundance coincides with that one obtained in [**1**].

In Figure 7.4.1, the resulting Ωh^2 is given as a function of μ for different values of $\tan\beta$ for both $\lambda = 1.5$ (on the left) and $\lambda = 2$ (on the right). The features of the curves of Figure 7.4.1 are mainly due to the dependence of the cross-section on the mass of the LSP. In fact, when $m_Z/2 < m_{LSP} < m_W$, the only annihilation channel is that one into fermions that is mediated by an off-shell Z boson, which yields a cross-section behaved as $\sigma \sim 1/m_{LSP}^2$. This means that the relic abundance increases with m_{LSP} until new channels open. When annihilations into WW and ZZ are available, the relic abundance has to decrease accordingly with the opening of the phase-space for the new modes. Altogether the curves have a rise-and-fall shape with a maximum corresponding to $m_{LSP} \simeq m_Z$ and a maximal value being determined by the mixing coefficient that affects the annihilation into fermions.

Generically the annihilation cross-section of the Higgsino DM is too large and the relic abundance is then too low to account for the observed amount of DM, $\Omega h^2 \simeq 0.11$ [**65**]. In spite of this general trend there are regions of the parameter space where $m_{\chi_1} \lesssim m_Z$ and $\tan\beta \lesssim 1.5$ where the LSP has a large singlino component [**1**, **66**] and the relic abundance is reproduced. In those regions of parameter space the model can be tested by direct searches of DM through elastic scattering which we describe in the following section.

7.5. Direct detection of the dark matter

Direct searches of DM particles stored in the halo of our galaxy have been performed and several bounds on the properties of the DM exist [**67**–**69**]. The quantity probed by these experiments is the local DM density times the cross-section of an elastic scattering between a DM particle of mass M and the nuclei of the experiment [**70**]. The local density is typically assumed to be

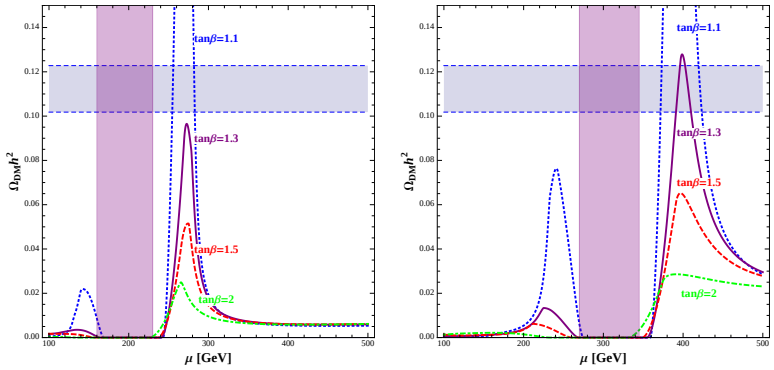

FIGURE 7.4.1. Relic abundance of neutralinos for $\lambda = 1.5$ (left) and $\lambda = 2$ (right). The horizontal blue band corresponds to the 3σ interval from the 7-years WMAP result [**65**]. Dotted blue lines are for $\tan\beta = 1.1$, purple solid lines for $\tan\beta = 1.3$, dashed red lines for $\tan\beta = 1.5$ and finally dot-dashed green lines for $\tan\beta = 2$. The vertical purple shaded area corresponds to $m_{LSP} < m_Z/2$ in the case $\tan\beta = 1.3$.

$0.3\ \mathrm{GeV/cm^3}$, so that bounds are given directly on the DM-nucleon cross-section. Therefore in the following we shall compute the cross-section for the scattering of the LSP of the model on a proton.

As we have already discussed, in our model the sfermions are heavy and the LSP is a mixture of Higgsinos and singlino. Therefore the only particle that can mediate a DM-nucleon scattering is a Higgs boson interacting via the Yukawa couplings dictated by the superpotential:

$$-\mathcal{L}_{yuk} = \frac{\lambda}{\sqrt{2}}(S\tilde{H}_1\tilde{H}_2 + H_1\tilde{S}\tilde{H}_2 + H_2\tilde{H}_1\tilde{S}) + \frac{k}{\sqrt{2}}S\tilde{S}^2 + h.c.\,.$$

These interactions contributes to the effective operator

$$\mathcal{O}_{SI} = \frac{1}{\Lambda^2}\bar{\chi}_1\chi_1\bar{N}N\,, \tag{7.5.1}$$

which mediates the spin-independent elastic scattering of the lightest neutralino χ_1 on a nucleus N probed in [**67–69**].

The elastic cross-section at zero transferred momentum can be written as

$$\sigma_{SI}(\chi_1 p \to \chi_1 p) = \frac{1}{16\pi(m_p + m_{LSP})^2}\,|\mathcal{M}|^2\,, \tag{7.5.2}$$

where the matrix element is given by

$$\mathcal{M} = \sum_m 2m_{LSP}\frac{1}{m_{s_m}^2}g_{\chi\chi s_m}\left[\frac{2m_p^2}{v}\left(\mathcal{U}_{mu}F_u + \mathcal{U}_{md}F_d\right)\right], \tag{7.5.3}$$

where

$$g_{\chi\chi s_m} = \frac{\lambda}{\sqrt{2}} \sum_{(a,b,c)} 2\mathcal{V}_{1a}\mathcal{V}_{1b}\mathcal{U}^{-1}_{cm} + \sqrt{2}k\mathcal{V}^2_{13}\mathcal{U}^{-1}_{3m}\,, \tag{7.5.4}$$

and the indices (a, b, c) run over all the ordered permutations of $(1, 2, 3)$, the matrix $\mathcal{V}$ is the matrix that brings the Higgsinos $\tilde{H}_1, \tilde{H}_2, \tilde{S}$ to the mass eigenstates χ_i and the matrix $\mathcal{U}$ brings the scalar CP-even interaction eigenstates h_1, h_2, S_1 to the mass eigenstates s_m. In particular the $\mathcal{V}$ matrix is related to the matrix V defined in (7.1.12) through $\mathcal{V} = V^t R^{(\pi/4)}$ and $\mathcal{U}$ is related to U of (7.1.10) through $\mathcal{U} = UR^{(\beta-\pi/2)}$.

The effect of heavy quarks in the nucleon is taken into account according to [**71**] and incorporated in the values of F_u and F_d which we take from chiral perturbation theory respectively equal to 0.11 ± 0.02 and 0.44 ± 0.13 [**72**] or, from QCD on the lattice, 0.14 ± 0.02 and 0.23 ± 0.01 [**73**].

The quantity affecting the most the cross-section σ_{SI} is the mass of the lightest Higgs boson which is the scale that suppresses the operator of the interaction (7.5.1). In fact, the spin-independent cross section can be estimated as

$$\sigma_{SI} \simeq \frac{1}{16\pi}\frac{m_p^2}{v^2}\frac{m_p^2}{m_{s_1}^4} \simeq 10^{-43}\mathrm{cm}^2 \left(\frac{200\ \mathrm{GeV}}{m_{s_1}}\right)^4\,, \tag{7.5.5}$$

that is of the order of the sensitivity of current experiments. Therefore direct searches of WIMPs can significantly restrict the allowed parameter space where $\Omega h^2 \lesssim 0.1$ [**65**]. From the previous section, we know that for $1.5 < \lambda < 2$ such interesting regions are those with $\tan\beta \lesssim 1.5$ and m_{H^+} and μ in the regions outlined in Figure 7.2.1.

Given the relevance of the mass of the lightest Higgs for the cross-section, the latter has a significant dependence on the parameters of the scalar sector μ and m_{H^+}. However none of the two is of direct significance for the experiments that, on the contrary, probe m_{LSP}. Thus we shall show our result trading μ for m_{LSP} and we shall fix some representative values of m_{H^+} taken in the range that is allowed by all the constraints on the scalar potential analyzed in Section 6.2. The resulting DM-nucleon cross-section is given in Figure 7.5.1 as a solid and a dashed thin line, obtained using hadronic matrix elements from [**73**] and [**72**] respectively and assuming that the LSP accounts for the entire dark matter in the Universe. However the actual rate of DM-nuclei scattering in the model is typically reduced by the scarce amount of thermal relic neutralinos, therefore in Figure 7.5.1 we give also thick lines which correspond to the prediction of the model taking this reduction into account.

From the thin lines in Figure 7.5.1, we see that the predicted cross section is typically above the lower bounds from experiments. This shows that in this model is difficult to reproduce the relic abundance of the dark matter without violating the experimental limits on WIMP scattering.

On the other hand when one takes into account the actual abundance of LSP computed in Section 7.4 the limits from direct detection experiments are

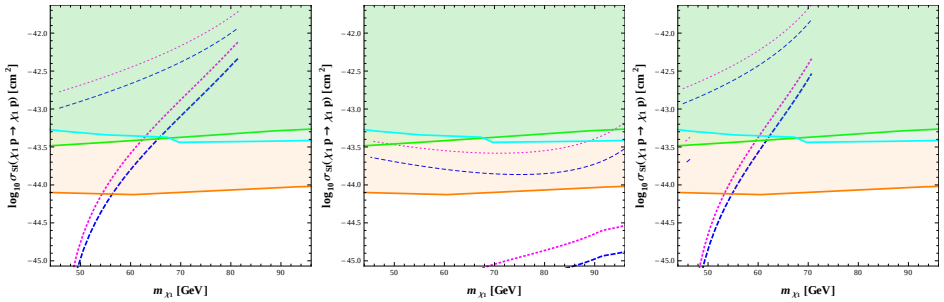

FIGURE 7.5.1. Three panels showing the prediction of the spin-independent DM-proton scattering cross-section fixing $\tan\beta = 1.5$. On the left for $\lambda = 1.5$ and $m_{H^+} = 500$ GeV, in the middle $\lambda = 2$ and $m_{H^+} = 550$ GeV, on the right $\lambda = 2$ and $m_{H^+} = 700$ GeV. The dashed and solid lines correspond to the prediction obtained taking the values of the hadronic matrix element from [**72**] and from [**73**] respectively. Thick lines show the prediction of the model once the actual relic abundance is taken into account. The shaded orange, green and cyan areas are those excluded by Xenon 2011 [**67**], Xenon 2007 [**68**] and CDMS 2009 [**69**] respectively.

less stringent. The region of low m_{H^+} tends to be below the limits because of a low nucleon-DM cross-section and a low relic abundance, while for larger m_{H^+} the regions corresponding to $m_{\chi_1} > 60$ GeV are typically excluded. In both cases the region that is compatible with direct WIMP searches indicates a preference for small of $\mu \sim (200 - 300)$ GeV.

CHAPTER 8

A strongish self-coupled Higgs sector at the LHC

In the preceding Chapters we have outlined and discussed in details a class of supersymmetric models where the Higgs boson is significantly heavier than the Z boson. The very origin of this large mass is the strongish self-coupling of the Higgs sector. The supersymmetric nature of the model enforces this strong coupling to appear in the Higgsino sector as well. Therefore we expect large Yukawa interaction among Higgs scalars and higgsinos.

We have already discussed the possible direct effects of this large coupling in the direct detection of the dark matter. In this Chapter we shall discuss the observable consequences of this strongish coupling for the LHC phenomenology. In this discussion we shall consider two possible λSUSY scenarios.

The first scenario is the scenario that naturally emerges in the model proposed to dynamically generate the μ term and discussed at length in the Chapters 6 and 7. It is characterized by a singlet S with VEV of the order of the VEV v of the MSSM Higgs. The scalar and pseudoscalar mass eigenstates are rather even mixtures of the interaction eigenstates. All the mass eigenstates are expected to be significantly coupled to the MSSM matter although with significant deviations from the coupling of a SM-like Higgs boson of the same mass. This scenario therefore is expected to offer many hints signaling deviations in the Higgs sector from the SM or MSSM picture.

The second scenario that we shall discuss is the scenario originally discussed in [**1**] and [**3**]. In this case the μ term of the superpotential is put by hand. The model breaks the PQ symmetry putting by hand a mass for the singlet S. The mass of this singlet can be large without reintroducing fine-tuning, as it has only limited impact on the RGE. For this reason the model can naturally go in a limit where the singlet is decoupled from the rest of the fields.

From the analysis of the EWPT, and to help to generate a large mass for the Higgs boson, this model prefers a moderate or small value of $\tan\beta \lesssim 3$. With such a small $\tan\beta$ the lightest Higgs boson is coupled in rather SM-like manner.

The luminosity needed at the LHC to discover such a SM-like Higgs boson is expected to be close to the luminosity needed to discover the gluino up to roughly 1 TeV. The same luminosity is expected to be sufficient for the evidence of squarks in a similar mass range. Hence in this scenario we expect the discovery of supersymmetry and the discovery of a Higgs boson with properties

completely different from those of the MSSM Higgs boson. The emerging picture will certainly compel to search the other states of the Higgs sector. Studying the properties of these heavier states, in Sections 8.5, 8.6 and 8.7 we shall find distinctive and observable signatures of λSUSY.

We shall articulate our discussion following the expected timeline of discoveries. Thus we shall first discuss the discovery of gluinos and stop in Section 8.1. Then in Section 8.2 we shall discuss the possibilities for the lightest Higgs in the two scenarios outlined above. We shall see that in the scenario with the largely mixed singlet there are clean and distinctive features of λSUSY that can be observed already at the time of the discovery of the lightest Higgs boson. In the following Sections 8.5 8.6 and 8.7 we shall discuss the distinctive signatures of λSUSY observable in the long run of LHC in the scenario with small mixing between the singlet and the doublet.

8.1. Gluino and stop

The standard way to discover SUSY at the LHC is via pair-production of squarks and gluinos [**74**, **75**]:

$$pp \to \tilde{g}\tilde{g},\, \tilde{q}\tilde{g},\, \tilde{q}\tilde{q}\ .$$

Since these sparticles are strongly interacting, the production cross section can be larger than a pb in a large range of masses that extends up to one TeV [**76**]. The produced sparticles give rise to well-studied cascade decays with lightest neutralinos in the final state, giving events with several jets, leptons and missing E_T. The invariant mass spectrum of the decay products allow to constrain the masses of the particles involved in the chain. In the following we shall assume to be able to roughly determine the mass of discovered sparticles [1].

The majority of available studies [**74**,**75**] of this signal focus on the mSUGRA case, which gives degenerate squark spectra. While the same discovery strategy will apply also in the λSUSY case, the discovery is expected to be more difficult due to the fact that only stop squarks may be light enough to be produced. For a rough estimate we can use the existing study [**77**] of the LHC discovery potential in the case of effective supersymmetry [**52**]. Indeed in this scenario the 1st and 2second generation squarks are decoupled, while sbottom and stop masses are similar. However, notice that in λSUSY the LSP is expected to be relatively light with respect to the gaugino and stop (see Section 5.4), which helps the discovery. According to [**77**], in this favorable case 10 fb^{-1} of integrated luminosity at $\sqrt{s} = 14$ TeV should be enough for a discovery of SUSY in the entire range (5.5.1) of stop and gluino masses suggested by Naturalness.

[1] A typical example could be $m_{\tilde{t}} > m(llq)_{max}$ in $\tilde{t} \to llq\chi_0^1$.

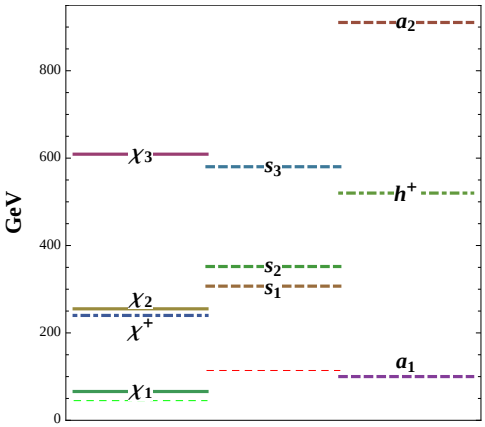

FIGURE 8.3.1. The spectrum of the model for fixed parameters as in eqs. (6.3.1) and (8.3.1). Solid lines correspond to neutral fermions, dashed lines to CP-even and CP-odd scalars, dot-dashed lines to charged particles. The two thin dashed lines correspond to $m_Z/2$ (in green) and 114 GeV (in red).

8.2. The lightest Higgs boson

The properties of the colored particles cannot tell much about the structure of the Higgs sector. To obtain information on the Higgs states it is necessary to discover the scalars and pseudoscalars of the model and study in detail their properties. We outlined two scenarios, one with a large singlet-doublet mixing and another with negligible mixing. In the two following sections we shall describe how their lightest Higgs boson appears at the LHC.

8.3. The case of the mixed singlet scalar

The spectrum of the model with large singlet-doublet mixing is described in Section 7.1. Here we shall fix a representative point of the parameter space given in eq. (6.3.1). Furthermore we shall fix the remaining parameters

$$\mu = 240 \text{ GeV}\,, \quad m_{H^+} = 520 \text{ GeV}\,. \tag{8.3.1}$$

The resulting spectrum is given in Figure 8.3.1 and shows several interesting features. We notice that there is a light neutralino as LSP, χ_1, a second lightest neutralino, χ_2, rather close to the chargino, χ^+, of mass μ, and a significantly heavier χ_3. In the scalar sector we find a relatively heavy lightest CP-even Higgs boson, s_1, that is rather close to its maximal mass (3.6.28) and to the second CP-even state, s_2. Both these scalar states have a mass of order λv and from the relation (6.4.8) we deduce that their closeness to the fermionic states χ^+ and χ_2 is in fact generic in the entire region of parameter space allowed by all the constraints discussed in Chapters 6 and 7. The pseudo-scalars always have a heavy state close to the TeV and a light state of roughly few hundreds of GeV. This large separation between the pseudo-scalars is the result

of a significant level-repulsion effect arising from the large mixing between the two states. Because of this effect, it is rather typical to have a spectrum with $2m_{a_1} < m_{s_1}$.

The precise values of the masses in the point defined by eqs. (6.3.1) and (8.3.1) are

$$m_{s_1} = 305 \text{ GeV}\,, \quad m_{s_2} = 353 \text{ GeV}\,, \quad m_{s_3} = 573 \text{ GeV}\,, \tag{8.3.2}$$

$$m_{\chi_1} = 66 \text{ GeV}\,, \quad m_{\chi_2} = 255 \text{ GeV}\,, \quad m_{\chi_3} = 609 \text{ GeV}\,, \tag{8.3.3}$$

$$m_{a_1} = 100 \text{ GeV}\,, \quad m_{a_2} = 905 \text{ GeV}\,. \tag{8.3.4}$$

8.3.1. Production of the new states. We want to focus on the production of the scalar particles as they provide a direct handle on λ, the characteristic coupling of the model. Furthermore the production of scalars is well studied in the SM and can be easily understood in terms of ratios between a coupling of a scalar of our model and the corresponding coupling of the SM Higgs boson of equal mass. In such a way one inherits all the studies available in the literature about (differential and inclusive) QCD effects in Higgs production. The ratios directly affecting the cross-section of the partonic production process

$$gg \to s_i, a_j \tag{8.3.5}$$

are those of the couplings of up-type quarks to CP-even and CP-odd scalars denoted respectively by ξ_{tts_i} and ξ_{tta_j} and given by

$$\xi_{tts_i} = (\sin\beta U^*_{i2} - \cos\beta U^*_{i1})^2\,, \tag{8.3.6}$$

$$\xi_{tta_j} = \cos\beta^2 P^2_{j1}\,, \tag{8.3.7}$$

where the matrices U and P are defined in (7.1.10) and (7.1.11) respectively.

The reduced couplings squared ξ_{tts_i} for the the CP-even Higgs bosons are shown in Figure 8.3.2 in the relevant region of the plane μ, m_{H^+} after that the constraints on the scalar potential, the constraints from direct searches at LEP, and from direct dark matter searches are imposed.

The state s_1 is in general significantly coupled to the up-type quarks and it has, over the majority of the parameter space, a cross-section of at least 50% of the one of the SM Higgs boson with the same mass. The state s_2, on the contrary, has at most 30% of the cross-section of the SM Higgs boson of equal mass. The converse of this slight decoupling of s_2 is the relatively large coupling of s_3, which can have a cross-section up to 15% of the one of the SM Higgs boson of the same mass. This quantitative analysis shows that the scalar CP-even sector consists altogether of three states all significantly coupled to up-type quarks. In particular we find remarkable to have such a large coupling for the heaviest state, s_3. In general such mixing scenario seems favorable for the discovery of states beyond the lightest one.

For the pseudo-scalars the value of the couplings to the up-type quarks are mainly determined by the fact that the two mass eigenstates are almost maximal admixtures of singlet and doublet interaction eigenstates. As such,

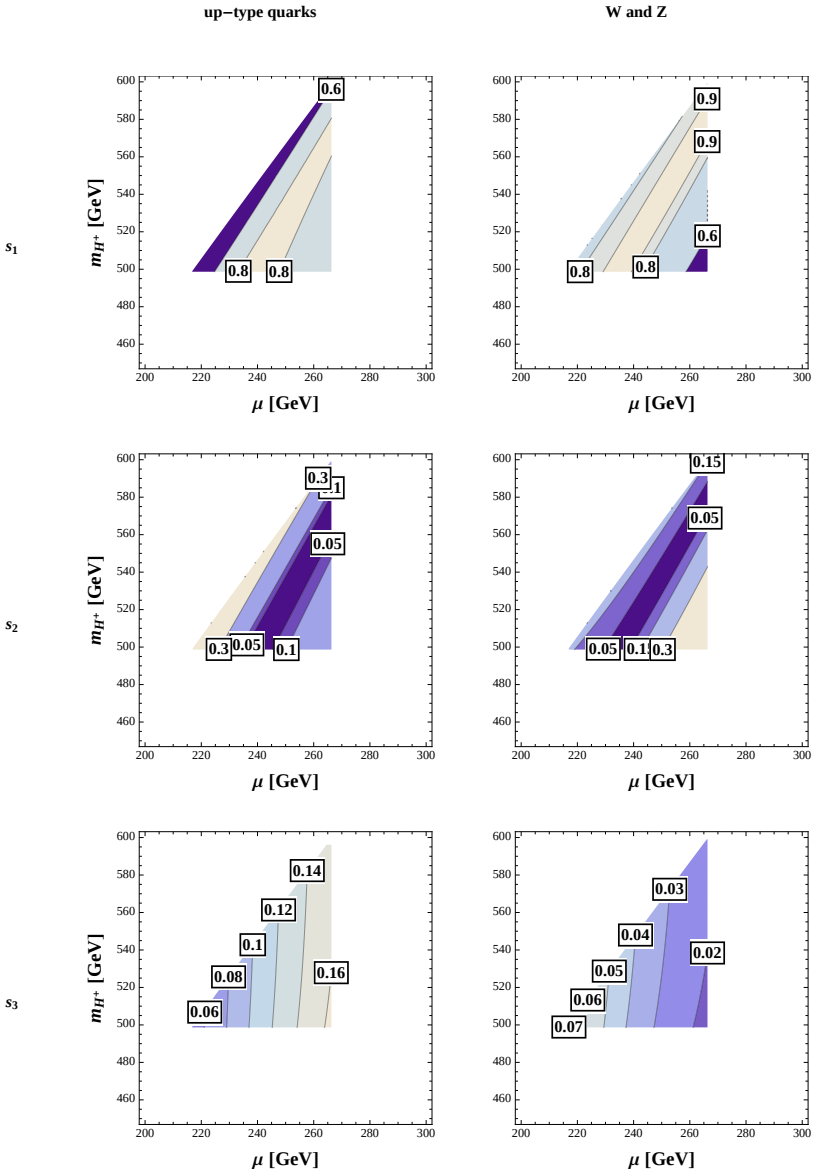

FIGURE 8.3.2. (Left column) Reduced couplings squared of the up-type quarks with the CP-even scalars as defined in (8.3.6). (Right column) Reduced couplings squared of the SM vectors with the CP-even scalars as defined in (8.3.9).

the two states nearly equally share a coupling equivalent to a fraction $\cos\beta$ of the Yukawa of the SM Higgs boson. In particular, for the case of the point of parameter space (6.3.1) and (8.3.1), we obtain $\xi_{tta_1} \simeq 0.16$ and $\xi_{tta_2} \simeq 0.14$.

For the partonic production processes

$$qq \to VVqq \to qqs_i \text{ and } q\bar{q} \to VVq\bar{q} \to q\bar{q}s_i\,, \tag{8.3.8}$$

we define the reduced couplings squared

$$\xi_{VVs_i} = U_{i2}^2\,. \tag{8.3.9}$$

In this case, as we observe in Figure 8.3.2, the heavy states s_2 and s_3 are more decoupled, thus their discovery in the vector boson fusion processes (8.3.8) is considerably more difficult than for a SM Higgs boson of the same mass.

Finally, the fermionic states $\chi_1, \chi_2, \chi_3, \chi^+$ are produced through their gauge couplings, as in the MSSM. Similarly, the production of H^+ will occur through its gauge and Yukawa interactions, as it happens in the MSSM.

8.3.2. Decays. The ordering of the masses shown in Figure 8.3.1 and dimensional considerations on the decay width allows for a rough determination of the relevant decay channels of each state. We discuss some of them beginning from the lowest lying states.

The state χ_1 is the lightest particle with negative R-parity and therefore it is stable. As well known its production results in large amount of missing transverse momentum.

The next lightest state is typically a_1 that, due to kinematics, can decay only in SM fermion pairs. Therefore its main decay modes are

$$a_1 \to b\bar{b}\,, \tag{8.3.10}$$

$$a_1 \to \tau\bar{\tau}\,. \tag{8.3.11}$$

The lightest CP-even state, s_1, has the usual decays into SM vector bosons

$$s_1 \to ZZ\,, \quad s_1 \to WW\,, \tag{8.3.12}$$

and the non-SM decays

$$s_1 \to a_1a_1\,, \tag{8.3.13}$$

$$s_1 \to a_1Z\,, \tag{8.3.14}$$

$$s_1 \to \chi_1\chi_1\,, \tag{8.3.15}$$

$$s_1 \to \chi_1\chi_2\,. \tag{8.3.16}$$

However, due to the fact that $m_{s_1} \simeq \mu \simeq m_{\chi_2}$, the decay $s_1 \to \chi_2\chi_1$ is not available over the majority of the interesting parameter space.

The state s_1 has a total width of several tens of GeV, as show in figure 8.3.3. The contribution from the non SM-like decays is sizeable and therefore the decays into W^-W^+, which would be dominant for a SM-like state, is always sub-dominant, as shown by the branching fraction into W^-W^+ shown in figure 8.3.4.

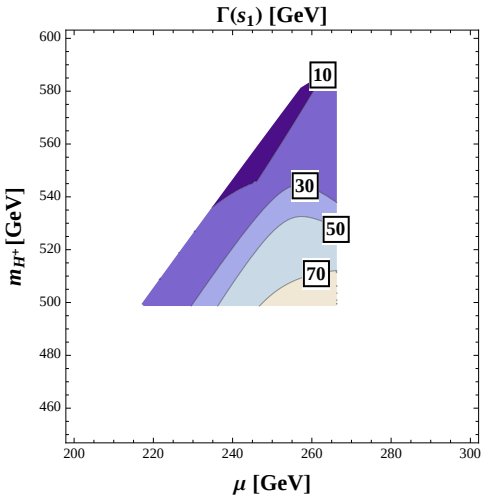

FIGURE 8.3.3. The total width of the lightest CP-even Higgs boson in the region of parameters space compatible with direct constraints from LEP, dark matter searches and the stability of the potential.

The reduced rate of the resonant production of W^-W^+ through Higgs states that results from the lessening of branching fraction and the Higgs production cross section is the first evidence of the non-SM nature of the Higgs boson that we expect to show up at the LHC. The reduced production rate of vectors motivates the search of the Higgs boson in other final states. As show in figure 8.3.5, when kinematically accessible, the decay into pseudoscalars $s_1 \to a_1 a_1$ is dominant. The process

$$gg \to h \to a_1 a_1 \to \tau\bar{\tau} b\bar{b}\,, \tag{8.3.17}$$

is potentially interesting to clarify the reason of the reduced production rate of resonant W^+W^- pairs. However we observe that the decay into pseudoscalar is dominant especially where the SM-like decay into vectors is more suppressed. As such we find that the Higgs boson could be observed earlier in the non-SM decay $s_1 \to a_1 a_1$. A search for the Higgs boson in the channel eq. (8.3.17) might well be in the reach of the first few fb^{-1} of luminosity of LHC at 7 TeV center of mass energy [**78**].

Among the non-SM decay modes of the state s_1 the decay into LSP is particularly interesting because it results in an invisible decay width of the Higgs boson of up to ~ 10 GeV, as shown in figure 8.3.6. The presence of a sizable invisible width is a sign of the strongish coupling λ and therefore represents an indication of λSUSY. The invisible width can be measured reconstructing the line-shape of the Higgs resonance using decay modes in clean final states as $s_1 \to ZZ \to 4\ell$ and comparing the total width of the resonance with the widths of the observable channels. The measurement becomes easier when the decay into pseudoscalars is absent as the decay into ZZ gets a larger branching fraction. As such the measurement of the invisible width helps to

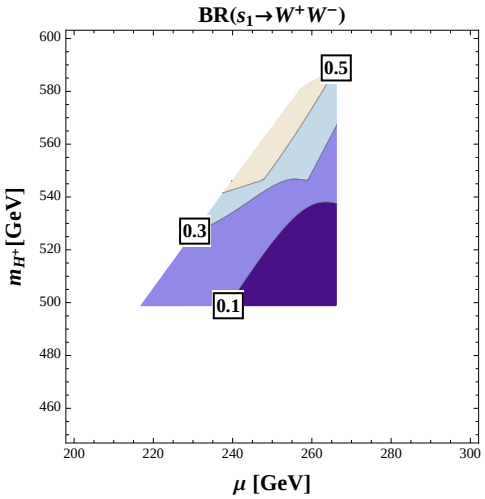

FIGURE 8.3.4. The branching fraction of the lightest CP-even Higgs boson into W^-W^+ in the region of parameters space compatible with direct constraints from LEP, dark matter searches and the stability of the potential.

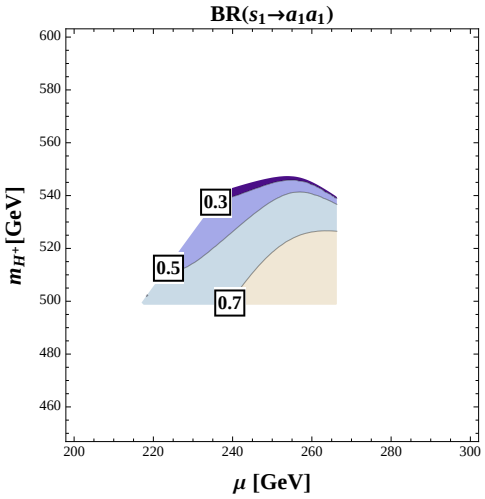

FIGURE 8.3.5. The branching fraction of the lightest CP-even Higgs boson into $a1a1$ in the region of parameters space compatible with direct constraints from LEP, dark matter searches and the stability of the potential.

cover the portion of parameters space where the decay into pseudoscalars is not available.

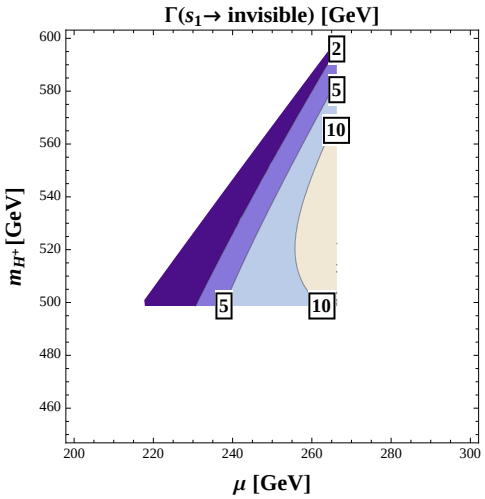

FIGURE 8.3.6. The invisible width of the lightest CP-even Higgs boson due to the decay into $\chi_1\chi_1$ in the region of parameters space compatible with direct constraints from LEP, dark matter searches and the stability of the potential.

	ZZ	WW	$t\bar{t}$	$\chi_1\chi_1$	$\chi_1\chi_2$	a_1Z	a_1a_1	Γ [GeV]
s_1	0.088	0.196	0	0.09	0	0.059	0.568	30.3
s_2	0.004	0.008	0.002	0.179	0.027	0.001	0.782	33.6
s_3	0.023	0.047	0.039	0.461	0.013	0.165	0.255	48.2

TABLE 1. The branching fractions and the total widths of the CP-even scalars computed with parameters fixed as in eqs. (6.3.1) and (8.3.1).

The states s_2 and s_3 are typically not heavy enough to decay into pairs of s_1, thus the results of previous studies contained in [**3**] are not applicable to this case. We have seen in Figure 8.3.2 that s_2 and s_3 are relatively decoupled from SM vectors, therefore the relevant modes are

$$s_{2,3} \to a_1 Z \text{ and } s_{2,3} \to a_1 a_1 \,, \tag{8.3.18}$$

and those into fermions. For the latter case we notice that the modes

$$s_{2,3} \to \chi_1\chi_2 \text{ and } s_{2,3} \to t\bar{t} \tag{8.3.19}$$

are always kinematically allowed. However, because of the mass dependence of the partial widths and the largeness of λ and k, we expect the decays involving a_1 of (8.3.18) to be dominant.

The branching fractions and the total widths of the CP-even scalars computed with parameters fixed as in (6.3.1) and (8.3.1) are given in Table 1.

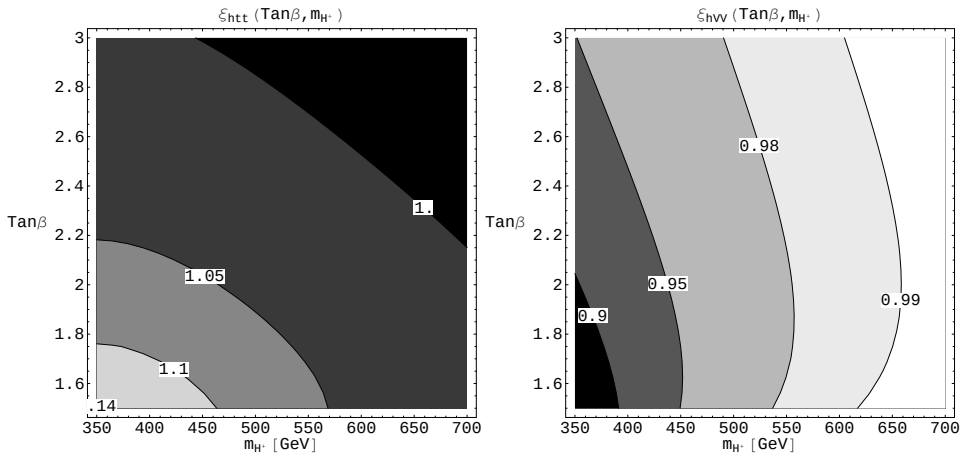

FIGURE 8.4.1. The couplings of h with SM matter normalized to the SM values: ξ_{htt} (left) and ξ_{hVV} (right) for $\lambda = 2$ and the rest of the parameters as in eq. (5.3.6).

Due to the heaviness of the charged Higgs boson H^+, the only two-body decay mode available for the chargino is

$$\chi^+ \to \chi_1 W^+ \,.$$

Similarly, the fact that $m_{s_1} \gtrsim m_{\chi_2}$ implies that the only relevant modes for χ_2 are the two-body decays

$$\chi_2 \to \chi_1 Z \text{ and } \chi_2 \to \chi_1 a_1 \,.$$

The situation for a_2 is more involved as it has all the following decay channels: $a_2 \to s_j a_1$, $a_2 \to Z s_k$, $a_2 \to f_{SM}\bar{f}_{SM}$, $a_2 \to \chi_i \chi_j$. Among the available decay modes, more than one involves large couplings and/or large final state multiplicities. As such, a detailed computation of the partial width is needed to determine which channel actually dominates.

8.4. The case of the decoupled singlet scalar

When the singlet has a large supersymmetric mass M or happen to not be mixed to the doublet fields, the Higgs sector tends to have branching ratios similar to the MSSM, despite the important difference of the large mass of the lightest Higgs boson.

To identify the production mechanism of this Higgs boson we first find the largest couplings of h with SM particles, which are the couplings with the top and with the W and Z bosons. In the case of small mixing between the singlet and the Higgs doublets we can use the standard 2 Higgs Doublet Model (2HDM) result for these couplings. They are equal to the coupling of the SM

Higgs boson times the following factors:

$$\xi_{htt} = \frac{\cos\alpha}{\sin\beta}, \quad \xi_{hVV} = \sin(\beta-\alpha)\,.$$

The values of the couplings normalized to the SM value are given in Fig. 8.4.1. We see that these factors are very close to one (within 10%) in the whole parameter space of Eq. (5.3.6), and thus the properties of h are very similar to those of the SM Higgs boson. In particular, the dominant production process is via the gluon fusion with top quark in the loop.

For the decay the total width of the Higgs boson is saturated by the decays into vectors, which is exactly what is expected for the SM Higgs in the $200-300$ GeV mass range. The discovery of the Higgs boson can be made with 5σ confidence level (CL) in the "gold-plated" channel $h \to ZZ \to l^+l^-l^+l^-$, with as little as 5 fb^{-1} of integrated luminosity [**74**], [**75**]. The mass of h will also be easily measurable thanks to good energy resolution of the final leptons. Ref. [**75**] report that 30 fb^{-1} will be enough to measure m_h with a relative error of order 10^{-3}.

At the time the discovery of this Higgs boson will be possible, there are serious chances that the colored superpartners will have been already discovered. In that case it will be necessary to investigate the differences of the Higgs boson h with respect to the SM Higgs boson. The gluon-fusion cross section of the Higgs boson originate from a coupling between the gluons and the Higgs that arise only at one-loop level. This fact makes the coupling of the Higgs to the gluons a very sensitive probe of the new physics seen by the Higgs [**79**]. In our model the major source of deviation from the SM is the stop loop contribution. The effect of the stop on the gluon fusion cross section can be parametrized by

$$K(\sigma_h)_{stop} = \frac{\sigma_h(stop+top)}{\sigma_h(top)}.$$

This factor is the ratio of the h production cross section summing stop and top diagrams over the cross section with only top loops.

We computed the cross section including the stop contribution using the results reported in [**29**]. Neglecting small effects from D-terms, the relevant parameters are: the SUSY breaking stop masses $m^2_{\tilde{t}_R}$ and $m^2_{\tilde{t}_L}$„ the top soft trilinear breaking A_t, μ, , α and β. Using Eq. (5.3.4) we can trade α for m_{H^+}. In Figure 8.4.2 we present the factor $K(\sigma_h)_{stop}$ as a function of A_t and the average stop mass $\bar{m}_{\tilde{t}} \equiv (m_{\tilde{t_1}} + m_{\tilde{t_2}})/2$ for the choice of parameters:

(8.4.1)
$$\tan\beta = 2, \;\; m_{H^+} = 500 \text{ GeV},$$
$$|m_{L,\tilde{t}} - m_{R,\tilde{t}}| = 100 \text{ GeV}, \;\; \mu = 250 \text{ GeV}.$$

The cross section results quite insensitive to variations of the fixed parameters. The stop loop contribution is less than 20% in most of the parameter

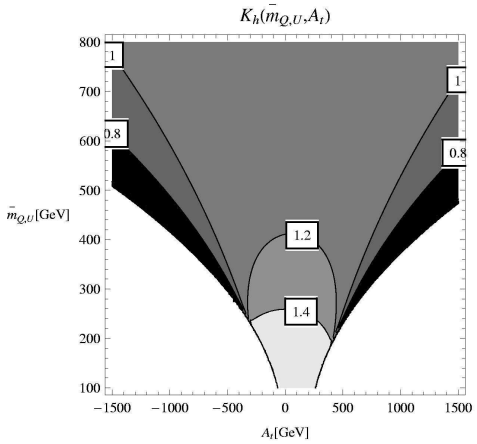

FIGURE 8.4.2. $K(\sigma_h)_{stop}$ plotted in the parameter space of the average stop mass, $\bar{m}_{\tilde{t}}$, and the top trilinear SUSY breaking term A_t. Parameters were fixed accordingly to Eq. (8.4.1). The two white areas in the lower left and lower right corners yields $m_{\tilde{t}} \leq 100$ GeV and are therefore excluded by direct stop searches [**80**] (see right panel in Fig. 8.6.3).

space, which is numerically comparable with NNLO QCD effect. The smallness of the supersymmetric contribution to the gluon fusion cross section renders very difficult to distinguish this Higgs boson from a SM one by looking at the production rate.

The generic difficulty to distinguish a SM Higgs boson from the lightest Higgs boson of the scenario with a decoupled singlet motivates the search for other states of the Higgs sector. The existence of such states would clearly signal a Higgs sector different from the SM and the detailed properties of these states can have traces of the strongish self-coupling of the Higgs sector of λSUSY.

8.5. The heavy Higgs bosons in the decoupled singlet scenario

The discovery of both a SM-like Higgs boson with a $200 - 300$ GeV mass and strongly-interacting cascade-decaying heavy particles will will give a strong evidence for supersymmetry but at the same time rule out the MSSM as the underlying theory. Indeed, in the MSSM, the lightest Higgs boson mass has a theoretical upper bound of about 140 GeV and there is no way to make the model compatible with the phenomenology of sections 8.1 and 8.4. Same conclusion holds for all other SUSY models considered in Section 3.6. For this reason, at the time 10 fb^{-1} will be available, we could have a very puzzling picture with a heavy Higgs on one side and typical supersymmetric events on the other side. Since $\lambda SUSY$ is a possible solution to this puzzle we should look closer to the heavier scalars and ask ourselves if their detection can give an experimental evidence for this model.

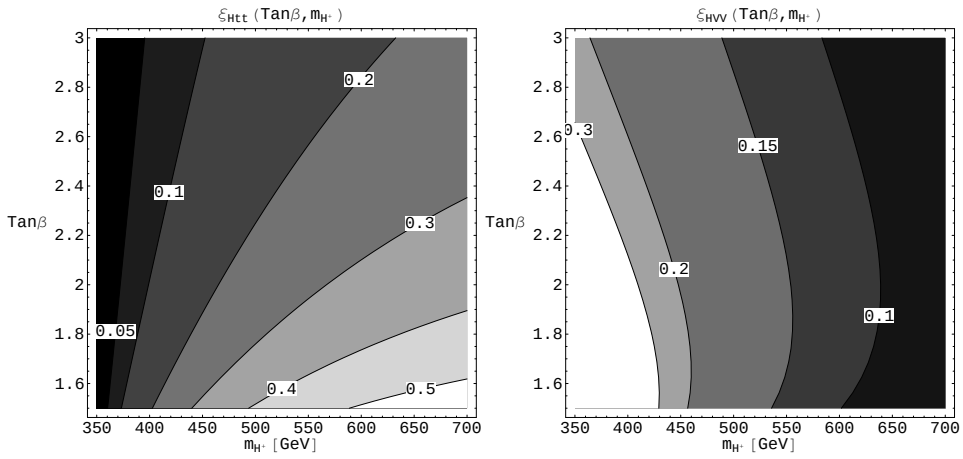

FIGURE 8.6.1. ξ_{Htt}(left) and ξ_{HVV}(right) plotted in the range (5.3.6) for $\lambda = 2$.

To answer this question we assume h, $\tilde{g}$ and $\tilde{t}$ have been observed and m_h is known, then we turn to study the discovery reach for H and A. In fact, measuring m_h,m_H and m_A we can determine $m_{H^\pm}, \tan\beta$ and λ (see Section 5.3) and make the theory predictive. Knowing λ, we can say what is the scale of compositeness/strong coupling, which is very important to support λSUSY hypothesis. Moreover, we can look for a charged Higgs boson whose mass is now given by the theory[2].

In our discussion we shall always assume $\lambda = 2$ and $\tan\beta$ and $m_{H^\pm}$ belonging to the preferred range (5.3.6). More specific Monte Carlo studies will be performed for a benchmark point

$$m_{H^\pm} = 500 \text{ GeV}, \quad \tan\beta = 2\,. \tag{8.5.1}$$

8.6. The heavy CP-even scalar

8.6.1. Production. From the discussion of the spectrum of the theory, and in particular eq. (5.3.4) and Fig. 5.3.2 , we see that the heavy CP-even Higgs boson H has mass in the 500-800 GeV range. Due to the large supersymmetric mass M of the singlet Its couplings to fermions and electroweak gauge bosons are equal to the couplings of the SM Higgs boson times the factors of the 2HDM

$$\xi_{Htt} = \frac{\sin\alpha}{\sin\beta}, \quad \xi_{Hbb} = \frac{\cos\alpha}{\cos\beta}, \quad \xi_{HVV} = \cos(\beta-\alpha)\,,$$

which we show in fig. 8.6. Couplings to stop can be found in Ref. [**29**].

Production can occur in both gluon fusion and weak boson fusion process. In particular gluon fusion can have both a top and stop loop diagrams. As a matter of fact the bottom loop contribution can safely be neglected because

[2]Although very important, the issue of observability of H^+ will not be covered here and we leave its study to the future.

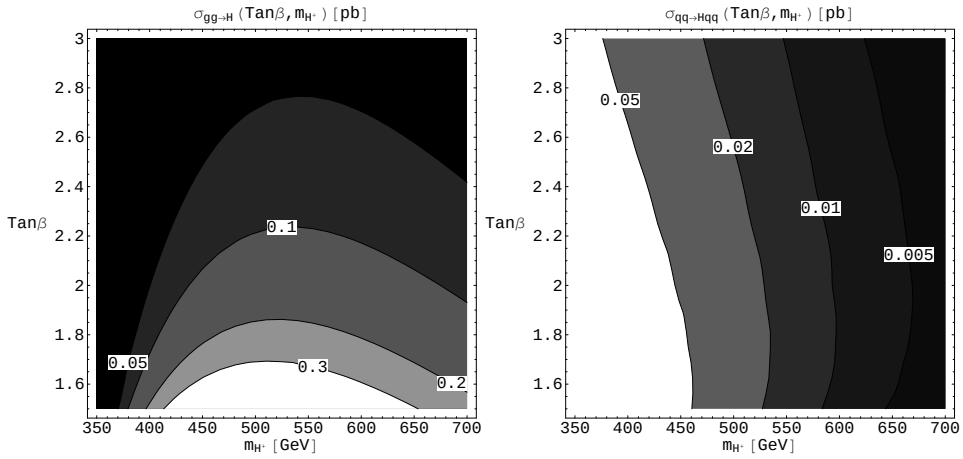

FIGURE 8.6.2. The NLO production cross section of the H via the gluon fusion (left) and the weak boson fusion (right) plotted in the range (5.3.6) for $\lambda = 2$.

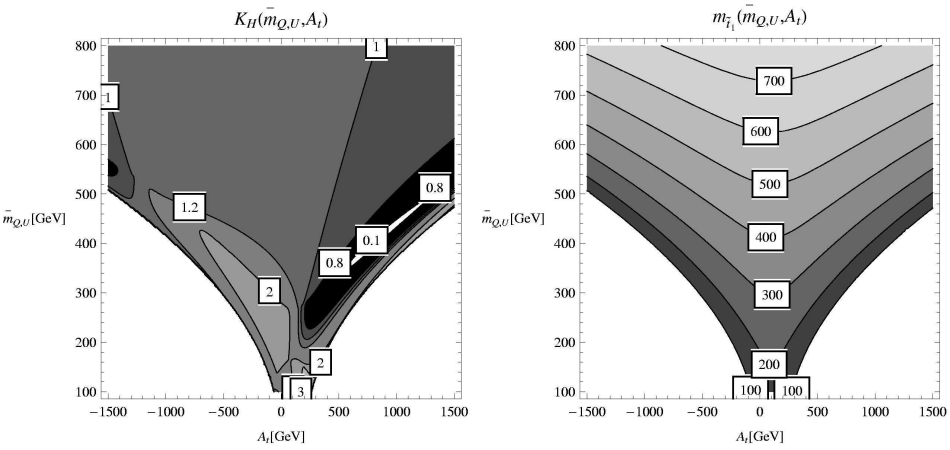

FIGURE 8.6.3. (left)The ratio of the cross section including the stop over the cross section with top only in the parameter space of the average stop mass, $\bar{m}_{\tilde{t}}$, and the top trilinear SUSY breaking term A_t. Parameters were fixed accordingly to Eq. (8.4.1). (right)Mass of the lightest stop for parameters fixed accordingly to Eq. (8.4.1). In both plots the two white areas in the lower left and lower right corners yields $m_{\tilde{t}} \leq 100$ GeV and are therefore excluded by direct stop searches [**80**].

ξ_{Hbb} is not large enough to make it comparable with the top loop for moderate $\tan\beta$ as in (5.3.6). In analogy with the light Higgs case, we define

$$K(\sigma_H)_{stop} = \frac{\sigma_H(stop + top)}{\sigma_H(top)},$$

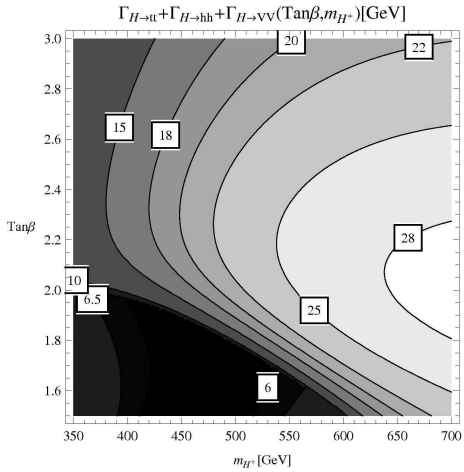

FIGURE 8.6.4. Γ_H omitting supersymmetric decays into Higgsino pairs, see Fig. 8.6.6.

the ratio of the H production cross section summing stop and top diagrams over the cross section with only top loops. Figure 8.6.3 shows this ratio for the choice of parameters given in eq. (8.4.1). At variance with the light Higgs case, stop contribution to H production can have a sizable effect. Looking at the lightest stop mass plotted in figure 8.6.3 one see that the largest contributions arise for a lighter stop, while the area corresponding to

$$m_{\tilde{t}} > 400 \text{ GeV} \tag{8.6.1}$$

is the area where $K(\sigma_H)_{stop}$ is close to one (deviation is less than 20%). This has to be ascribed to decoupling of the stop contribution as it gets heavier. Variations of choice of parameters are inessential to conclude that, when Eq. (8.6.1) holds, the stop is decoupled enough to induce effects as small as NNLO QCD or less. In the following we shall assume to work in this scenario, neglecting possible contribution from the stop.

With the priors explained above, we obtain the gluon fusion (GF) and weak boson fusion (WBF) production cross sections of the H by simply rescaling the NLO results for the SM Higgs boson of the same mass, generated by HIGLU [**81**] and VV2H [**82**] codes. For instance the gluon fusion production cross section is given by:

$$\sigma^{GF}(H) = \xi^2_{Htt}\sigma^{GF}_{SM}\,.$$

The resulting production cross sections are given in Fig. 8.6.2. The main channel is gluon fusion, which has a production cross section of the order of 100 fb. From the order of magnitude of the cross-section we expect that at least tens of 1/fb are needed to observe this state.

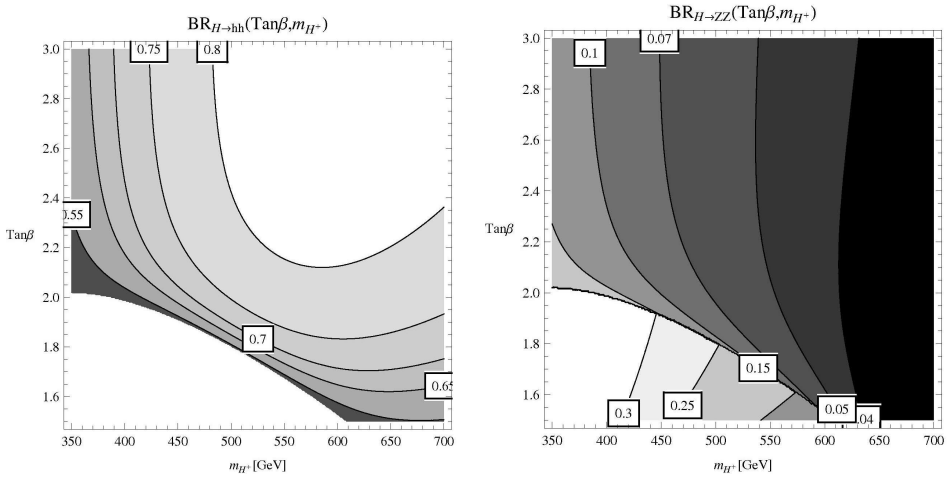

FIGURE 8.6.5. $BR(H \to hh)$ (left) and $BR(H \to ZZ)$ (right) in the preferred range (5.3.6) of the parameter space. The H decay width into Higgsinos $\Gamma_{\chi\chi}$ is neglected. For nonzero $\Gamma_{\chi\chi}$, these branching ratios have to be multiplied by a factor $\Gamma/(\Gamma + \Gamma_{\chi\chi})$, where Γ is the visible decay width plotted in Fig. 8.6.4. The $H \to hh$ decay mode is dominant except for the lower left corner of the parameter space where this decay channel is closed ($m_H < 2m_h$).

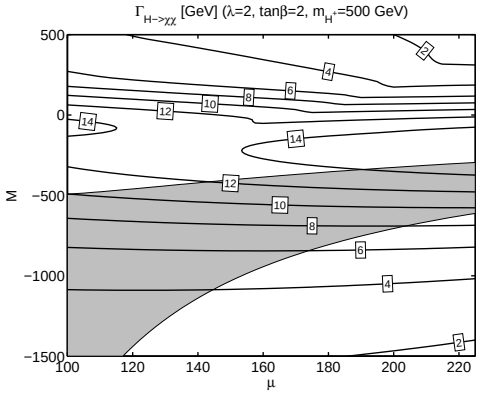

FIGURE 8.6.6. The H decay width into Higgsino pairs for $\lambda = 2$, m_{H^+} and $\tan\beta$ at the benchmark point (8.5.1), and for μ (chargino mass) and M within their ranges determined by stability of the potential and Naturalness considerations [**1**]. The gray area corresponds to $m_{\rm LSP} < m_Z/2$ and is excluded.

8.6.2. Decays. The visible decay width of the H is dominated by decays into hh, $t\bar{t}$ and VV pairs[3]).Decays into a stop pair are not considered because of the heavy stop assumption Eq. (8.6.1). The Hhh coupling is proportional to

[3]Here and below V stands for W, Z.

λ^2 and is given by[4]

$$g_{Hhh} = \frac{v\lambda^2}{2\sqrt{2}}[\sin(\alpha+\beta) - 3\sin(3\alpha-\beta)] \ .$$

The total visible decay width is given in Fig. 8.6.4 and ranges between 5 and 25 GeV. The branching ratio for decays into hh and, for comparison, into ZZ pairs, is plotted in Fig. 8.6.5. Because λ is large, decay into hh pairs is a dominant decay mode whenever this channel is open, which happens in most of the parameter space.

The H will also decay into Higgsino pairs. This decay width depends on the neutralino parameters μ and M. Fig. 8.6.6 gives the decay width of H into Higgsinos for the benchmark point (8.5.1) and for μ, M within their ranges (determined by stability of the potential and Naturalness considerations [**1**]): it takes values between a few and 15 GeV. Thus the Higgs can be a considerable source of neutralinos. This can result in visible final states accompanied by substantial missing energy or even completely invisible decays of the Higgs boson H.

For sake of simplicity in most of our discussion below we shall neglect the decay width into Higgsinos. This means that in a realistic situation for fixed M and μ all branching ratios and signal rates will have to be multiplied by a factor $\Gamma/(\Gamma+\Gamma_{\chi\chi})$.

8.6.3. Detection strategies. Let us first discuss the lower left corner of the parameter space, where the $H \to hh$ decay channel is closed (see Fig. 8.6.5). In this region $BR(H \to VV)$ becomes significant. We believe that H could be discovered in this region via $H \to ZZ \to 4l, \nu\nu ll$ combined with $H \to WW \to l\nu l\nu$. A rough estimate of the discovery reach can be obtained using results of the SM Higgs boson studies [**74**,**75**], and then taking into account that the width of our H scalar is significantly smaller that the width of the SM Higgs boson of the same mass. More precisely, the discovery significance can be estimated by rescaling the corresponding significances in the SM case with a factor

$$\frac{(\sigma_H \times BR)_{\lambda SUSY}}{(\sigma_H \times BR)_{SM}} \sqrt{\frac{\Gamma_{SM}}{\Gamma_H}}$$

where the quantities marked by SM refer to the SM Higgs boson of the same mass as the H. The factor $\sqrt{\Gamma_{SM}/\Gamma_H}$ reflects the reduction of background events passing the event selection in the mass window $\pm const.\Gamma$. This rescaling procedure gives a $5-6\sigma$ significance with 100 fb^{-1} for the H discovery in $H \to VV$ when $H \to hh$ is closed [5]

In the remaining, larger region of the parameter space, $BR(H \to VV)$ is too small for a convincing H discovery in the VV decay channel. In what follows, we shall discuss how H could be discovered in that region using the

[4] The corresponding Lagrangian term is $g_{Hhh}Hh^2/2$.

[5] The preceding discussion used the gluon fusion production mechanism. This result can presumably be improved using vector boson fusion, which is not normally used in the SM for this range of the Higgs mass, but becomes significant in λSUSY for low m_{H^+} (see Fig. 8.6.2).

decay mode $H \to hh$. The fact that this decay mode is dominant when open reflects a very basic property of λSUSY: the large value of λ.

8.6.4. Signal. For $H \to hh$ decay we cannot rely on existing SM studies. To perform a careful analysis, we shall consider a benchmark point (8.5.1). This point is generic rather than chosen for some special properties. The relevant particle parameters at this point take the following values[6]:

$$\begin{aligned} \sigma_H^{GF} &= 150 \text{ fb}, & \sigma_H^{VBF} &= 27 \text{ fb}, \\ m_H &= 555 \text{ GeV}, & m_h &= 250 \text{ GeV}, \\ \Gamma_H &= 21 \text{ GeV}, & \Gamma_h &= 3.8 \text{ GeV}, \\ \xi^2_{Htt} &= 0.058, & \xi^2_{HVV} &= 0.060, \\ BR(H \to hh) &= 0.76, & BR(H \to VV) &= 0.2\,. \end{aligned} \tag{8.6.2}$$

As discussed in Section 8.6.1, the H is mainly produced via gluon fusion; in the following we shall consider only this channel. Once produced, most of the Hs will decay into hh and then into $4V$, resulting in $\sigma_{gg\to H\to 4V} = 110$ fb. The final weak bosons can decay leptonically, but the branching fractions in this case are so small that relevant decay modes have at most one leptonic decay, while the remaining weak bosons have to be allowed to decay handronically. Our choice for a quantitative study is therefore[7]

$$gg \to H \to hh \to 2Z2V \to l^+l^-6J\,, \quad \sigma \times BR = 2.67 \text{ fb}\,. \tag{8.6.3}$$

To increase the signal cross section, we assumed that final state jets J are *generic jets,* i.e. $J = j, b, c$, where j is a usual gluon or light-quark jet. Flavor labels are not necessary, since we shall not deal with flavor tagging issues at all.

To produce a sample of signal events, we first used MADGRAPH [**84**] to produce matrix-element-generated $gg \to H \to VVZl^+l^-$ events, and then we decayed the remaining weak bosons through the DECAY routine by F. Maltoni [**84**].

8.6.5. Backgrounds. We scanned the long list of SM processes with l^+l^-6J final state and used ALPGEN [**85**] or MADGRAPH+DECAY to compute their cross sections for the total invariant mass near the H mass[8]. We found that only $Z6J$ and $t\bar{t}Z$ processes are relevant, i.e. have cross section large enough to potentially compete with the signal.

---

[6] The reported decay widths and branching ratios are calculated assuming zero decay widths into Higgsinos. See discussion in Section 8.6.2.

[7] The alternative channel $H \to WWVV \to l\nu 6J$ benefits from a higher rate and could perhaps yield a higher statistical significance. Another promising channel is $H \to WWWW$ with several same-sign or opposite sign-different flavor leptons in the final state, which was recently used in a related study of non-SUSY $H \to hh$ decays [**83**]. We preferred channel (8.6.3) to avoid discussing additional sources of missing energy among which there are particularly delicate detector effects (jet energy scale, finite cone size effects, calibration, etc.).

[8] Possible SUSY backgrounds like sparticle mediated diffuse hh production and $l^+l^-6J + LSP$ in gluino and squark decay have been estimated to be negligible.

Process	specific cuts	σ
$(Z \to l^+l^-)6j$	—	$1118(2)$ fb
$(Z \to l^+l^-)b\bar{b}4j$	$p_T^l > 10$ GeV	$94(2)$ fb
$(Z \to l^+l^-)c\bar{c}4j$	$p_T^l > 10$ GeV	$92(1)$ fb
$(Z \to l^+l^-)(t\bar{t} \to 6J)$	$\eta_l < 2.5$,$p_T^l > 10$ GeV	$5.86(2)$ fb

TABLE 2. Simulation of the relevant SM backgrounds for $H \to l^+l^-6J$. Apart from the shown specific cuts, all l^+l^- pairs and jets fulfill Eq. (8.6.4). Final state total invariant mass is between 400 and 2400 GeV except for $Zt\bar{t}$, which is produced without invariant mass restrictions.

We then proceeded with a more complete analysis of these two relevant backgrounds. Samples of $(Z \to l^+l^-)6j$ and $(Z \to l^+l^-)4jQ\bar{Q}$ events were generated with ALPGEN using the CTEQ5L parton distribution functions (pdf) enforcing the cuts

$$\Delta R_{JJ} > 0.7\,, \quad p_T^J > 20 \text{ GeV}, \quad \eta_J < 2.5, \qquad 80 \text{ GeV} < m_{ll} < 100 \text{ GeV}, \quad \eta_l < 10. \tag{8.6.4}$$

We also enforced the total invariant mass cut

$$400 \text{ GeV} < m_{tot,inv} < 2400 \text{ GeV}, \tag{8.6.5}$$

covering by a large margin the region near the H mass. This allows us to properly introduce a jet spectrum smearing and take into account possible effects from high invariant mass tails[9]. With these cuts, our results for the cross section are reported in Table 2. These results were obtained for the ALPGEN factorization and renormalization scale set at $\mu_F^2 = m_Z^2 + p_{T,Z}^2$. Our motivation for choosing this scale is twofold. First, the Tevatron experiments [**86**] have confronted the observed rates of $Z + N$ *jets* events with ALPGEN simulations for various μ_F^2, finding μ_F^2 values not far from our choice as best fitting the observations. Second, our μ_F^2 yields nearly the largest cross section we found trying out several possibilities available in ALPGEN. Thus we believe that the systematic uncertainty of background normalization is conservatively taken into account.

The $(Z \to l^+l^-)t\bar{t}$ process, with subsequent $6J$ decay of the $t\bar{t}$ pair, was simulated with MADGRAPH+DECAY using the CTEQ6L1 PDF. We generated a sample using cuts (8.6.4) setting the renormalization and factorization scale at $\mu_F^2 = m_Z^2$. The resulting cross section is given in Table 2 and results subdominant with respect to the $Z6J$ background.

8.6.6. Analysis. The total background cross section reported in Table 2 is much bigger than that of the signal Eq. (8.6.3). However, we expect signal

[9]At the same time the lower invariant mass cut is indispensable with our limited computer resources, since it improves greatly ALPGEN unweighting efficiency.

events to have a very specific structure due to the presence of intermediate resonances (h, W, Z). Typical background events are not expected to have such structure and can be rejected by imposing *reconstruction cuts*, i.e. requiring that the intermediate state resonances be reconstructed by final state jets and leptons. This is the general idea of the analysis described below. The main issue is whether the rejection efficiency will be enough to sufficiently suppress the backgrounds.

The details of the analysis (performed with ROOT [**87**]) are as follows. First of all, our analysis is completely partonic, so neither showering nor jet reconstruction effects are taken into account. We also ignore flavor tagging and trigger issues, but our inclusive definition of jet and final selection cuts for leptons, respectively, make these simplifications fully justified. However, in order to make the analysis more realistic, we do introduce a smearing of energies of individual jets using the expression

$$\frac{\sigma}{E} = \frac{0.5}{\sqrt{E/\text{GeV}}} + 0.03 \tag{8.6.6}$$

to generate the smearing coefficient, as prescribed in Table 9-1 of [**88**][10].

After smearing, we impose the kinematical cuts (8.6.4) on the jets and slightly tighten the corresponding leptonic cuts

$$\Delta R_{lJ} > 0.1, \quad p_T^l > 10 \text{ GeV}, \quad \eta_l < 2.5\,. \tag{8.6.7}$$

Background and signal events not passing these cuts are removed from the samples. The signal events passing these cuts correspond to $0.48(1)$ fb of cross section to be compared with 2.47 fb without any kinematical cuts, see eq. (8.6.3). The backgrounds cross section are reduced by these tighter cuts only by a small amount compared to the values reported in Table 2.

Finally, we impose the *reconstruction cuts*, proceeding as follows[11].

R1. For each event we try to group the 6 final jets into 3 pairs so that the jets in each pair *reconstruct* a W or a Z. By this we mean that the invariant mass m_{inv} of each pair has to satisfy the requirement:

$$M_V - \delta_V \leq m_{inv} \leq M_V + \delta_V, \quad \delta_V = 8 \text{ GeV}, \quad V \in \{W, Z\}\,.$$

In practice, the value of δ_V cannot be taken too small because otherwise too many signal events will be rejected. The given value was motivated by the finite resolution of the W and the Z peaks which is determined by their natural widths as well as by the energy resolution of the detector as taken into account by the smearing procedure described above.

R2. If a grouping into jet pairs reconstructing a W or a Z each is found, we proceed to impose a further condition that two h's be reconstructed by four jets from two of these three pairs, say pair 1 and 2, and by two jets of pair 3 and the

[10] This is also the smearing adopted in the ATLFAST++ detector simulator [**89**]

[11] Geometrical discrimination has been attempted too, but turned out not to be very helpful, since both signal and background result in a largely boosted system.

Process	σ
$H \to 6Jl^+l^-$	$0.286(9)$ fb
$(Z \to l^-l^+)6j$	$0.15(1)$ fb
$(Z \to l^-l^+)Q\bar{Q}4j$	$0.032(5)$ fb
$(Z \to l^-l^+)(t\bar{t} \to 6J)$	$0.022(1)$ fb

TABLE 3. Signal and background cross sections after imposing the reconstruction cuts. For $ZQ\bar{Q}4j$ the given value is the sum over $Q = b, c$.

two leptons. In this case the precise reconstruction cut that we used is

$$m_h - \delta_h \leq m_{pair_1+pair_2} \leq m_h + \delta_h, \quad \delta_h = 33 \text{ GeV},$$
$$m_h - \frac{\delta_h}{\sqrt{2}} \leq m_{pair_3+l^+l^-} \leq m_h + \frac{\delta_h}{\sqrt{2}},$$

where $m_{pair_1+pair_2}$ and $m_{pair_3+l^+l^-}$ are the invariant masses of the $4J$ and $2Jl^+l^-$ final states. The value of δ_h is again motivated by the natural width of h (with an additional spreading caused by the jet energy resolution). We also check that the gauge boson reconstructed by the jets of pair 3 is a Z, while the two gauge bosons reconstructed by the jets of pairs 1 and 2 have the same type (both W or both Z).

If no grouping of 6 jets into 3 pairs satisfying both R1 and R2 can be found (we go over all combinations), the event is rejected, otherwise it is retained. The retained events show the expected intermediate state resonance structure of the signal.

We ran the reconstruction analysis on the signal sample and on each of the relevant background samples shown in Table 2. The signal and background cross sections *after the reconstruction cuts* are given in Table 3. For each sample the number of events which passed the reconstruction cuts was large enough so that the statistical uncertainty in determining the rejection efficiency is reasonably small[12]. In fact it is this statistical uncertainty (determined from the usual $\sqrt{N}$ fluctuations of the number of events passing the reconstruction cuts) which underlies the errors for the cross sections quoted in Table 3.

Two basic conclusions are evident from Table 3. On the one hand, we see that for the chosen parameters $\delta_{V,h}$ the reduction in the signal cross section from what we had after the kinematical cuts is reasonably small (from 0.48 to 0.36 fb). On the other hand, we see that the reconstruction cuts have huge effect on backgrounds, giving the rejection efficiency of about 10^{-3}. The final background cross section is comparable to that of the signal, making the discovery possible.

Finally, in Figure 8.6.7 we show the distribution of the signal and the total background cross section versus the total invariant mass of the event.

[12]For example, we had 1481 events in the signal sample which passed all the cuts.

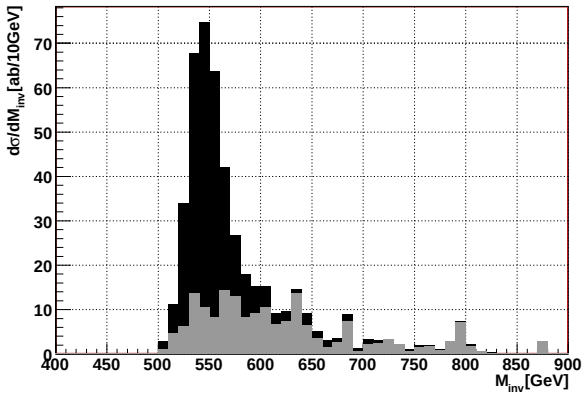

FIGURE 8.6.7. λSUSY at the benchmark point (8.5.1), (8.6.2) (black) and Standard Model (gray) expectation for the differential cross section $d\sigma/dM_{inv}(l^+l^-6j)$ after the kinematical and reconstruction cuts discussed in Section 8.6.6.

8.6.7. Discovery potential after 100 fb^{-1}. From Figure 8.6.7 we see that signal and backgrounds peak in the same invariant mass range. The discovery of H will thus comes not from an observation of a new peak, but rather from an overall excess of events compared to the SM prediction, as well as from the enhanced prominence of the SM peak.

For an integrated luminosity of 100 fb^{-1}, the expected number of events passing all the cuts is 20 in the SM, and 49 in λSUSY at the benchmark point (8.5.1), (8.6.2), giving 3.4σ if one uses the significance estimator formula given in Eq. (A.3) of [**75**]. Of course, once this global excess is found, it is worth to scan the invariant mass range to find where the excess is localized. Optimizing the range, much better discovery significance can be achieved. For instance, for 510 GeV$< M_{inv} < 590$ GeV we have 3 events in the SM, and 23 events in λSUSY, 7.2σ away from the SM. When going beyond benchmark-point analysis (something we do not attempt for the time being), such localized excess can be used to determine m_H.

Our conclusion is that the λSUSY signal (8.6.3) is indeed observable at the LHC with 100 fb^{-1} of integrated luminosity. If observed, it can provide clean evidence for the heavy scalar H as well as for the $H \to hh$ dominant decay chain.

8.7. The CP-odd scalar

8.7.1. Production and decays. The pseudo-scalar Higgs boson A has mass in the same 500-800 GeV range as the heavy scalar H but is always heavier than H (see Fig. 5.3.2). Its couplings to the third generation SM fermions are given by [**29**]:

$$g_{Att} = \frac{m_t}{v}\cot\beta\,, \quad g_{Abb} = \frac{m_b}{v}\tan\beta.$$

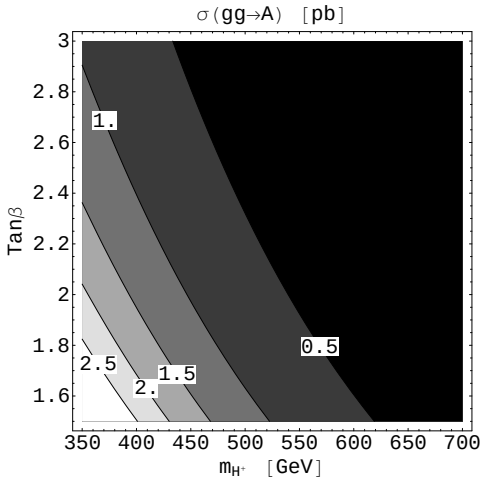

FIGURE 8.7.1. Pseudo-scalar Higgs boson production cross section plotted in the parameter space of Eq. (5.3.6) for $\lambda = 2$.

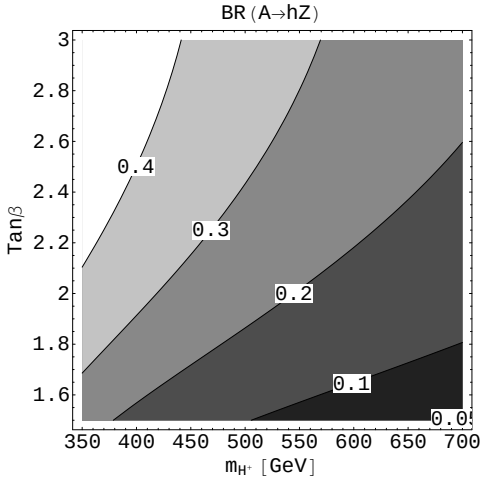

FIGURE 8.7.2. BR($A \to Zh$) plotted in the parameter space of Eq. (5.3.6) for $\lambda = 2$, assuming negligible decay width into Higgsinos. BR($A \to t\bar{t}$)$\approx 1-$BR($A \to Zh$).

There is also a coupling with the Z boson and the lightest CP-even Higgs boson h from the interaction Lagrangian term $g_{AhZ}(A \overleftrightarrow{\partial}_\mu h)Z_\mu$ where [**29**]

$$g_{AhZ} = \frac{g}{2\cos\theta_w}\cos(\beta-\alpha),$$

and g is the SU(2) gauge coupling.

By CP-invariance AVV couplings vanish, therefore the only relevant production mechanism of A is gluon fusion via the top loop. The production cross section has been evaluated at NLO with HIGLU [**81**] and is plotted in Fig. 8.7.1.

The total width of A ranges between 5 and 30 GeV and is dominated by $A \to t\bar{t}$ and $A \to hZ$ decays. Although the branching ratio of $A \to t\bar{t}$ is almost always dominant (see Fig. 8.7.2), we cannot exploit this channel. Indeed, [**90**] showed that for the mass values we are interested in, the $t\bar{t}$ SM background does not allow discovery of a scalar resonance decaying into $t\bar{t}$. Therefore, we focus on $A \to hZ$, whose BR is smaller, but still significant. Most of the produced h's will decay into vectors, yielding $\sigma_{tot}(gg \to A \to ZVV) \sim 10$ fb over all the parameter space. Such a cross section will give too small event rate if more than one V is allowed to decay leptonically. Therefore we concentrate on the signature

$$gg \to A \to hZ \to VVZ \to 4Jl^+l^- \quad \text{(signal)}. \tag{8.7.1}$$

For a detailed study we go to our benchmark point (8.5.1), which gives the following numerical values [13]:

$$m_A = 615\ \text{GeV}, \quad \Gamma_A = 11\ \text{GeV}, \quad \sigma \times \text{BR} = 5.5\ \text{fb}. \tag{8.7.2}$$

8.7.2. Analysis and discovery potential. The analysis is quite analogous to what was done in Section 8.6 for the heavy CP-even Higgs. We will therefore be relatively brief.

We generated a sample of signal events with MADGRAPH+DECAY.

We then computed cross sections for all SM processes with $4Jl^+l^-$ final state and we found that only the $Z4j$ and $ZW2j$ processes are relevant[14]. Table 4 contains details about the relevant and neglected backgrounds.

Event samples of relevant backgrounds were generated for a more complete analysis. The $Z4j$ process was simulated with ALPGEN using the CTEQ5L PDF, setting $\mu_F^2 = m_Z^2 + p_{T,Z}^2$ and enforcing cuts:

$$\begin{gathered} 500\ \text{GeV} < M_{inv} < 750\ \text{GeV} \\ p_T^j > 20\ \text{GeV}\,, \quad p_T^l > 10\ \text{GeV}\,, \\ \Delta R_{jj,lj,ll} > 0.4, \quad \eta^{j,l} < 2.5 \\ 80\ \text{GeV} < m_{ll} < 100\ \text{GeV}\,. \end{gathered} \tag{8.7.3}$$

The $ZW2j$ process was simulated with MADGRAPH using the CTEQ6L1 pdf, setting $\mu_F^2 = m_Z^2$ and imposing the same cuts. The resulting background cross sections are the ones given in Table 4. Finally, to model finite detector energy resolution, we apply energy smearing to the signal and background events using the smearing function (8.6.6).

From Table 3 we see that the background cross section in the relevant interval of m_{inv} is more than 3 orders of magnitude above the signal. To reduce the background, we proceed by imposing the reconstruction cuts. Namely, we

[13] The quoted value of Γ_A does not include the width into Higgsino pairs depending on μ and M. The latter can be as large as 10 GeV, but in most of the parameter space is below 2 GeV. See the analogous discussion for the H in Section 8.6.2.

[14] In particular, backgrounds $ZZ2j$, VVV, $h2j$ were analyzed and found negligible.

Channel	σ
$A \to (Z \to l^+l^-)4J$	3.02(4) fb
$(Z \to l^+l^-)4J$	7.006(4) pb
$(Z \to l^+l^-)W2j$	176.0(8) fb
Sum of neglected	$\simeq 90$ fb

TABLE 4. Cross sections of the signal and of the relevant SM backgrounds after the kinematical cuts (8.7.3).

require that the 4 final jets can be divided into 2 pairs reconstructing a vector boson each. Moreover, we require that these two vector bosons be of the same type. If they are both W, then we require that they reconstruct an h. If they are both Z, we require that out of the 3 final Z's (the two from jets and the one reconstructed by the leptons) we should find two reconstructing an h. Reconstruction parameters $\delta_{V,h}$, having the same meaning as in Section 8.6.6, are chosen

$$\delta_V = 8 \text{ GeV}\,, \quad \delta_h = 18 \text{ GeV}.$$

If the above requirements can be satisfied, the event is retained, otherwise it is rejected.

The fraction of the signal event sample which passes the reconstruction cuts amounts to 2.2 fb, i.e. the cross section is reduced only by a small factor compared to the value after kinematical cuts given in Table 4. Under the reconstruction cuts the total SM background cross section in $500 - 750$ GeV invariant mass range drops down by a factor about 200, i.e. to 51.1 fb.

The differential cross sections versus the invariant mass for both the background and signal+background are plotted in Fig. 8.7.3. We see that the signal distribution presents a clearly visible peak above the background. The discovery significance can be optimized choosing a range with largest $S/\sqrt{B}$ ratio. For example, assuming 100 fb^{-1} of integrated luminosity, in the $595 - 635$ GeV range we expect 816 events in the SM, and 989 events in λSUSY at the benchmark point of eqs. (8.5.1) and (8.7.2), which amounts to 6.1σ discovery significance.

In summary, we showed that the CP-odd Higgs boson of λSUSY has a clear experimental signature in the $4jl^+l^-$ channel, allowing for its discovery at the LHC with ~ 100 fb^{-1} of integrated luminosity. Moreover, the peaked shape of the signal distribution should allow background extraction from data and an easy mass measurement. Even though the $A \to Zh$ decay mode is less distinctive of λSUSY than the $H \to hh$ mode discussed in Section 8.6, its signature is much simpler and cleaner, and it could be the easiest channel to pursue when looking for λSUSY signals.

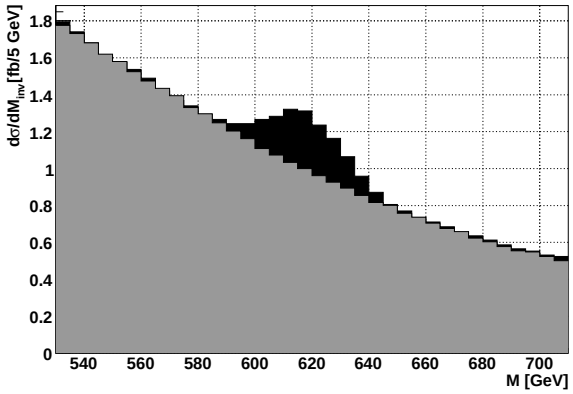

FIGURE 8.7.3. λSUSY (black) and SM (grey) expected differential cross section $d\sigma/dM_{inv}(4jl^+l^-)$ for process (8.7.1) at the benchmark point (8.5.1), (8.7.2).

CHAPTER 9

Conclusions and outlook

In this thesis we have examined in detail the properties and the phenomenology of a class of supersymmetric models characterized by a large mass of the Higgs boson arising from a term $\lambda S H_1 \cdot H_2$ in the superpotential.

This class of models can emerge as the low energy theory of a class of UV complete theories where the Higgs sector has some degree of compositeness. Within these UV complete models we discussed examples that are manifestly compatible with the gauge couplings unification to the same extent of the MSSM. The existence of such models constitutes a great motivation to study the low energy phenomenology of the theories with largish λ that, still being compatible with the greatest indirect hint of SUSY, can result in a phenomenology significantly different from the MSSM. To perform a phenomenological study we disregarded the details of the particular UV complete models and introduced $\lambda SUSY$, a supersymmetric effective theory that corresponds to the usual NMSSM with strongish couplings in the Higgs sector. This model, as an effective field theory, has the merit to describe the phenomenology relevant for the LHC and the other experiments performed and foreseeable so far, thus capturing the essence of the physical picture of the whole class of UV complete models.

In the context of λSUSY we found two phenomenologically interesting regions of the parameter space. In one region the models is such that all the physics connected to the new singlet S is decoupled, thus leaving a phenomenology that resembles very closely that of the MSSM, except for a Higgs boson mass around 200 or 300 GeV. The other region, on the contrary, corresponds to the regime where the singlet fully participates in the dynamics of the whole Higgs sector leading to order one deviations with respect to the phenomenology of the MSSM in addition to the large Higgs mass. This last scenario has been studied in closer detail with particular focus on the issue of the dynamical generation of the μ term.

Indeed the generation of the μ term by means of the dynamics that breaks the electroweak symmetry is one of the motivation for the extension of the MSSM to the NMSSM. In this thesis we assessed how the NMSSM with a strongish self coupling in the Higgs sector is very well suited to generate the μ term in a natural way. Indeed we found that in the regime of $\lambda SUSY$ in which the singlet is not decoupled is very natural to have its VEV, s, of the same order of magnitude, and typically very close to, the VEV of the Higgs doublets. Together with our choice of largish coupling λ, *i*.e. $\lambda \simeq 1$, this leads naturally to

the generation of

$$\mu = \lambda s \gtrsim m_Z \, .$$

More in detail, we have been able to prove that when the singlet is not decoupled from the rest of the scalars, that is generically the case when $v \simeq s$, the generation of the mass of the Higgs and of the μ term are very closely connected phenomena, as one would expect in a theory that is characterized by only one physical scale, λv, and generates the two masses at the moment of the breaking of the same symmetry. Thus our result

$$m_h \sim \lambda v \, , \quad \frac{\lambda v}{\sqrt{2}} \sin 2\beta < \mu < \frac{3}{2} \lambda v \sin 2\beta$$

appears completely natural and expected.

We also quantified how natural is our model. We examined the logarithmic sensitivity of the electroweak scale to the change of the fundamental parameters of the model and we found that the most natural region is that where the Higgs boson mass is well above m_Z. This also implies that μ is preferred to be at least slightly heavier than m_Z. Assuming a messengers mass around 100 TeV we have made predictions for the masses of the colored sparticles, in particular of the stop and the gluino. We found that they can be easily heavier than 1 TeV still not rendering our model unnatural. This quantitative assessment of the fine tuning of the model and the consequent bounds of the masses show that the null results of Higgs bosons and superpartners searches of LEP is not necessarily a killer of low energy supersymmetry but rather an element of tension for the MSSM and its extensions with *perturbative* gauge couplings unification.

The model in the regime of not decoupled singlet has been extensively checked against the current experimental data. In particular we examined the bounds from direct searches at LEP and the indirect constraints coming from precision measurements. We find that direct observations do not pose any serious bound on the model. More constraints arise from the analysis of the electroweak precision observables that forces the model to have a small $\tan\beta$ and self couplings in the Higgs sector not too large. Interestingly the couplings allowed are large enough to obtain a Higgs boson above 200 GeV. Furthermore the range of $\tan\beta$ preferred by precision data maximizes the effect of the coupling λ on the Higgs mass.

We also computed the thermal relic abundance of the lightest neutralino, that is a dark matter candidate. The model parameter space left after the consideration of the several constraint from particle physics experiments can accommodate a lightest neutralino with the correct relic abundance. This requires some particular choice of the parameters such that the lightest neutralino is an almost pure singlino interaction eigenstate with mass close to the mass of the Z boson.

The limits from direct detection of dark matter that scatters with heavy nuclei in underground experiments have been taken into account as well. We find that the higgsino and singlino components of the lightest neutralino both scatter

rather efficiently on ordinary matter through the exchange of the lightest Higgs boson. The bounds in the case of a not decoupled singlet are more stringent than in the decoupling case as the mixing of the singlet with the doublet adds up a whole new class of diagrams for the scattering of the LSP with ordinary matter mediated by the self-coupling of the singlet and by mixed singlet-doublet interactions. We find that the model is more easily compatible with the current data when the Higgs boson is heavier that about 200 GeV, which is rather natural in this class of models. However, the bounds from the spin-independent cross section of the LSP on the proton constitutes an important constraint for the model.

The model has very striking and observable consequences for the LHC, which we studied in detail for both the scenarios with the mixed and unmixed singlet.

The mixed scenario offers more immediate observable deviations from the SM and the MSSM as it substantially modifies the properties of the lightest Higgs boson. Indeed the lightest Higgs boson is rather strongly coupled to the whole sector of Higgs and higgsino states. This leads to a number of unsuppressed decay channels that in the MSSM are at best sub-dominant and typically nearly absent. This will result in a substantial deviation from the SM rate for the process

$$gg \to h \to WW, ZZ\,.$$

The low rate for the gluon fusion process and the large mass of the Higgs boson will point toward scenario beyond the SM and beyond the MSSM. The case of $\lambda SUSY$ with a mixed singlet offers a number of possible observations to be carried on right after the establishing of a non-standard Higgs boson. A notable possibility is the decay of the Higgs to a pair of LSP, which lead to an invisible decay of the Higgs, *i.e.* to an invisible decay width that can potentially be measured [1]. Furthermore in a large fraction of the allowed parameters space the Higgs boson can decay to a pair of pseudoscalar states with mass of the order of 100 GeV. In this case the Higgs boson can be observed in processes as

$$gg \to h \to aa \to b\bar{b}b\bar{b},\, b\bar{b}\tau\bar{\tau}\,, \quad gg \to h \to Za \to b\bar{b}\ell\bar{\ell}\,,$$

that might be observable with few fb^{-1} of integrated luminosity at $\sqrt{s} = 7$ TeV [**78**].

The unmixed singlet scenario, on the contrary, manifests itself in a more subtle manner. The deviations of the properties of the lightest Higgs boson from the ones of the SM are too tiny to be observed at the LHC and we established that it will be necessary to search for the heavy states of the Higgs sector of λSUSY to find evidence for a non SM Higgs sector. We studied the observability of the heavy CP-even Higgs boson H and the lightest CP-odd boson A that in this regime have masses of several hundreds of GeV. Our study shows

[1] See for instance page 1419 of Ref. [**91**] for the estimates of ATLAS for the direct measurement of signals of the invisible decay of the Higgs boson.

that these states are observable in the channels

$$gg \to H \to hh\, VV \to \ell\bar{\ell}6j\,, \quad gg \to A \to hZ \to \ell\bar{\ell}4j\,,$$

with an integrated luminosity of 30 to 100 fb^{-1} at $\sqrt{s} = 14$ TeV.

In summary, we have studied in detail the phenomenology of λSUSY, the low energy realization of supersymmetric UV complete models with composite Higgs states having strongish self-coupling. The supersymmetric structure of our model can be captured by the NMSSM with large coupling of the Higgs sector. This large coupling results in a generically heavy Higgs boson, easily heavier than 200 GeV, in striking contrast with the MSSM case and the usual NMSSM.

We studied the generation of the μ terms and the fine-tuning of the model finding that the model can naturally give a dynamical generated μ term of a phenomenologically acceptable size. The request of a dynamically generated μ term favors the regime of the model in which the singlet state does not decouple. We have studied in detail the limits from high energy particle physics and dark matter experiments finding that the least tuned region of the parameter space is preferred by the current data.

Finally we have studied the observability of this model for both the case of a mixed and an unmixed singlet field. We have argued that the LHC might have the potential to observe signals of deviation from the SM and the MSSM already in the first few fb^{-1}. In the case of a mixed singlet the same amount of luminosity might be sufficient to find evidences of λSUSY in most of the parameters space. For the unmixed singlet case we studied the observability of the heavier states of the Higgs sector finding that they can be observed with 30 to 100 fb^{-1}.

This work shows that λSUSY is a viable and motivated alternative to the MSSM. Indeed it can result in a relieve of the tensions between the LEP results and the MSSM, still maintaining desirable features of the MSSM as the stabilization of the electroweak scale, the presence of a dark matter candidate, and the possibility of gauge couplings unification. Very interestingly, the model has verifiable predictions for the LHC, that is certainly in position to test thoroughly the idea of a strongish self-coupling in a supersymmetric Higgs sector.

Acknowledgments

I would like to thank R. Barbieri for having drawn my attention on λSUSY and for the encouragement, the support and the inputs that he gave me along all my work.

I also want to thank R. Rattazzi and A. Wulzer for the many comments they made about this work and for the many suggestions they gave me.

I am thankful to Stefania Gori who is co-author of the results about the generation of the μ term and the phenomenological study of the results about the mixed singlet case.

I wish to thank L. Cavicchia and V.S. Rychkov, who are co-authors of the study about the LHC phenomenology of the Higgs sector with an unmixed singlet.

I also thank G. Corcella, F. Maltoni, M. Mangano, A. Messina for useful discussions. A final thank goes to M. Herquet for useful advices on using MadGraph.

APPENDIX A

One loop contributions to S and T

We collect here the one loop functions used through the paper.

For a boson loop with internal masses m_1 and m_2 and coupling the the gauge boson W_μ given by $iW_\mu\phi_1^*\partial_\mu\phi_2$, we have

$$2\alpha_{\rm em}v^2A(m_1,m_2) \equiv \frac{1}{16\pi^2}\left[\frac{m_1^2+m_2^2}{2}-\frac{m_1^2m_2^2}{m_1^2-m_2^2}\ln\frac{m_1^2}{m_2^2}\right], \tag{A.0.4}$$

$$\begin{aligned}\frac{1}{4\pi}F(m_1,m_2) &\equiv \frac{1}{96\pi^2}\left[-\ln\frac{\Lambda^4}{m_1^2m_2^2}+\frac{4m_1^2m_2^2}{(m_1^2-m_2^2)^2}+\right.\\ &+ \left.\frac{m_1^6+m_2^6-3m_1^2m_2^2(m_1^2+m_2^2)}{(m_1^2-m_2^2)^3}\ln\frac{m_1^2}{m_2^2}\right].\end{aligned} \tag{A.0.5}$$

Additionally, also the diagram in which the gauge boson W_μ and the Higgs boson ϕ propagate in the loop contributes to the parameter S, giving as loop function

$$G(m_1,m_2)\equiv\frac{1}{2\pi}\left[\frac{2m_1^2m_2^2}{(m_1^2-m_2^2)^3}\ln\frac{m_1^2}{m_2^2}-\frac{m_1^2+m_2^2}{(m_1^2-m_2^2)^2}\right]. \tag{A.0.6}$$

For a fermion loop with internal masses m_1 and m_2 and a vector coupling $W_\mu\bar{\psi}_i\gamma^\mu\psi_2$, we have

$$\begin{aligned}2\alpha_{\rm em}v^2\tilde{A}(m_1,m_2) &\equiv \frac{1}{16\pi^2}\left[(m_1-m_2)^2\ln\frac{\Lambda^4}{m_1^2m_2^2}-2m_1m_2+\right.\\ &+ \left.\frac{2m_1m_2(m_1^2+m_2^2)-m_1^4-m_2^4}{m_1^2-m_2^2}\ln\frac{m_1^2}{m_2^2}\right],\end{aligned} \tag{A.0.7}$$

$$\begin{aligned}\frac{1}{4\pi}\tilde{F}(m_1,m_2) &\equiv \frac{1}{24\pi^2}\left[-\ln\frac{\Lambda^4}{m_1^2m_2^2}-\frac{m_1m_2(3m_1^2-4m_1m_2+3m_2^2)}{(m_1^2-m_2^2)^2}+\right.\\ &+ \left.\frac{m_1^6+m_2^6-3m_1^2m_2^2(m_1^2+m_2^2)+6m_1^3m_2^3}{(m_1^2-m_2^2)^3}\ln\frac{m_1^2}{m_2^2}\right].\end{aligned} \tag{A.0.8}$$

Differently, for an axial coupling, the result can be obtained by letting $m_1\to -m_1$. These expressions are valid for both Dirac and Majorana fermions, with an extra factor of 2 in the case of identical Majorana fermions.

Bibliography

[1] R. Barbieri, L. J. Hall, Y. Nomura, and V. S. Rychkov, "Supersymmetry without a light higgs boson," *Phys. Rev.* **D75** (2007) 035007, hep-ph/0607332.

[2] R. Franceschini and S. Gori, "Solving the μ problem with a heavy Higgs boson," *JHEP* **1105** (2011) 084, arXiv:1005.1070 [hep-ph].

[3] L. Cavicchia, R. Franceschini, and V. S. Rychkov, "Supersymmetry without a light Higgs boson at the LHC," *Phys. Rev.* **D77** (2008) 055006, arXiv:0710.5750 [hep-ph].

[4] R. Franceschini, T. Hambye, and A. Strumia, "Type-III see-saw at LHC," *Phys.Rev.* **D78** (2008) 033002, arXiv:0805.1613 [hep-ph].

[5] M. Cirelli, R. Franceschini, and A. Strumia, "Minimal Dark Matter predictions for galactic positrons, anti-protons, photons," *Nucl.Phys.* **B800** (2008) 204–220, arXiv:0802.3378 [hep-ph].

[6] **LEP** Collaboration, "A Combination of preliminary electroweak measurements and constraints on the standard model," arXiv:hep-ex/0312023.

[7] **ALEPH** Collaboration, S. Schael *et al.*, "Improved measurement of the triple gauge-boson couplings gamma W W and Z W W in e+ e- collisions," *Phys. Lett.* **B614** (2005) 7–26.

[8] **LEP Working Group for Higgs boson searches** Collaboration, R. Barate *et al.*, "Search for the standard model Higgs boson at LEP," *Phys. Lett.* **B565** (2003) 61–75, arXiv:hep-ex/0306033.

[9] M. Dine, N. Seiberg, and S. Thomas, "Higgs physics as a window beyond the MSSM (BMSSM)," *Phys.Rev.* **D76** (2007) 095004, arXiv:0707.0005 [hep-ph]. M. Carena, K. Kong, E. Ponton, and J. Zurita, "Supersymmetric Higgs Bosons and Beyond," *Phys.Rev.* **D81** (2010) 015001, arXiv:0909.5434 [hep-ph]. I. Antoniadis, E. Dudas, D. Ghilencea, and P. Tziveloglou, "MSSM Higgs with dimension-six operators," *Nucl.Phys.* **B831** (2010) 133–161, arXiv:0910.1100 [hep-ph]. I. Antoniadis, E. Dudas, D. Ghilencea, and P. Tziveloglou, "MSSM with Dimension-five Operators (MSSM(5))," *Nucl.Phys.* **B808** (2009) 155–184, arXiv:0806.3778 [hep-ph]. I. Antoniadis, E. Dudas, D. Ghilencea, and P. Tziveloglou, "Higher Dimensional Operators in the MSSM," *AIP Conf.Proc.* **1078** (2009) 175–180, arXiv:0809.4598 [hep-ph]. I. Antoniadis, E. Dudas, and D. Ghilencea, "Supersymmetric Models with Higher Dimensional Operators," *JHEP* **0803** (2008) 045, arXiv:0708.0383 [hep-th]. A. Brignole, J. A. Casas, J. R. Espinosa, and I. Navarro, "Low-scale supersymmetry breaking: Effective description, electroweak breaking and phenomenology," *Nucl. Phys.* **B666** (2003) 105–143, arXiv:hep-ph/0301121.

[10] P. Lodone, "Naturalness bounds in extensions of the MSSM without a light Higgs boson," *JHEP* **05** (2010) 068, arXiv:1004.1271 [Unknown].

[11] S. Chang, C. Kilic, and R. Mahbubani, "The new fat Higgs: Slimmer and more attractive," *Phys. Rev.* **D71** (2005) 015003, arXiv:hep-ph/0405267.

[12] R. Harnik, G. D. Kribs, D. T. Larson, and H. Murayama, "The minimal supersymmetric fat Higgs model," *Phys. Rev.* **D70** (2004) 015002, arXiv:hep-ph/0311349.

[13] A. Birkedal, Z. Chacko, and Y. Nomura, "Relaxing the upper bound on the mass of the lightest supersymmetric Higgs boson," *Phys. Rev.* **D71** (2005) 015006, arXiv:hep-ph/0408329.

[14] A. Delgado and T. M. P. Tait, "A fat Higgs with a fat top," *JHEP* **07** (2005) 023, arXiv:hep-ph/0504224.

[15] R. Barbieri, L. J. Hall, A. Y. Papaioannou, D. Pappadopulo, and V. S. Rychkov, "An alternative NMSSM phenomenology with manifest perturbative unification," *JHEP* **03** (2008) 005, arXiv:0712.2903 [hep-ph]. M. Quiros and J. R. Espinosa, "What is the upper limit on the lightest supersymmetric Higgs mass?," arXiv:hep-ph/9809269.

[16] G. Giudice and R. Rattazzi, "Theories with gauge mediated supersymmetry breaking," *Phys.Rept.* **322** (1999) 419–499, arXiv:hep-ph/9801271 [hep-ph]. M. Dine and A. E. Nelson, "Dynamical supersymmetry breaking at low-energies," *Phys.Rev.* **D48** (1993) 1277–1287, arXiv:hep-ph/9303230 [hep-ph]. M. Dine, A. E. Nelson, Y. Nir, and Y. Shirman, "New tools for

low-energy dynamical supersymmetry breaking," *Phys.Rev.* **D53** (1996) 2658–2669, arXiv:hep-ph/9507378 [hep-ph].

[17] G. Dvali, G. Giudice, and A. Pomarol, "The Mu problem in theories with gauge mediated supersymmetry breaking," *Nucl.Phys.* **B478** (1996) 31–45, arXiv:hep-ph/9603238 [hep-ph].

[18] T. S. Roy and M. Schmaltz, "Hidden solution to the mu/Bmu problem in gauge mediation," *Phys.Rev.* **D77** (2008) 095008, arXiv:0708.3593 [hep-ph]. Z. Chacko and E. Ponton, "Yukawa deflected gauge mediation," *Phys.Rev.* **D66** (2002) 095004, arXiv:hep-ph/0112190 [hep-ph]. A. de Gouvea, A. Friedland, and H. Murayama, "Next-to-minimal supersymmetric standard model with the gauge mediation of supersymmetry breaking," *Phys.Rev.* **D57** (1998) 5676–5696, arXiv:hep-ph/9711264 [hep-ph]. H. Murayama, Y. Nomura, and D. Poland, "More visible effects of the hidden sector," *Phys.Rev.* **D77** (2008) 015005, arXiv:0709.0775 [hep-ph]. G. F. Giudice, H. D. Kim, and R. Rattazzi, "Natural mu and B mu in gauge mediation," *Phys.Lett.* **B660** (2008) 545–549, arXiv:0711.4448 [hep-ph]. Z. Komargodski and N. Seiberg, "mu and General Gauge Mediation," *JHEP* **0903** (2009) 072, arXiv:0812.3900 [hep-ph]. C. Csaki, A. Falkowski, Y. Nomura, and T. Volansky, "New Approach to the mu-Bmu Problem of Gauge-Mediated Supersymmetry Breaking," *Phys.Rev.Lett.* **102** (2009) 111801, arXiv:0809.4492 [hep-ph].

[19] G. Giudice and A. Masiero, "A Natural Solution to the mu Problem in Supergravity Theories," *Phys.Lett.* **B206** (1988) 480–484.

[20] A. Delgado, G. Giudice, and P. Slavich, "Dynamical mu term in gauge mediation," *Phys.Lett.* **B653** (2007) 424–433, arXiv:0706.3873 [hep-ph].

[21] J. Cao and J. M. Yang, "Current experimental constraints on NMSSM with large lambda," *Phys. Rev.* **D78** (2008) 115001, arXiv:0810.0989 [hep-ph].

[22] B. W. Lee, C. Quigg, and H. B. Thacker, "Weak interactions at very high-energies: The role of the higgs boson mass," *Phys. Rev.* **D16** (1977) 1519.

[23] M. Schmaltz and D. Tucker-Smith, "Little higgs review," *Ann. Rev. Nucl. Part. Sci.* **55** (2005) 229–270, hep-ph/0502182.

[24] M. Perelstein, "Little higgs models and their phenomenology," *Prog. Part. Nucl. Phys.* **58** (2007) 247–291, hep-ph/0512128.

[25] G. F. Giudice, C. Grojean, A. Pomarol, and R. Rattazzi, "The strongly-interacting light higgs," *JHEP* **06** (2007) 045, hep-ph/0703164.

[26] E. Farhi and L. Susskind, "Technicolor," *Phys. Rept.* **74** (1981) 277.

[27] C. Csaki, "Tasi lectures on extra dimensions and branes," hep-ph/0404096. C. Csaki, J. Hubisz, and P. Meade, "Electroweak symmetry breaking from extra dimensions," hep-ph/0510275.

[28] M. Drees, R. Godbole, and P. Roy, *Theory and phenomenology of sparticles: An account of four-dimensional N=1 supersymmetry in high energy physics*. Hackensack, USA: World Scientific (2004) 555 p. S. P. Martin, "A supersymmetry primer," hep-ph/9709356.

[29] A. Djouadi, "The anatomy of electro-weak symmetry breaking. ii: The higgs bosons in the minimal supersymmetric model," hep-ph/0503173.

[30] R. Rattazzi, "Electroweak symmetry breaking waiting for the lhc," *Plenary Talk given at "Workshop on Higgs Boson Phenomenology" - ETH and University of Zürich, Switzerland 7 - 9 January 2009* .

[31] K. G. Wilson and J. B. Kogut, "The Renormalization group and the epsilon expansion," *Phys. Rept.* **12** (1974) 75–200.

[32] R. Barbieri, "Electroweak precision tests: what do we learn?,". CERN-TH-6659-92.

[33] R. Barbieri, A. Pomarol, R. Rattazzi, and A. Strumia, "Electroweak symmetry breaking after lep1 and lep2," *Nucl. Phys.* **B703** (2004) 127–146, hep-ph/0405040.

[34] Y. Nir, "The physics of heavy flavors," *Lectures given at the '2007 CERN-FERMILAB Hadron Collider Physics Summer School', CERN, Geneva* (2007) .

[35] R. Barbieri and A. Strumia, "The 'lep paradox'," hep-ph/0007265. R. Barbieri and A. Strumia, "What is the limit on the higgs mass?," *Phys. Lett.* **B462** (1999) 144–149, hep-ph/9905281. R. Barbieri and L. J. Hall, "Improved naturalness and the two higgs doublet model," hep-ph/0510243. R. Barbieri, L. J. Hall, and V. S. Rychkov, "Improved naturalness with a heavy Higgs: An alternative road to LHC physics," *Phys. Rev.* **D74** (2006) 015007, arXiv:hep-ph/0603188.

[36] M. F. Sohnius, "Introducing Supersymmetry," *Phys. Rept.* **128** (1985) 39–204. J. Terning, "Non-perturbative supersymmetry," arXiv:hep-th/0306119.

[37] L. Girardello and M. T. Grisaru, "Soft Breaking of Supersymmetry," *Nucl. Phys.* **B194** (1982) 65. S. Dimopoulos and H. Georgi, "Softly Broken Supersymmetry and SU(5)," *Nucl. Phys.* **B193** (1981) 150.

[38] K. N. et al (Particle Data Group), "Review of particle physics," *Journal of Physics G 37, 075021 (2010)* .

[39] S. Weinberg, "Effective Gauge Theories," *Phys. Lett.* **B91** (1980) 51.

[40] R. Barbieri, P. Ciafaloni, and A. Strumia, "Light thresholds in grand unified theories," *Nucl. Phys.* **B442** (1995) 461–471, arXiv:hep-ph/9411255. P. Langacker and N. Polonsky, "Uncertainties in coupling constant unification," *Phys. Rev.* **D47** (1993) 4028–4045, arXiv:hep-ph/9210235.

[41] J. C. Romao, "Spontaneous cp violation in susy models: a no-go theorem," *Phys. Lett.* **B173** (1986) 309.

[42] J. R. Ellis, G. Ridolfi, and F. Zwirner, "Radiative corrections to the masses of supersymmetric higgs bosons," *Phys. Lett.* **B257** (1991) 83–91.

[43] R. Barbieri, M. Frigeni, and F. Caravaglios, "The Supersymmetric Higgs for heavy superpartners," *Phys. Lett.* **B258** (1991) 167–170.

[44] S. P. Martin, "Extra vector-like matter and the lightest Higgs scalar boson mass in low-energy supersymmetry," *Phys. Rev.* **D81** (2010) 035004, arXiv:0910.2732 [Unknown].

[45] P. Batra, A. Delgado, D. E. Kaplan, and T. M. P. Tait, "The Higgs mass bound in gauge extensions of the minimal supersymmetric standard model," *JHEP* **02** (2004) 043, arXiv:hep-ph/0309149.

[46] G. Marandella, C. Schappacher, and A. Strumia, "Little-Higgs corrections to precision data after LEP2," *Phys. Rev.* **D72** (2005) 035014, arXiv:hep-ph/0502096.

[47] R. Barbieri, L. J. Hall, A. Y. Papaioannou, D. Pappadopulo, and V. S. Rychkov, "An alternative NMSSM phenomenology with manifest perturbative unification," *JHEP* **03** (2008) 005, arXiv:0712.2903 [hep-ph].

[48] C. T. Hill, "Quark and Lepton Masses from Renormalization Group Fixed Points," *Phys. Rev.* **D24** (1981) 691.

[49] K. A. Intriligator and N. Seiberg, "Lectures on supersymmetric gauge theories and electric- magnetic duality," *Nucl. Phys. Proc. Suppl.* **45BC** (1996) 1–28, arXiv:hep-th/9509066.

[50] U. Ellwanger, C. Hugonie, and A. M. Teixeira, "The Next-to-Minimal Supersymmetric Standard Model," arXiv:0910.1785 [Unknown].

[51] P. Gambino and M. Misiak, "Quark mass effects in B -> Xs gamma," *Nucl. Phys.* **B611** (2001) 338–366, arXiv:hep-ph/0104034.

[52] A. G. Cohen, D. B. Kaplan, and A. E. Nelson, "The more minimal supersymmetric standard model," *Phys. Lett.* **B388** (1996) 588–598, arXiv:hep-ph/9607394.

[53] R. Barbieri, E. Bertuzzo, M. Farina, P. Lodone, and D. Pappadopulo, "A Non Standard Supersymmetric Spectrum," arXiv:1004.2256 [Unknown].

[54] B. Allanach, C. Balazs, G. Belanger, M. Bernhardt, F. Boudjema, *et al.*, "SUSY Les Houches Accord 2," *Comput.Phys.Commun.* **180** (2009) 8–25, arXiv:0801.0045 [hep-ph].

[55] E. Bertuzzo and M. Farina, "Higgs boson signals in lambda-SUSY with a Scale Invariant Superpotential," arXiv:1105.5389 [hep-ph].

[56] J. P. Derendinger and C. A. Savoy, "Quantum Effects and SU(2) x U(1) Breaking in Supergravity Gauge Theories," *Nucl. Phys.* **B237** (1984) 307.

[57] R. Barbieri and G. F. Giudice, "Upper Bounds on Supersymmetric Particle Masses," *Nucl. Phys.* **B306** (1988) 63.

[58] S. P. Martin and M. T. Vaughn, "Two loop renormalization group equations for soft supersymmetry breaking couplings," *Phys. Rev.* **D50** (1994) 2282, arXiv:hep-ph/9311340.

[59] **Particle Data Group** Collaboration, C. Amsler *et al.*, "Review of particle physics," *Phys. Lett.* **B667** (2008) 1.

[60] **LEP Higgs Working Group for Higgs boson searches** Collaboration, "Search for charged Higgs bosons: Preliminary combined results using LEP data collected at energies up to 209- GeV," arXiv:hep-ex/0107031.

[61] **ALEPH** Collaboration, S. Schael *et al.*, "Search for neutral MSSM Higgs bosons at LEP," *Eur. Phys. J.* **C47** (2006) 547–587, arXiv:hep-ex/0602042.

[62] "Http://www.cern.ch/lepewwg/,".

[63] P. Hut, "Limits on masses and number of neutral weakly interacting particles," *Phys. Lett.* **B69** (1977) 85. B. W. Lee and S. Weinberg, "Cosmological lower bound on heavy-neutrino masses," *Phys. Rev. Lett.* **39** (1977) 165–168. M. I. Vysotsky, A. D. Dolgov, and Y. B. Zeldovich, "Cosmological limits on the masses of neutral leptons," *JETP Lett.* **26** (1977) 188–190.

[64] H. Goldberg, "Constraint on the photino mass from cosmology," *Phys. Rev. Lett.* **50** (1983) 1419. M. Drees and M. M. Nojiri, "The Neutralino relic density in minimal $N = 1$ supergravity," *Phys. Rev.* **D47** (1993) 376–408, arXiv:hep-ph/9207234.

[65] N. Jarosik *et al.*, "Seven-Year Wilkinson Microwave Anisotropy Probe (WMAP) Observations: Sky Maps, Systematic Errors, and Basic Results," arXiv:1001.4744 [Unknown].

[66] S. A. Abel, S. Sarkar, and I. B. Whittingham, "Neutralino dark matter in a class of unified theories," *Nucl. Phys.* **B392** (1993) 83–110, arXiv:hep-ph/9209292. B. R. Greene and P. J. Miron, "Supersymmetric cosmology with a gauge singlet," *Phys. Lett.* **B168** (1986) 226. G. Belanger, F. Boudjema, C. Hugonie, A. Pukhov, and A. Semenov, "Relic density of dark matter in the NMSSM," *JCAP* **0509** (2005) 001, arXiv:hep-ph/0505142.

[67] **XENON100** Collaboration, E. Aprile *et al.*, "Dark Matter Results from 100 Live Days of XENON100 Data," arXiv:1104.2549 [astro-ph.CO].

[68] **XENON** Collaboration, J. Angle *et al.*, "First Results from the XENON10 Dark Matter Experiment at the Gran Sasso National Laboratory," *Phys. Rev. Lett.* **100** (2008) 021303, arXiv:0706.0039 [astro-ph].

[69] **The CDMS-II** Collaboration, Z. Ahmed *et al.*, "Results from the Final Exposure of the CDMS II Experiment," arXiv:0912.3592 [Unknown].

[70] R. Barbieri, M. Frigeni, and G. F. Giudice, "Dark matter neutralinos in supergravity theories," *Nucl. Phys.* **B313** (1989) 725. M. W. Goodman and E. Witten, "Detectability of certain dark-matter candidates," *Phys. Rev.* **D31** (1985) 3059.

[71] M. A. Shifman, A. I. Vainshtein, and V. I. Zakharov, "Remarks on Higgs Boson Interactions with Nucleons," *Phys. Lett.* **B78** (1978) 443.

[72] J. R. Ellis, K. A. Olive, and C. Savage, "Hadronic Uncertainties in the Elastic Scattering of Supersymmetric Dark Matter," *Phys. Rev.* **D77** (2008) 065026, arXiv:0801.3656 [hep-ph].

[73] J. Giedt, A. W. Thomas, and R. D. Young, "Dark matter, the CMSSM and lattice QCD," *Phys. Rev. Lett.* **103** (2009) 201802, arXiv:0907.4177 [hep-ph].

[74] A. Collaboration, "Atlas detector and physics performance vol. 2. no. atlas tdr 15, cern/lhcc 99-15.,".

[75] C. Collaboration, "Cms physics technical design report - volume ii: Physics performance. no. cern/lhcc 2006-021.,".

[76] W. Beenakker, R. Hopker, M. Spira, and P. M. Zerwas, "Squark and gluino production at hadron colliders," *Nucl. Phys.* **B492** (1997) 51–103, arXiv:hep-ph/9610490.

[77] S. I. Bityukov and N. V. Krasnikov, "The LHC (CMS) discovery potential for models with effective supersymmetry and nonuniversal gaugino masses," *Phys. Atom. Nucl.* **65** (2002) 1341–1351, arXiv:hep-ph/0102179.

[78] R. Franceschini and R. Torre, "Heavy scalars with leptons and bottom jets signatures at the early lhc," *In preparation* .

[79] I. Low, R. Rattazzi, and A. Vichi, "Theoretical Constraints on the Higgs Effective Couplings," *JHEP* **04** (2010) 126, arXiv:0907.5413 [hep-ph].

[80] **Particle Data Group** Collaboration, C. Amsler *et al.*, "Review of particle physics," *Phys. Lett.* **B667** (2008) 1.

[81] M. Spira, "HIGLU: A Program for the Calculation of the Total Higgs Production Cross Section at Hadron Colliders via Gluon Fusion including QCD Corrections," arXiv:hep-ph/9510347.

[82] http://people.web.psi.ch/spira/proglist.html.

[83] K. Tobe and J. D. Wells, "Higgs boson mass limits in perturbative unification theories," *Phys. Rev.* **D66** (2002) 013010, hep-ph/0204196.

[84] F. Maltoni and T. Stelzer, "MadEvent: Automatic event generation with MadGraph," *JHEP* **02** (2003) 027, arXiv:hep-ph/0208156.

[85] M. L. Mangano, M. Moretti, F. Piccinini, R. Pittau, and A. D. Polosa, "ALPGEN, a generator for hard multiparton processes in hadronic collisions," *JHEP* **07** (2003) 001, arXiv:hep-ph/0206293.

[86] C. Collaboration, "Measurement of the inclusive jet cross section in z(-> ee) + jets pro- duction, cdf note 8827,". D. Collaboration, "Z+jet production in the d0 experiment: A comparison between data and the pythia and sherpa monte carlo, d0 note 5066-conf.,".

[87] "http://root.cern.ch/,". I. Antcheva *et al.*, "ROOT: A C++ framework for petabyte data storage, statistical analysis and visualization," *Comput. Phys. Commun.* **180** (2009) 2499–2512.

[88] A. Collaboration, "Atlas detector and physics performance vol. 1. no. atlas tdr 14, cern/lhcc 99-14.,".

[89] "http://root.cern.ch/root/atlfast.html,".

[90] V. Barger, T. Han, and D. G. E. Walker, "Top Quark Pairs at High Invariant Mass: A Model-Independent Discriminator of New Physics at the LHC," *Phys. Rev. Lett.* **100** (2008) 031801, arXiv:hep-ph/0612016.

[91] **The ATLAS Collaboration** Collaboration, G. Aad *et al.*, "Expected Performance of the ATLAS Experiment - Detector, Trigger and Physics," arXiv:0901.0512 [hep-ex].